

NOAA Technical Memorandum OAR ARL-241

**AIRCRAFT MEASUREMENTS IN THE COUPLED BOUNDARY LAYERS AIR-SEA
TRANSFER (CBLAST) LIGHT WIND PILOT FIELD STUDY**

Gennaro H. Crescenti
Jeffrey R. French
Timothy L. Crawford

Field Research Division
Idaho Falls, Idaho

Air Resources Laboratory
Silver Spring, Maryland
December 2001

**UNITED STATES
DEPARTMENT OF COMMERCE**

**Donald L. Evans
Secretary**

**NATIONAL OCEANIC AND
ATMOSPHERIC ADMINISTRATION**

**Condrad C. Lautenbacher, Jr.
Under Secretary for Oceans
and Atmosphere/Administrator**

Oceanic and Atmospheric
Research Laboratories

**David L. Evans
Director**



Notice

This document was prepared as an account of work sponsored by an agency of the United States Government. The views and opinions of the authors expressed herein do not necessarily state or reflect those of the United States Government. Neither the United States Government, nor any of their employees, makes any warranty, express or implied, or assumes any legal liability or responsibility for the accuracy, completeness, or usefulness of any information, product, or process disclosed, or represents that its use would not infringe privately owned rights. Mention of a commercial company or product does not constitute an endorsement by NOAA/OAR. Use of information from this publication concerning proprietary products or the tests of such products for publicity or advertising purposes is not authorized.

Table of Contents

	<u>Page</u>
Notice	ii
Table of Contents	iii
List of Figures	v
List of Tables	vii
List of Abbreviations and Acronyms	viii
List of Symbols and Variables	ix
Abstract	x
1 Introduction	1
2 Aircraft	2
3 Instrumentation	4
3.1 Wind Measurement System	4
3.2 Temperature and Humidity Sensors	7
3.3 Radiometers	9
3.4 Ocean Surface Remote Sensors	11
3.5 Other Sensors	13
4 Data Acquisition System	14
5 Post Flight Data Processing	16
5.1 Differential GPS Corrections	17
5.2 NetCDF Conversion	17
5.3 Quality Control	17
5.4 Final Processing	17
6 Data	20
6.1 NCR Files	20
6.2 NCP Files	22
6.3 MKR Files	22
6.4 LOG Files	24
6.5 Known Problems	24

7	Flight Summaries	26
	7.1 Flight 1 (21 JUL 01)	26
	7.2 Flight 2 (22 JUL 01)	26
	7.3 Flight 3 (23 JUL 01)	26
	7.4 Flight 4 (25 JUL 01)	28
	7.5 Flight 5 (27 JUL 01)	28
	7.6 Flight 6 (27 JUL 01)	28
	7.7 Flight 7 (28 JUL 01)	28
	7.8 Flight 8 (29 JUL 01)	28
	7.9 Flight 9 (29 JUL 01)	29
	7.10 Flight 10 (30 JUL 01)	29
	7.11 Flight 11 (31 JUL 01)	29
	7.12 Flight 12 (01 AUG 01)	29
	7.13 Flight 13 (01 AUG 01)	29
	7.14 Flight 14 (02 AUG 01)	30
	7.15 Flight 15 (03 AUG 01)	30
	7.16 Flight 16 (05 AUG 01)	30
	7.17 Flight 17 (05 AUG 01)	30
	7.18 Flight 18 (07 AUG 01)	30
	7.19 Flight 19 (08 AUG 01)	30
	7.20 Flight 20 (08 AUG 01)	31
	Acknowledgments	32
	References	33
	Appendix A: Marker Files	36
	Appendix B: N3R Flight Tracks	63

List of Figures

	<u>Page</u>
Figure 1	N3R in flight during a research mission 2
Figure 2	BAT probe and GPS antenna 4
Figure 3	Calibration curves for BAT probe pressure sensors 5
Figure 4	Calibration curves for BAT probe accelerometers 6
Figure 5	Calibration curves for backseat accelerometers 6
Figure 6	Demonstration of accuracy of DGPS-derived aircraft velocity. Eastward (Nu), northward (Nv), and vertical (Nw) velocity components are reported for a one-minute period when N3R was stationary on 22 JUL 01 7
Figure 7	Calibration curve for slow-response thermistor (TBar) 8
Figure 8	Scatter plot of temperature acquired by the fast-response thermistor (Tp1) against the slow response thermistor temperature (TBar) acquire by N3R on 21 JUL 01 ... 8
Figure 9	Calibration curve for IRGA 9
Figure 10	Everest Interscience 4000.4GXL infrared radiometer with a flexible heater and a temperature controller 9
Figure 11	Calibration curves for PAR sensors 10
Figure 12	Calibration curve for Everest Interscience 4000.4GL (sky) radiometer 11
Figure 13	Calibration curve for Everest Interscience 4000.4GXL (SST) radiometer 11
Figure 14	N3R instrument pod 11
Figure 15	Riegl LD90-3100VHS laser altimeter 12
Figure 16	NASA Ka-band scatterometer 12
Figure 17	N3R data acquisition PC, BAT auxiliary box, Ashtech dual-frequency GPS, and PCMCIA flash disk 14
Figure 18	Flowchart summarizing N3R data post-processing steps 16

Figure 19	N3R track for Flight 1 (21 JUL 01)	63
Figure 20	N3R track for Flight 2 (22 JUL 01)	64
Figure 21	N3R track for Flight 3 (23 JUL 01)	65
Figure 22	N3R track for Flight 4 (25 JUL 01)	66
Figure 23	N3R track for Flight 5 (27 JUL 01)	67
Figure 24	N3R track for Flight 6 (27 JUL 01)	68
Figure 25	N3R track for Flight 7 (28 JUL 01)	69
Figure 26	N3R track for Flight 8 (29 JUL 01)	70
Figure 27	N3R track for Flight 9 (29 JUL 01)	71
Figure 28	N3R track for Flight 10 (30 JUL 01)	72
Figure 29	N3R track for Flight 11 (31 JUL 01)	73
Figure 30	N3R track for Flight 12 (01 AUG 01)	74
Figure 31	N3R track for Flight 13 (01 AUG 01)	75
Figure 32	N3R track for Flight 14 (02 AUG 01)	76
Figure 33	N3R track for Flight 15 (03 AUG 01)	77
Figure 34	N3R track for Flight 16 (05 AUG 01)	78
Figure 35	N3R track for Flight 17 (05 AUG 01)	79
Figure 36	N3R track for Flight 18 (07 AUG 01)	80
Figure 37	N3R track for Flight 19 (08 AUG 01)	81
Figure 38	N3R track for Flight 20 (08 AUG 01)	82

List of Tables

	<u>Page</u>
Table 1	N3R specifications 3
Table 2	Summary of data files 18
Table 3	Calibration constants and switches used in <i>makepod</i> 19
Table 4	Summary of NCR file variables 21
Table 5	Summary of NCP file variables 23
Table 6	Summary of N3R flights 27

List of Abbreviations and Acronyms

A/D	Analog-to-Digital
ARA	Airborne Research Australia
ARL	Air Resources Laboratory
ASCII	American Standard Code for Information Interchange
BAT	“Best” Aircraft Turbulence
CBLAST	Coupled Boundary Layers Air-Sea Transfer
CG	Center of Gravity
DGPS	Differential Global Positioning System
DRI	Defense Research Initiative
DSP	Design Stagnation Point
ELT	Emergency Locator Transmitter
FAA	Federal Aviation Administration
FUST	Fast Ultra-Sensitive Temperature
GOES	Geostationary Operational Environmental Satellite
GPS	Global Positioning System
IR	Infrared
IRGA	Infrared Gas Analyzer
MABL	Marine Atmospheric Boundary Layer
MVCO	Martha’s Vineyard Coastal Observatory
NASA	National Aeronautics and Space Administration
NCAR	National Center for Atmospheric Research
netCDF	Network Common Data Format
NOAA	National Oceanic and Atmospheric Administration
OAR	Office of Atmospheric Research
ONR	Office of Naval Research
PAR	Photosynthetically Active Radiation
PC	Personal Computer
PSP	Precision Spectral Pyranometer
REM	Remote
SAR	Synthetic Aperture Radar
SST	Sea Surface Temperature
TANS	Trimble Advanced Navigation System
UTC	Coordinated Universal Time
UW	University of Washington
WHOI	Woods Hole Oceanographic Institution

List of Symbols and Variables

α_0	Angle of Attack at Zero Lift
δ_h	Heading Offset for Relative Velocity
δ_p	Pitch Offset for Relative Velocity
δ_q	Adjustment to Dynamic Pressure
δ_r	Roll Offset for Relative Velocity
g	Gravitational Acceleration Constant (9.81 m s^{-2})
K_α	Pitch Calibration Constant
K_β	Yaw Calibration Constant
K_{up}	Upwash Factor
mss	Mean Square Slope
R_T	Temperature Recovery Factor
r	Linear Calibration Coefficient
SE	Standard Error
2	Accelerometer Angle

Abstract

A research aircraft was used in the low-wind pilot field study of the Coupled Boundary Layers Air-Sea Transfer (CBLAST) Departmental Research Initiative (DRI) to acquire high-resolution *in situ* atmospheric turbulent fluxes in the marine atmospheric boundary layer while simultaneously documenting the characteristics of the surface wave field with various remote sensors. The CBLAST-Low pilot study was successfully conducted during a three-week period from late July to early August 2001 off the south shore of Martha's Vineyard Island, Massachusetts. Twenty missions (~ 48 flight hours) were flown by the LongEZ (registration N3R) on days with light winds ($< 7 \text{ m s}^{-1}$) under various atmospheric stabilities. Data acquired by N3R in CBLAST-Low will support the test and refinement of parameterizations used in air-sea models for light wind regimes. In addition, such measurements will provide important boundary conditions to determine boundary layer turbulence and other atmospheric processes controlling the exchange of energy across the air-sea interface. This report summarizes the data acquired by N3R in the CBLAST-Low pilot field study.

1 Introduction

Existing parameterizations of heat, moisture, and momentum fluxes in the marine atmospheric boundary layer (MABL) perform poorly under weak wind regimes, especially in regions of inhomogeneity (e.g., Ramage 1984; Mahrt et al. 1996; Sun et al. 1996; Serra et al. 1997; Drennan et al. 1999; Greischar and Stull 1999; Lambert and Durand 1999). These problems are due to a variety of processes including averaging techniques, gravity/capillary wave spacing, surfactants and surface tension, free convection effects, and frequency-dependent differences between wind, waves, and stress. In order to improve our understanding of air-sea interaction in extremely light wind regimes, the Office of Naval Research (ONR) created the Coupled Boundary Layers Air-Sea Transfer (CBLAST) Defense Research Initiative (DRI). The objectives of the CBLAST light-wind initiative are:

C to measure vertical fluxes of momentum and heat in the lower atmospheric boundary layer and in the ocean surface layer;

C to identify the processes that influence these fluxes (e.g., shear, convection, surface wave breaking, Langmuir cells);

C to close budgets for heat and momentum;

C to test parameterizations of fluxes; and

C to obtain other measurements (e.g., horizontal variability of pressure and temperature) sufficient to provide boundary conditions for a large eddy simulation or local application of a regional-scale simulation.

A research aircraft was used in the CBLAST-Low pilot field study to acquire high-resolution *in situ* atmospheric turbulent fluxes in the MABL and simultaneously document the characteristics of the surface wave field with various remote sensors. The LongEZ (registration N3R) research aircraft has proven to be an especially powerful tool for studying the spatial variability of air-sea interaction (Crawford et al. 1993; Vogel and Crawford 1997, 1999; Crescenti et al. 1999; Mahrt et al. 1999, 2001; Mourad 1999; Sun et al. 1999, 2001; Vogel et al. 1999; Vandemark et al. 1999a, 1999b, 2001; French et al. 2000, Mourad et al. 2000; Vickers et al. 2000, 2001). Data acquired by N3R in CBLAST-Low will support the test and refinement of parameterizations used in air-sea models. In addition, such measurements will provide important boundary conditions to determine boundary layer turbulence and other atmospheric processes controlling the exchange of energy across the air-sea interface.

The CBLAST-Low pilot study was conducted during a three-week period from late July to early August 2001 off the south shore of Martha's Vineyard Island, Massachusetts. Twenty missions (~ 48 flight hours) were flown on days with light winds ($< 7 \text{ m s}^{-1}$) under various atmospheric stabilities. This report summarizes the data acquired by N3R in the CBLAST-Low pilot field study.

2 Aircraft

Over the last ten years, N3R has been used by the National Oceanic and Atmospheric Administration's (NOAA) Air Resources Laboratory (ARL) in a number of air-sea interaction research studies. The differences between N3R and that of a standard airplane are obvious (Fig. 1). Far more than just being visually striking, these design features are ideally suited for high-fidelity turbulent flux measurements, especially at low altitudes.



Fig. 1. N3R in flight during a research mission.

The LongEZ was designed in the early 1980's by Burt Rutan as a high-performance sport aircraft. N3R is a custom-built aircraft licensed by the Federal Aviation Administration (FAA) under an experimental amateur-built airworthiness category. It is a safe and reliable aircraft with exceptional performance characteristics. Unlike most aircraft that are constructed with metal, N3R is fabricated from light-weight, high-strength fiberglass and foam composite that is resistant to structural fatigue and corrosion. Another important feature is that the engine is mounted on the rear of the airframe. The large main laminar-flow wing is set back further than that of conventional aircraft. Vertical winglets found on either end of the main wing enhance aircraft lift. A smaller second wing (canard) is found near the nose of the aircraft. This forward lifting surface is designed to increase aircraft stability and to prevent the main wing from stalling.

An important characteristic of an aircraft with a pusher engine and a canard is that it responds to turbulence far less than conventional aircraft with the same wing loading (weight per unit area). Since the canard contributes to both lift and stability, it can be heavily loaded relative to the main wing. For conventional aircraft with a rear-mounted elevator, an upward wind gust will tend to make the aircraft pitch up. This increases the lift generated by the wings and amplifies the aircraft response to an upward wind gust. In contrast, canard aircraft have their elevators forward of their center of gravity (CG). The same upward wind gust will push the canard elevator up which results in a compensating downward pitch response. Aircraft pitch response to either upward or downward wind gusts is opposed to the gust direction, thus giving canard-type aircraft their superior turbulent response characteristics. A canard aircraft is also stall-resistant. As the angle of attack on the airplane is increased, the canard loses lift before the main wing. This causes the nose to drop, which decreases the angle of attack, thereby providing automatic stall recovery without allowing the main wing to stall.

The unique aerodynamic design features of N3R make it ideally suited for making high-fidelity turbulence measurements with minimal flow distortion at low altitudes (~ 10 m) and slow aircraft flight speeds (~ 50 m s⁻¹). The small low-drag airframe and rear-mounted pusher engine have clear advantages for minimizing flow distortion and exhaust contamination (Crawford and Dobosy 1992). Instruments mounted on the aircraft nose avoid flow distortion, engine vibration,

and engine exhaust. On N3R, the wind measurement probe is five wing-widths (chord lengths) ahead of the canard. The resulting flow distortion is extremely low compared to other aircraft (Crawford et al. 1996).

The utility of N3R is illustrated by its impressive specifications and performance (Table 1). There are few aircraft that will carry its own weight as payload. Typically, N3R will fly a research mission at 50 m s^{-1} consuming fuel at a rate of only 11 kg hr^{-1} . Its fast cruise speed and long-range allow it to reach anywhere in the world. Because of its classification under FAA's experimental category, modifications can be made easily. N3R has been modified for scientific research with a larger engine, redundant high-output alternators, extended fuel tanks, and hard-points and port holes for instrument mounting. Fiberglass construction allows flexibility in modifying the airframe to mount sensors and instrument pods.

Table 1. N3R specifications.

Engine	Lycoming O-320 160 HP
Seats	2
Electrical	72 Amp @ 12 VDC
Fuselage Length (with probe)	5.0 m (5.6 m)
Wing Span	8.5 m
Wing Area	10 m^2
Canard Span (Chord)	3.7 m (0.38 m)
Propeller Diameter	1.80 m
Weight (empty)	430 kg
Payload	370 kg
Fuel Capacity (with aux tank)	200 kg (300 kg)
Range (extended)	3300 km (3800 km)
Ceiling	8000 m
Endurance	10 - 18 hr
Cruise Speed	90 m s^{-1}
Stall Speed	$25 - 30 \text{ m s}^{-1}$
Fuel Use @ 50 m s^{-1} (90 m s^{-1})	11 kg hr^{-1} (20 kg hr^{-1})

A number of important safety features have been incorporated into N3R. A 406-MHz Emergency Locator Transmitter (ELT) can send a distress signal via a NOAA Geostationary Operational Environmental Satellite (GOES) to a U. S. Coast Guard station or other rescue facility within seconds of activation. In the event of a catastrophic airframe or engine failure, a solid rocket ballistic parachute can be deployed in $\sim 1 \text{ s}$. The parachute, which is attached to the airframe, can safely lower the aircraft and pilot to the surface. A four-point harness and foam impact seat are capable of withstanding a 40-G impact. The auto-pilot is used to reduce pilot stress and fatigue for long flights. Routine radio communications are maintained with a ground-station on a regular basis. Other safety features include a life jacket, survival suit, inflatable raft, flare gun, signal mirrors, flashlights, chemical light sticks, and emergency rations.

3 Instrumentation

3.1 Wind Measurement System

The center piece of the N3R instrumentation package is the “best” aircraft turbulence (BAT) probe (Fig. 2). This device was designed, tested, and built as a result of a collaboration between ARL and Airborne Research Australia (ARA) (Crawford and Dobosy 1992; Hacker and Crawford 1999). The housing consists of a 15-cm diameter carbon-fiber hemisphere mounted on a tapered carbon-fiber cone. The housing and cone are mounted on a roughly 2-m long cylinder protruding forward from the nose of the aircraft. The housing contains four solid-state pressure sensors used to measure differential (three) and static (one) pressure from nine pressure ports symmetrically distributed on the hemisphere. The nominal accuracy of these sensors is ± 0.05 mb with a response of about 1 KHz. These measurements provide the pressure distribution over the housing from which the relative air velocity may be computed.

Two global positioning systems (GPS) are used on N3R. A dual-frequency Ashtech GPS antenna is mounted on the tapered cone of the BAT probe just aft of the housing. By using differential GPS (DGPS) correction techniques, aircraft position can be measured to within several centimeters relative to a fixed point and ground velocity can be computed to an accuracy of better than 1 cm s^{-1} in the horizontal and 2 cm s^{-1} in the vertical. These data are acquired at a rate of 5 Hz. Three orthogonally-mounted accelerometers contained in the BAT housing are used to augment the GPS position and velocity data to a frequency of 50 Hz.

Aircraft attitude (pitch, roll, and heading) is measured using a Trimble Advanced Navigation System (TANS) vector GPS. The TANS-vector consists of four antennas mounted on the BAT probe housing, on both wings, and the rear of the cockpit. Using carrier-phase techniques, the position of three antennas is measured relative to a master antenna. Manufacturer specified accuracy for aircraft attitude given the geometry of N3R is 0.05° . The TANS-vector GPS acquires attitude data at a maximum rate of 10 Hz. By differencing measurements acquired by accelerometers in the BAT probe housing and by three accelerometers mounted on the aircraft centerline in the back of



the fuselage, the frequency range for aircraft pitch and heading are extended up to 50 Hz. Similarly, the frequency can be extended to 50 Hz for aircraft roll by differencing two accelerometers mounted on either wing. This “blending” technique of aircraft position, velocity, and attitude from data acquired by GPS and accelerometers is described by Eckman et al. (1999).

Fig. 2. BAT probe and GPS antenna.

Calibration of the differential pressure sensors is accomplished using a Mensor 4040 digital pressure transducer. The Mensor transducer and the pressure sensors are connected in parallel to a syringe that is used to adjust the pressure applied to both the calibration standard and sensors. The y- and z-axis sensors (lateral and vertical, respectively) are designed to respond to differential pressure of ± 15 mb corresponding to an output of ± 5 V. The x-axis sensor (longitudinal) ranges from 0 to 28 mb with a corresponding output of ± 5 V. Figure 3 shows the linear calibration curves for the P_x (longitudinal), P_y (lateral), and P_z (vertical) pressure sensors. At least seven independent calibration points (N) were acquired for each sensor. A nearly perfect linear correlation r exists for all three sensors. The standard error SE , (i.e., the standard deviation about the linear fit) varies between 0.013 and 0.023 mb.

The accelerometers are calibrated by tipping the sensors to known angles and calculating the contribution due to gravity g as a function of angle θ (i.e., $g\sin\theta$ or $g\cos\theta$). It is possible to produce a calibration curve over the entire range of the device by making measurements over several angles. Figure 4 shows the linear calibration curves for the A_x (longitudinal), A_y (lateral), and A_z (vertical) accelerometers located in the BAT probe. At least seven independent calibration points were acquired for each sensor. A nearly perfect linear correlation r exists for all three sensors while values of SE vary between 0.024 and 0.053 $m\ s^{-2}$. The same calibration procedure was performed on the “backseat” accelerometers located along the aircraft centerline in the back of the fuselage (Fig. 5). Once again, values of r approach unity. Values of SE for all three backseat accelerometers are quite small (~ 0.008 to $0.015\ m\ s^{-2}$).

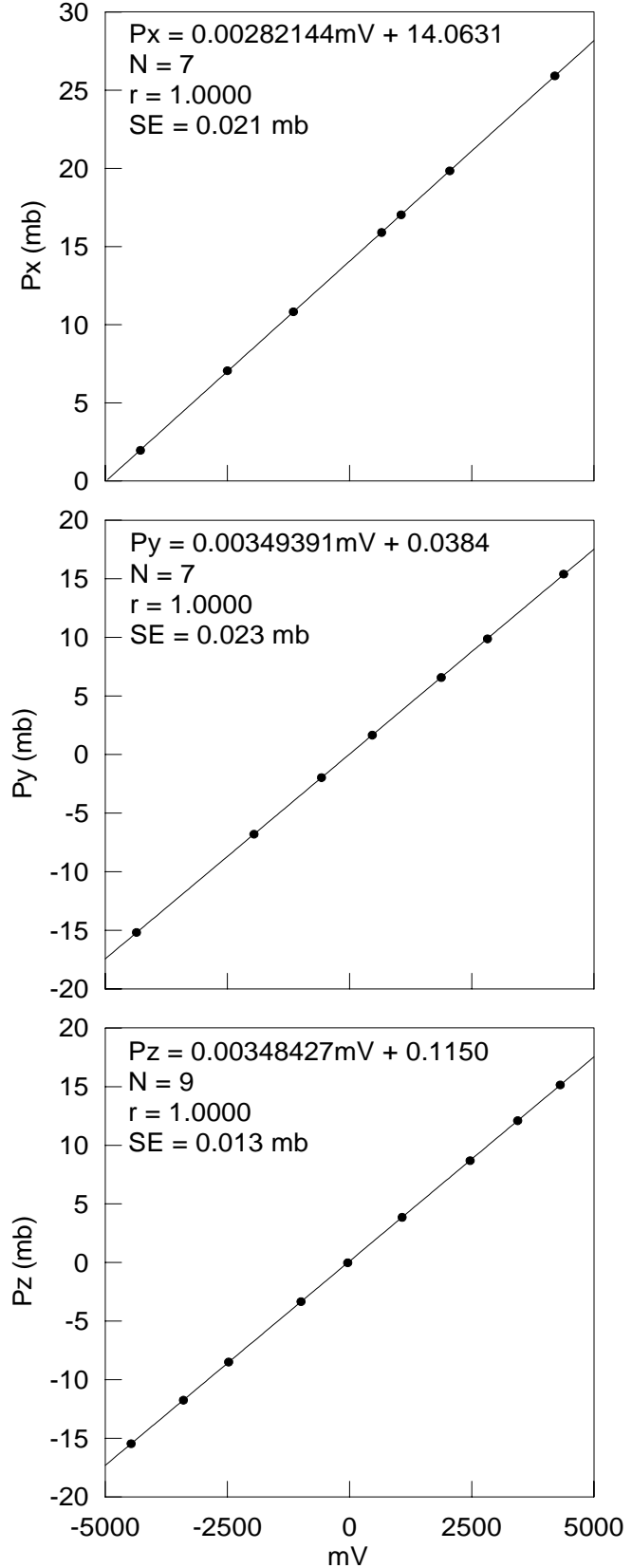


Fig. 3. Calibration curves for BAT probe pressure sensors.

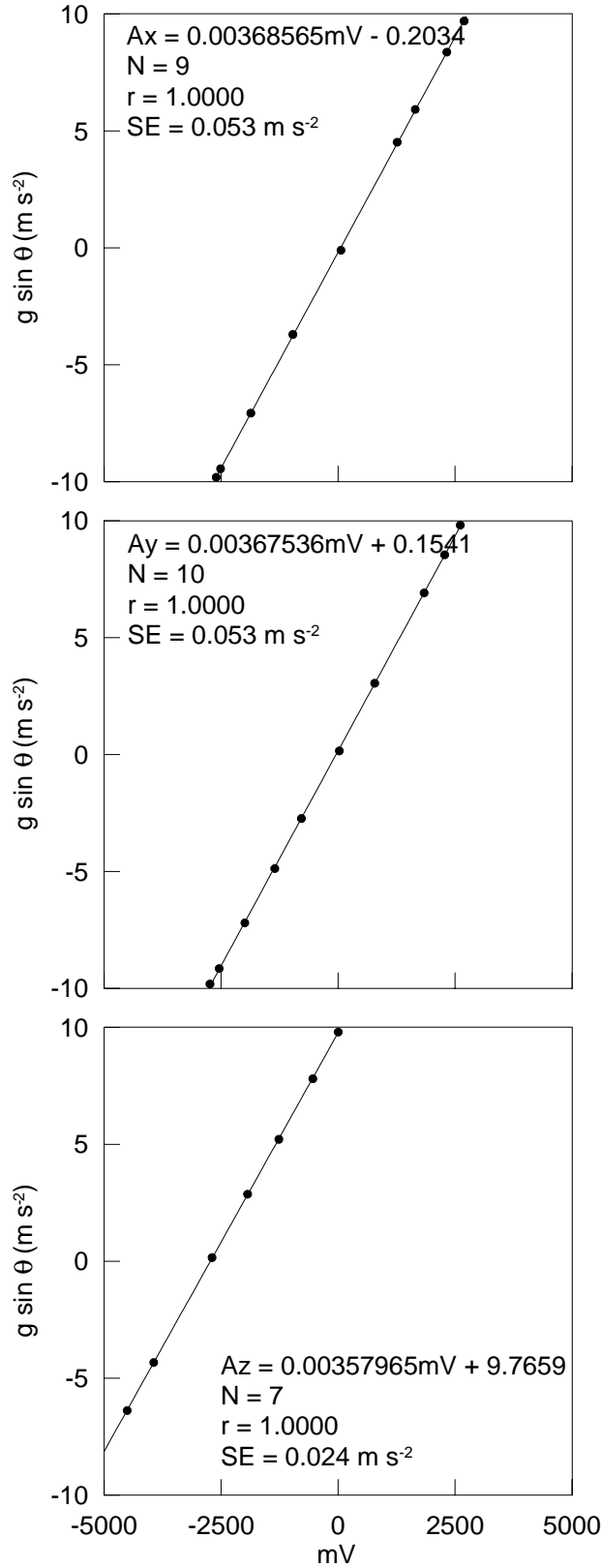


Fig. 4. Calibration curves for BAT probe accelerometers.

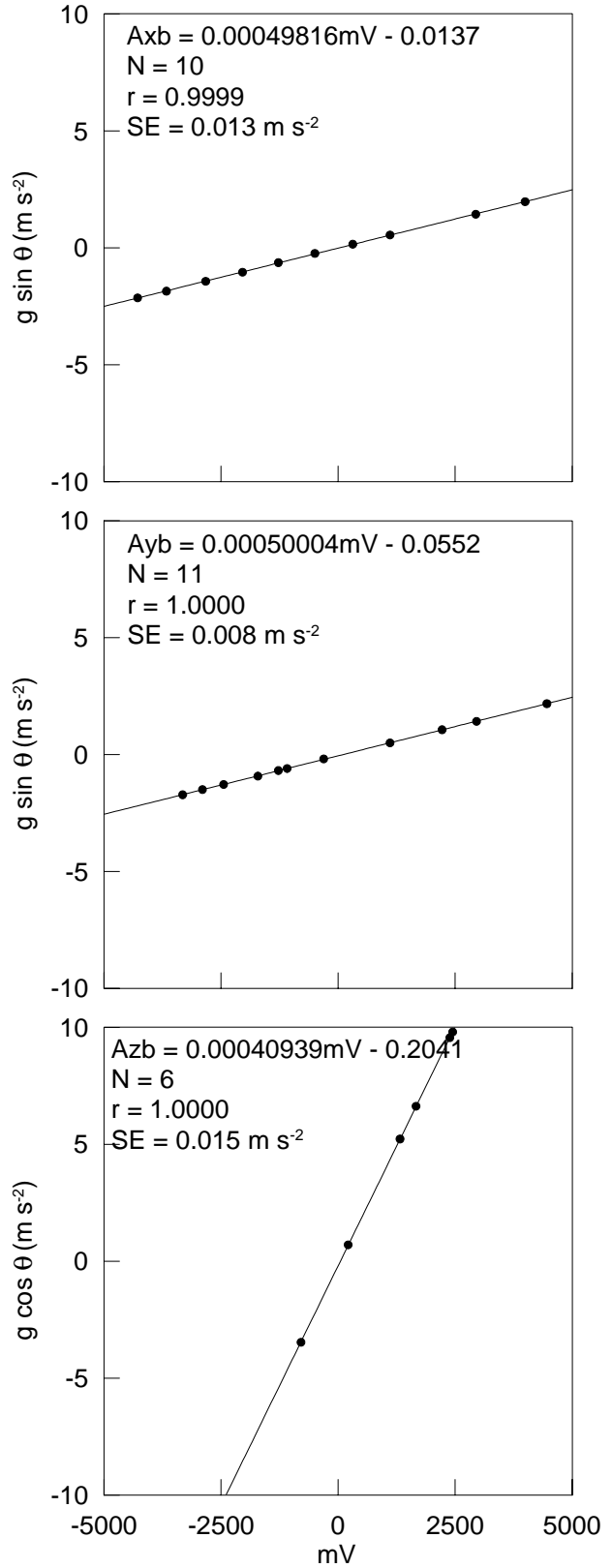


Fig. 5. Calibration curves for backseat accelerometers.

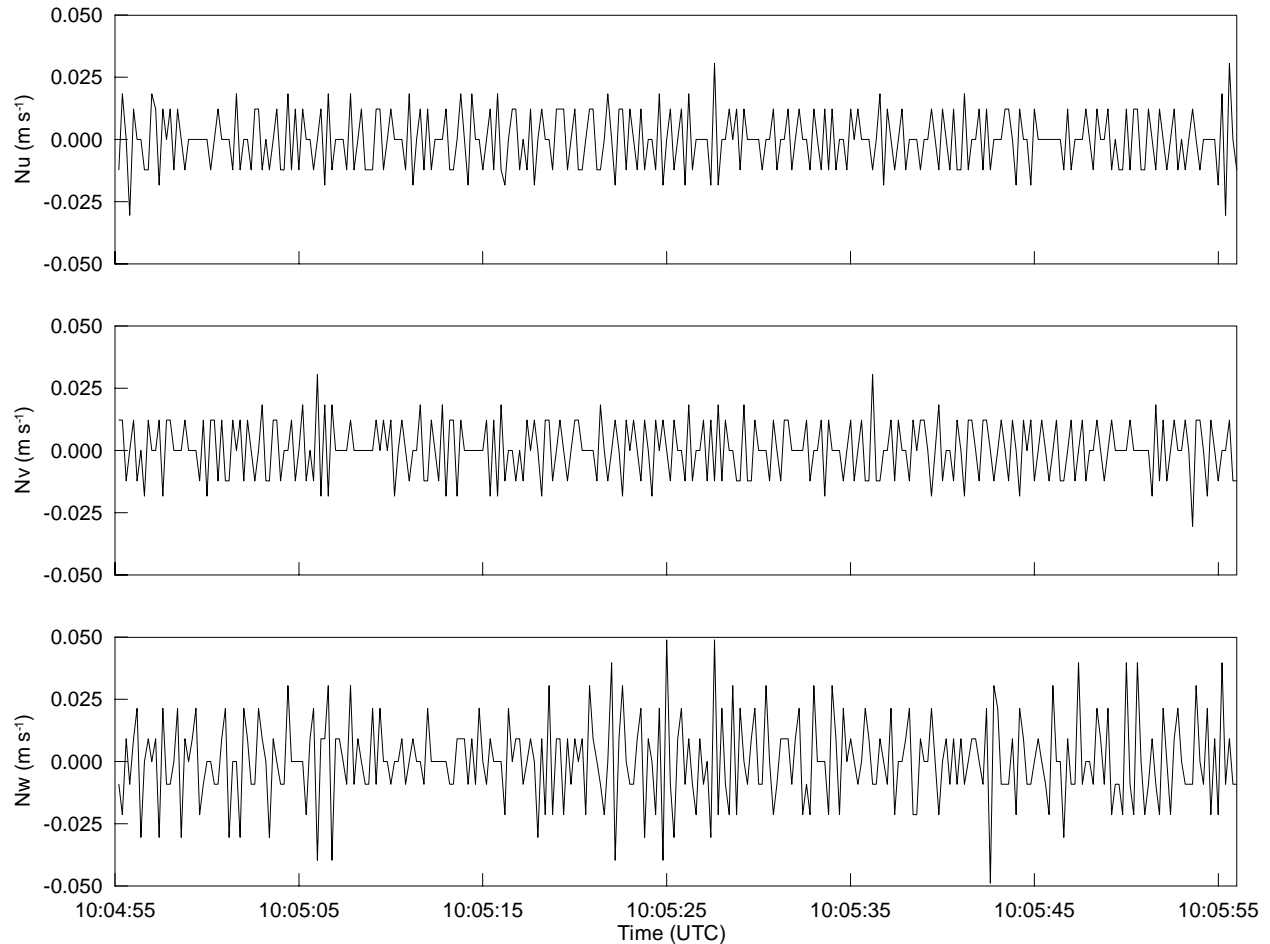


Fig. 6. Demonstration of accuracy of DGPS-derived aircraft velocity. Eastward (Nu), northward (Nv), and vertical (Nw) velocity components are reported for a one-minute period when N3R was stationary on 22 JUL 01.

The Ashtech and TANS-vector GPS are not calibrated per se, but checks are incorporated to ensure the data are within tolerance levels. For example, aircraft velocity data should be zero when N3R is parked on the tarmac. Figure 6 is an example of the DGPS eastward (Nu), northward (Nv), and vertical (Nw) aircraft velocity during a static test. This segment corresponds to a time when N3R was parked on the tarmac for about 60 s on 22 JUL 01. Over the course of the study, data from these static tests show a mean aircraft velocity of zero with a standard deviation of 1 to 2 cm s^{-1} . Spectra indicate the noise in the velocity data appears white (i.e., random). Prior studies have shown a standard deviation of 4 to 5 cm s^{-1} (French et al. 2000). This improvement is due in part to a combination of an upgraded GPS system (from the signal-frequency NovAtel GPS to the dual-frequency Ashtech GPS) and the elimination of selective availability (i.e., artificially inserted noise or variance) in the GPS satellite signals (Showstack 2000).

3.2 Temperature and Humidity Sensors

Three different probes are used to measure air temperature. A slow-response, multi-element

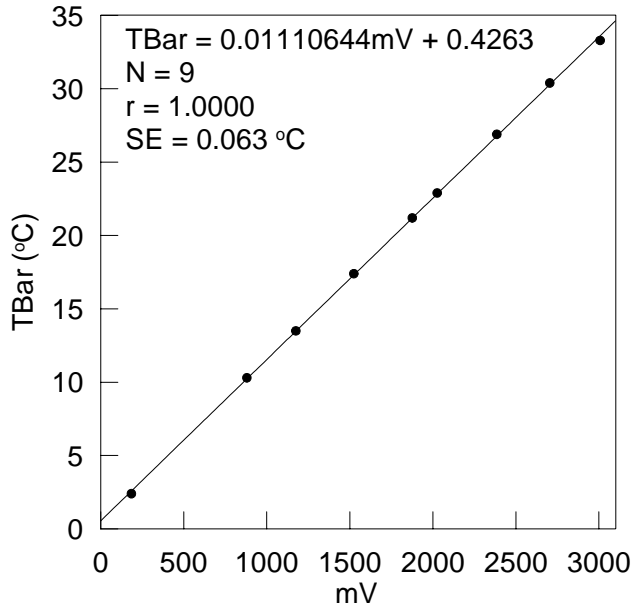


Fig. 7. Calibration curve for slow-response thermistor (TBar).

experimental development stage. Results from this new sensor will be documented at a later date.

Humidity is measured with two different sensors. An EG&G 200 chilled mirror sensor provides dew point temperature. This sensor has a relatively long response time (as much as a few seconds). An ARL designed and built fast-response (~ 50 Hz) open-path infrared gas analyzer (IRGA) measures the attenuation of light due to H₂O and CO₂ through a known path (Auble and Meyers 1992).

The slow-response thermistor is calibrated against an accurate mercury-bulb thermometer in a well mixed water bath over a range of temperatures. This method provides a stable calibration. The calibration curve for this thermistor (TBar) is shown in Figure 7. The correlation coefficient is nearly perfect with a standard error of about 0.06 °C.

The fast-response micro-bead thermistor is calibrated in flight against the output from the slow-response thermistor. Figure 8 is a scatter plot of the calibrated temperature acquired by the fast-response thermistor (Tp1) as a function of the slow response thermistor temperature (TBar).

linear thermistor provides low frequency (1 Hz) temperature measurements. This sensor is mounted within the center-hole, or design stagnation point (DSP) port, on the BAT hemisphere. A second fast-response (~ 20 Hz) 0.13-mm micro-bead thermistor is also mounted inside the DSP port. The recovery factor for micro-bead thermistor is 0.82 (the current housing/element combination has a time constant of ~ 0.07 s). The calculation of the correction factor due to compression is simpler than that of conventional temperature probes because of the location of the sensors within the DSP. The third sensor is the fast ultra-sensitive temperature (FUST) probe (French et al. 2001). This sensor is a Cu-Co 0.025-mm thermocouple and has a response time of better than 20 ms (50 Hz). The probe is mounted on a post below the hemisphere of the BAT probe. The FUST probe is still in the

Results from this new sensor will be documented at a later date.

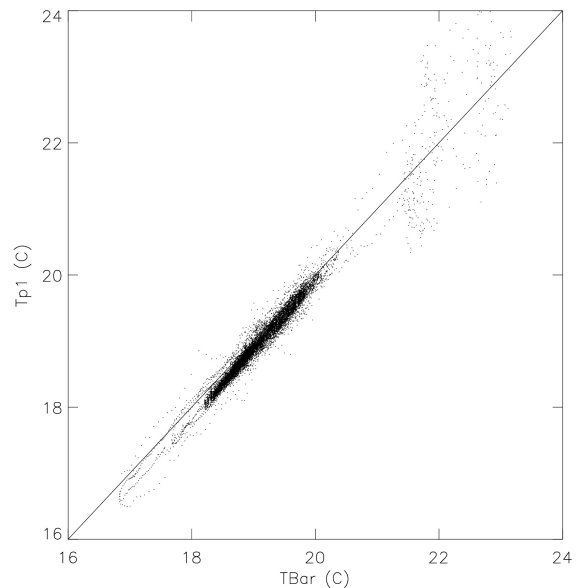


Fig. 8. Scatter plot of temperature acquired by the fast-response thermistor (Tp1) against the slow response thermistor temperature (TBar) acquire by N3R on 21 JUL 01.

In general, temperature data acquired by the micro-bead thermistor is highly correlated with data from the slow-response probe with correlation coefficients usually exceeding 0.9. It should be pointed out that some departures, especially for extreme values, represent real differences in the response time of the two sensors. For example, there are instances where the temperature from the slow-response thermistor changes more slowly than that of the micro-bead thermistor when N3R is flying through strong temperature gradients.

The factory calibration was used for the chilled mirror dew point sensor. Data output from this sensor were checked against humidity data acquired by a fan-aspirated psychrometer. The IRGA was calibrated by placing the sensor inside a chamber with known concentrations of water vapor between 2 and 19 g m⁻³. The calibration curve for the IRGA is a second-order polynomial (Fig. 9). It should be pointed out that values outside this range can be subject to larger errors. For very dry conditions, the IRGA can not acquire reliable data when absolute humidity is less than 1.7 g m⁻³ (corresponding to the minimum sensor output voltage of -5000 mV). Extrapolation of the calibration curve for absolute humidity greater than 19 g m⁻³ can also lead to uncertainty.

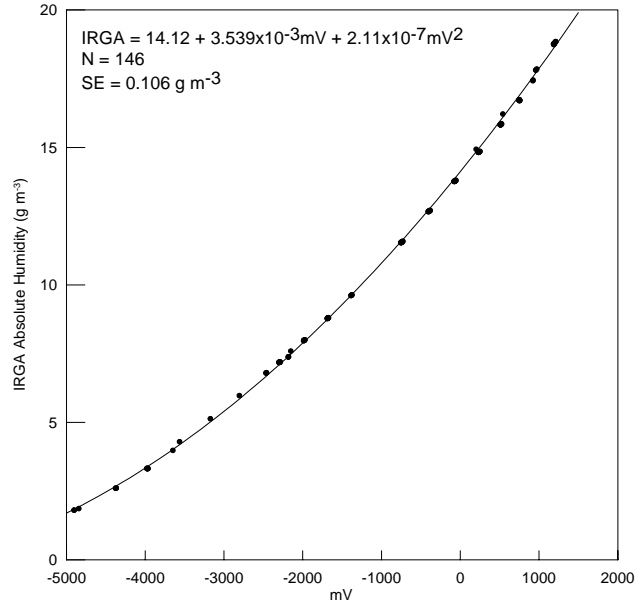


Fig. 9. Calibration curve for IRGA.

3.3 Radiometers

Radiometric sensors mounted on N3R measure both upwelling and downwelling (with respect to the aircraft) radiation. Upward looking and downward looking LI-COR photosynthetically active radiation (PAR) sensors measure the incoming and reflected portion of the visible solar spectrum, respectively. Upward and downward looking Everest Interscience 4000.4GL and 4000.4GXL infrared (IR) radiometer are used to measure sky and sea surface temperature (SST), respectively. The SST radiometer is shown in Figure 10. The upward looking radiometer has a response time of 0.25 s while the downward looking SST sensor has a response time of 0.02 s. The

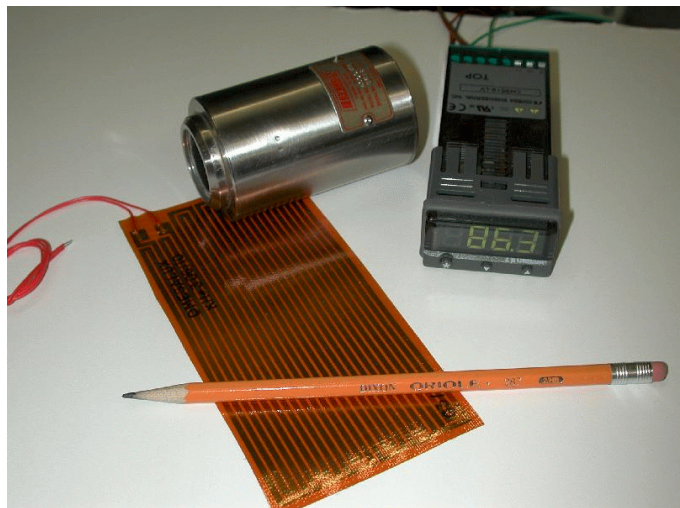


Fig. 10. Everest Interscience 4000.4GXL infrared radiometer with a flexible heater and a temperature controller.

manufacturer specified accuracy for both sensors is $\pm 0.5 \text{ } ^\circ\text{C}$.

The PAR sensors were calibrated against an Eppley Precision Spectral Pyranometer (PSP). These radiometers were placed outdoors under a clear, unobstructed sky for more than eight hours. One minute averages were acquired during this time and were used to determine the calibration curves for the PAR sensors (Fig. 11). Unlike the PSP which is responsive to the entire solar spectrum (0.285 to 2.8 : m), the PAR sensors are responsive only to the visible portion of the spectrum (0.4 to 1.1 : m). Thus, considerable scatter exists when clouds are present.

The upward looking Everest Interscience 4000.4GL (sky) radiometer was calibrated over a well-mixed water bath over a temperature range of 0 to 40 °C (Fig. 12). The linear regression over this range provides a good fit with an excellent correlation and a standard error of about 0.2 °C. It should be noted that a calibration could not be extended down to -40 °C which is the expected sky temperature for clear conditions.

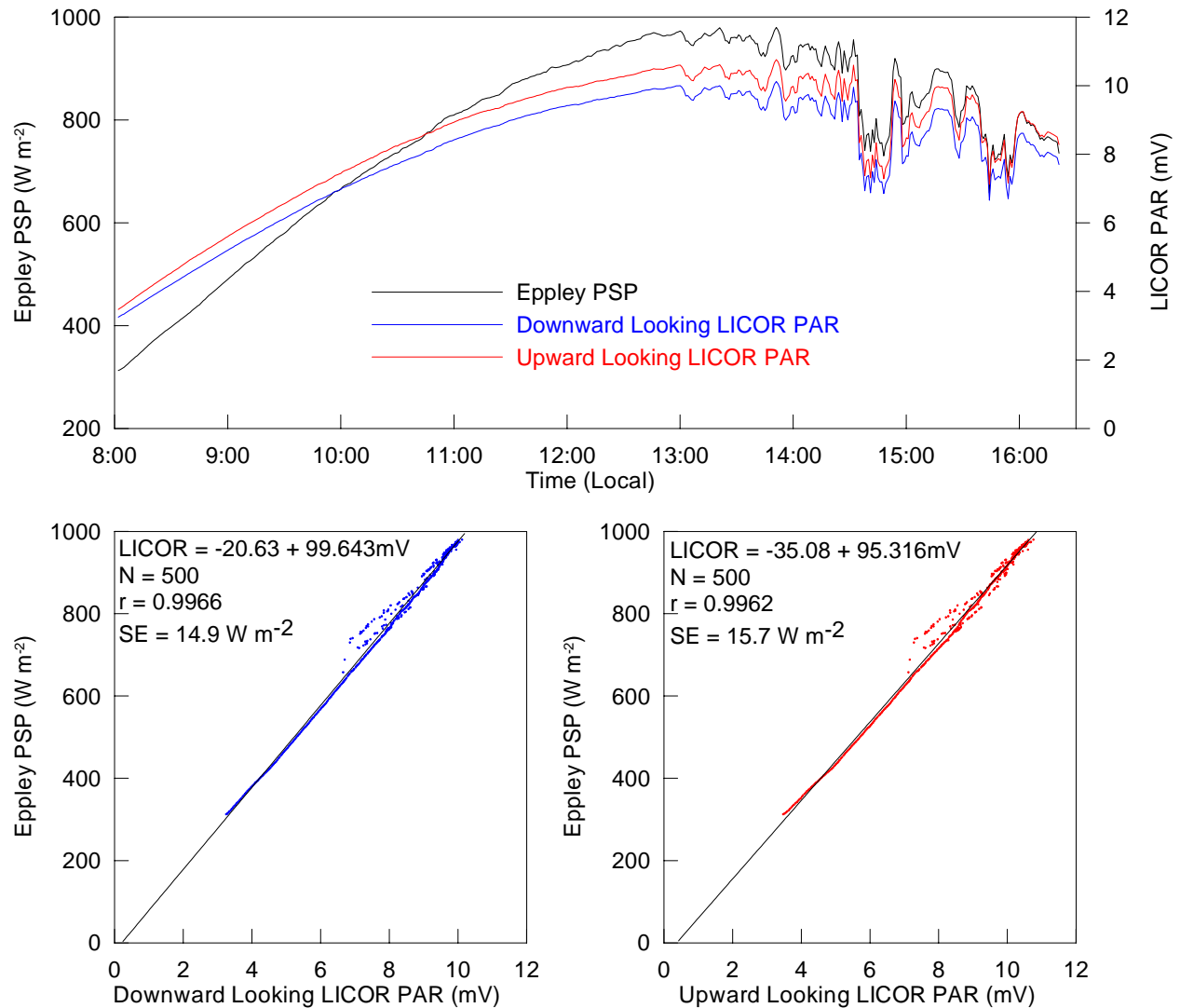


Fig. 11. Calibration curves for PAR sensors.

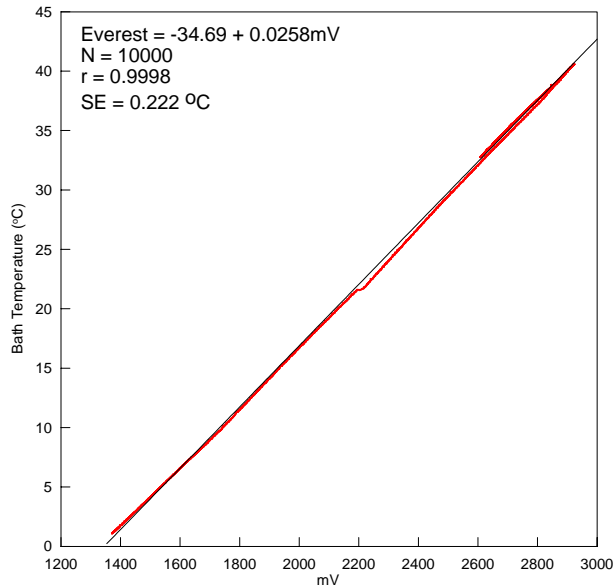


Fig. 12. Calibration curve for Everest Interscience 4000.4GL (sky) radiometer.

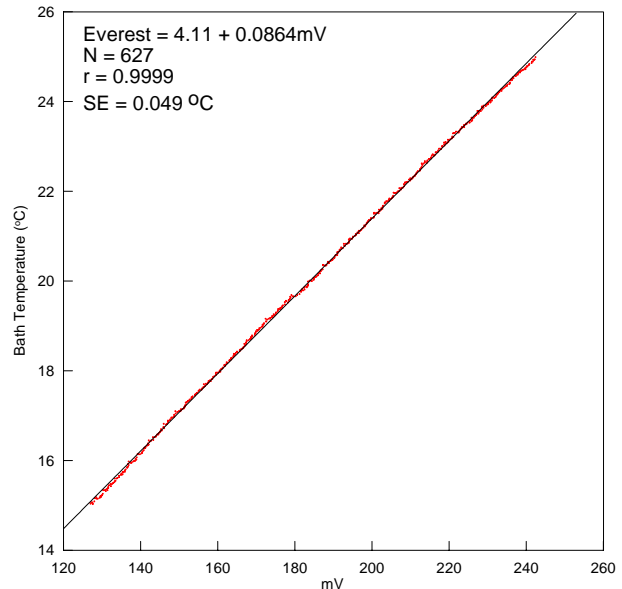


Fig. 13. Calibration curve for Everest Interscience 4000.4GXL (SST) radiometer.

Previous air-sea studies have shown that the SST data are subject to significant errors (> 1 to 2 °C) due to a temperature dependency of the sensor. Laboratory testing showed that SST measurements could be improved to better than 0.2 °C if the body temperature of the radiometer could be kept at a constant temperature. A flexible heater was wrapped around the body of the Everest 4000.4GXL radiometer and encased in a plastic shell with a layer of insulation. A controller is used to maintain a constant sensor body temperature of 30 °C. While the body temperature of the sensor is maintained at a constant value, no corrections are applied for the effects of the intervening atmosphere. The SST radiometer was calibrated over a well mixed water bath over a temperature range of 15 to 25 °C (expected SST off the coast of Martha's Vineyard in the summer). A nearly perfect linear correlation was found for this calibration with a standard error of about 0.05 °C (Fig. 13).

3.4 Ocean Surface Remote Sensors

A laser altimeter array and a nadir-pointing Ka-band scatterometer are used to determine long and short wave characteristics, respectively, of the sea surface. The data obtained from these remote sensors is unique in that it provides wave information from small capillary waves to long swells coupled with wind stress and turbulence measurements acquired by the BAT probe in the atmospheric surface layer. One of the lasers and the scatterometer are carried in an instrument pod suspended beneath the fuselage of N3R (Fig. 14).



Fig. 14. N3R instrument pod.



Fig. 15. Riegl LD90-3100VHS laser altimeter.

An array of three Riegl downward looking laser altimeters is designed to measure the sea surface profile and the one- and two-dimensional slopes of intermediate scale waves on the order of 1 to 10 m (Fig. 15). The laser array consists of three downward looking lasers mounted on the vertices of an equilateral triangle with 1-m separation. Two are mounted under either wing (model LD90-3100VHS) while the third is mounted in the instrument pod (model LD90-3100EHS). These lasers simultaneously measure sea surface height at points about the 1-m diameter circular footprint of the radar scatterometer. The circular footprint of each laser is about 7.5 mm in diameter at an altitude of 15 m. The two lasers mounted in either wing operate with a pulse repetition frequency of 2 KHz while the third laser in the pod operates at a frequency of 12 KHz. The individual pulses are averaged down to a rate of 150 Hz to reduce noise resulting in 13 pulses per scan for the 2-KHz lasers and 80 pulses per scan for the 12-KHz laser. The lasers output distance, normalized amplitude of the returned pulse, and number of valid returns. The focal length of the lasers was set to 15 m providing a nominal accuracy of ± 2 mm. The maximum altitude for which the lasers provide useful data is about 50 m. Given the laser measurements and aircraft attitude at any given time, matrix multiplications yield the vector normal to the sea surface plane. Other derived products include significant wave height, dominant wavelength of the wind sea, and the slope variance of the measured two-dimensional probability density function. This last parameter is denoted as the mean square slope (*mss*) of long waves. The *mss* can be considered as the slope variance associated with intermediate scale gravity waves. A fourth Riegl LD90-3100VHS laser was installed in the left wing of N3R at angle of 15° from the vertical. This sensor will serve as a “glint” laser during those instances when the vertically pointing lasers receive few or no returns.

Along-track changes in the integrated roughness of short ocean waves on the order of 2 to 100 cm are determined using a nadir-pointing 36-GHz (8.3 mm) continuous wave scatterometer (Fig. 16). This sensor, developed and built at the National Aeronautics and Space Administration (NASA) by Douglas C. Vandemark, is used to infer the short wave characteristics by relating backscatter intensity to the surface slope variance. The two-antenna remote sensor has a two-way, 3-dB beamwidth of 4.1° which corresponds to a 1.1-m footprint diameter at 15 m. Coincident laser altimeter



Fig. 16. NASA Ka-band scatterometer.

measurements provide the precise range information for computation of the normalized radar cross section which is used in turn to derive the *mss*. The radar/laser combination leads to high fidelity observations of the long-wave, short-wave hydrodynamic modulation transfer function.

3.5 Other Sensors

An independent suite of remote sensors was also flown by N3R during the CBLAST-Low pilot study. An SST imaging system was developed by Andrew T. Jessup of the University of Washington (UW) and Christopher J. Zappa of the Woods Hole Oceanographic Institution (WHOI). The UW/WHOI system incorporates a Raytheon Galileo IR imager, a Pulnix video camera, a Heitronics KT-15 radiometer, and GPS. The IR imager and video camera were mounted in the rear portion of the instrument pod. The KT-15 radiometer was mounted under the right wing of N3R. These data were acquired and stored on a separate computer and are not included with the N3R data acquisition system.

4 Data Acquisition System

The N3R data acquisition system consists of a modified personal computer (PC) powered by a Intel® Celeron® 600-MHz processor (Fig. 17), two remote (REM) analog-to-digital (A/D) modules, and flash card drive, flat-panel display, and a control switch box for the pilot. The PC and most associated electronics are mounted on the floor of the backseat of N3R. The data acquisition programs, written in C, run on top of the Microsoft DOS 6.22 operating system.



Fig. 17. N3R data acquisition PC, BAT auxiliary box, Ashtech dual-frequency GPS, and PCMCIA flash disk.

Analog sensor signals are digitized by the REM modules. This electronics package was developed by ARA to provide high-speed, high-resolution, multi-channel data logging. Each REM module consists of two 8-channel A/D boards with 16-bit resolution. The analog input voltage ranges from -5 to +5 volts, translating to a digital resolution of about 0.15 mV. The incoming analog signals are filtered using a 5-pole Butterworth anti-aliasing filter with a low-pass cutoff of 30 Hz. The signals are over-sampled by a factor of 32 before being averaged to 50 Hz for further noise reduction. The digital signals are transmitted to the PC for data storage via RS-422 serial lines. Two REM modules are currently used in the data acquisition system for a total of 32 A/D channels. One is contained in the tapered carbon fiber cone of the BAT probe to the rear of the pressure port dome. The second is inside the BAT auxiliary box located next to the data acquisition PC.

Calibration of the A/D channels for both REM modules was done prior to the CBLAST-Low pilot field study. Precise inputs of -4500, 0, and 4500 mV were inserted into each A/D channel. Simple linear calibration curves were computed for each input channel.

Most of the sensors described in the previous section provide analog signals that are digitized by the REMs. The exceptions include the Ashtech and TANS-vector GPS, and the Riegl lasers. These instruments transmit their respective digital data directly to the PC via RS-232 lines. The GPS data are ingested by the PC at 10 Hz while the Riegl lasers transmit their data at 150 Hz. All of the data are written to the PC hard disk once per second and are copied to a flash card at the end of each flight for post processing.

The Ashtech GPS provides the primary time reference for the data acquisition system. The clock utilized by the Ashtech receiver is synchronized with the time transmitted by the GPS satellites. The clock outputs a one pulse per second signal to the PC. The pulse is also used to synchronize flow of data transmitted to the PC from the REM modules and other digital sensors.

Three separate files are created for each flight. These files have the same 8-digit root name which is based on the PC clock when the data acquisition system is started (UTC). The convention is: month (2 digits), day (2 digits), hour (2 digits), and minute (2 digits). Each file has a unique 3-character suffix: ORG, BIN, and MKR.

The ORG file contains binary data from all of the *in situ* and remote sensors which are written in 1-s blocks. This file also contains information (i.e., a “header” listing) regarding device and channel assignments, measurement frequencies, engineering units, ranges, voltage scale factors and offsets, and calibration coefficients.

The BIN file contains binary satellite pseudo-range, carrier phase and Doppler data acquired by the Ashtech GPS during the flight.

The MKR file contains an ASCII listing of specific times and locations during the flight when the pilot toggles the “on”, “off”, or “event” switch on the control switch box. This file is used to mark the start and end of flux legs, profiles, or other specific maneuvers.

In addition to the three files collected by the N3R data acquisition system, two files are collected from a stationary ground-based Ashtech GPS. These data, when combined with GPS data acquired by N3R, are used to generate differentially corrected positions and velocities for the aircraft. A BIN file contains binary satellite pseudo-range, carrier phase and Doppler data acquired by the Ashtech GPS ground station while N3R was in flight. An EPH file contains the ephemeris information. The location of the ground station was 41° 22' 29.9" N, 70° 31' 38.3" W.

5 Post Flight Data Processing

Upon completion of each flight, files are transferred off the N3R data acquisition system to a ground-based PC for post-flight processing. These data are put through a series of post-flight processing programs with each performing a specific task. All programs are written in GNU C and are executed on a PC under a Linux operating system. The following is a brief outline of the processing steps. Raw GPS data from the aircraft and ground station are combined to produce a set of differentially-corrected GPS aircraft positions and velocities. Next, the *in situ* and remote sensor data are merged with the differentially corrected GPS data and converted into a network common data format (netCDF). Quality control programs are implemented on these data to remove spikes and outliers and to perform a series of other data quality checks. Finally, the calibrations are applied, low- and high-rate data are merged, winds are computed, and dynamic heating corrections are applied to the air temperature. During each step, time stamps are written in the output file header. These stamps describe when the data were processed and the version of the processing programs. This information is carried through to the final product. Additionally, the marker files are manually edited to reflect special notes regarding the flight and designate special legs for analysis purposes. Figure 18 contains a flow chart illustrating the steps for data post-processing. The rectangles in the figure represent specific data files while the ovals represent individual programs. Table 2 is a summary of the various acquired and processed data files.

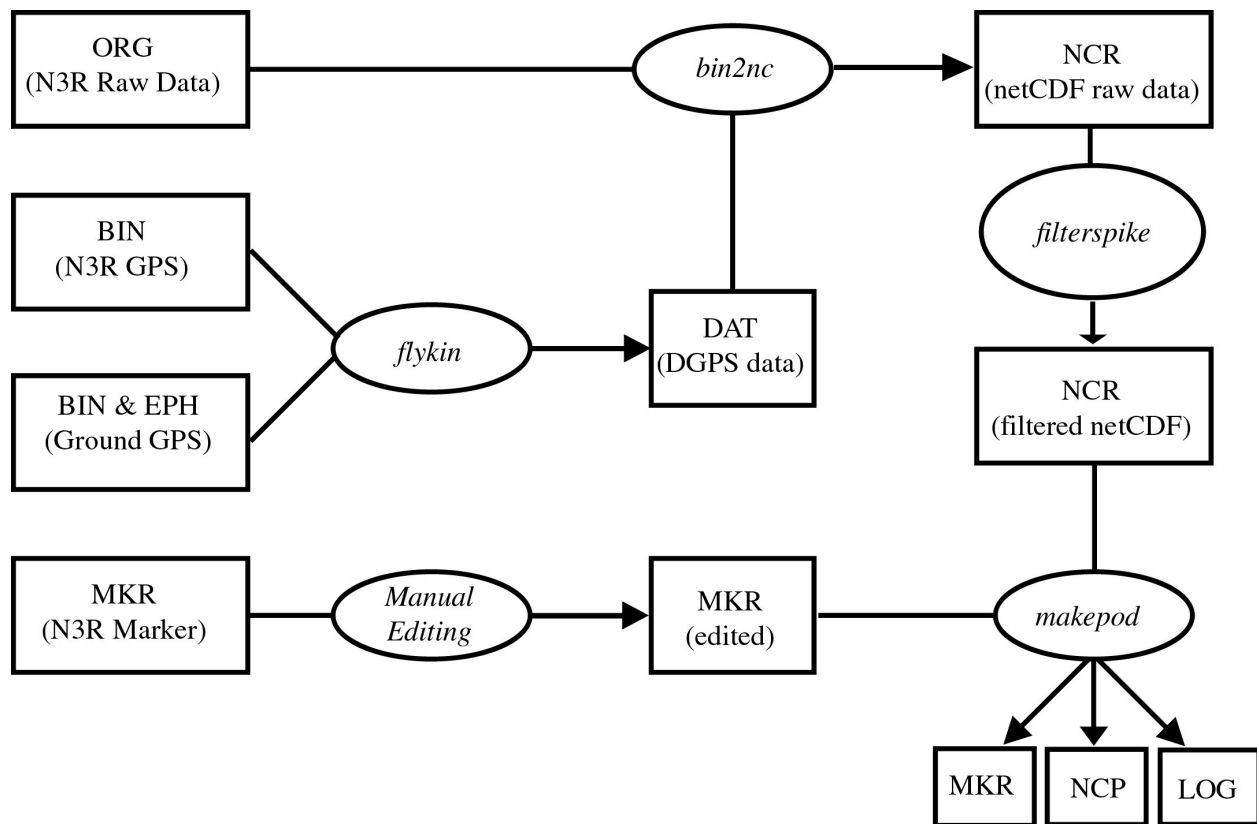


Fig. 18. Flowchart summarizing N3R data post-processing steps.

5.1 Differential GPS Corrections

The initial step in post-flight processing calculates positions and velocities using differential GPS techniques. Although the raw GPS data from N3R contains positions and velocities, accuracies are coarse (even after the elimination of selective availability) and are of little scientific use. The raw GPS data used in the corrections algorithm contain satellite navigation information and, for each epoch, signal phase, pseudo-range, and satellite number. Based on these data collected from two separate locations, one of which is precisely known (the ground-station), it is possible to calculate very accurate position and speed of the remote observing station (N3R). For this purpose, an algorithm (*flykin*) developed by the Department of Geomatics Engineering at the University of Calgary is used (Cannon et al. 1993). The algorithm, written in C, uses advanced filtering techniques and phase information to resolve ambiguities resulting from the determination of position based solely on pseudo-range. The source code for this software package was modified by ARL for our application on N3R. The algorithm creates an ASCII file of precise GPS information with the same root name and a DAT extension.

5.2 NetCDF Conversion

The next step in the data post-processing converts the files from their native format into netCDF (Rew et al. 1997). This program (*bin2nc*) executes a simple file conversion of the ORG data file. It also merges output from the differentially corrected GPS data, replacing the uncorrected GPS data stored in the original aircraft files. During the merging process, flags are set for missing GPS data. Also, because data are stored either as short- or long-word integers, a scale factor and offset must be computed. These values are assigned to variable attributes in the netCDF file. This binary file has the same root name with a NCR (netCDF “raw”) extension.

5.3 Quality Control

The next program applies quality control checks on the raw NCR data file and applies corrections as necessary. A despiking routine (*filterspike*) checks the data for regions where values fall outside of a prescribed range or are equal to some predefined “fill” value. In these regions, data are linearly interpolated based on the last and next “good” value. After completing the interpolation, flags are set for those regions where data were interpolated. Flags are set to mark these records.

5.4 Final Processing

The final step in the post processing algorithms is to carry through the actual computation of winds, apply recovery factors based on aircraft velocity, and to merge data from slow- and fast-response sensors. A program (*makepod*) calculates winds based on the raw pressure measurements from the BAT probe in combination with data from the GPS. High- and low-frequency measurements of position, velocity, temperature, and water vapor are blended by first performing Fourier transforms followed by passing the data through appropriate high- and low-pass filters, merging the sets, and finally calculating the inverse transform (Eckman et al. 1999). The final output file has the same root name and is given the extension NCP (netCDF “processed”). In

addition, a LOG file is created by *makepod*. This ASCII file contains calibration information and statistics (e.g., mean, standard deviation, skewness, kurtosis, minimum, maximum) for all variables.

Wind calculations use a method similar to the National Center for Atmospheric Research (NCAR) method described by Leise and Masters (1991). Modifications to the NCAR method result from the unique configuration of the BAT probe in that a reference pressure (not a true static pressure) is provided by the pneumatic average of the four reference pressure ports. Consequently, the dynamic pressure must be corrected not only for variations in attack angle and sideslip, but also for deviations of reference pressure from the static pressure. The computation of accurate wind measurements requires the empirical determination of several BAT probe calibration constants. Of particular interest are the angle offsets, roll, pitch, heading, angle of attack offset, and dynamic pressure adjustment (Table 3). The values of these constants are determined by minimizing the variance of the three individual wind components for various flight legs. These legs include straight and level flight, dynamic and steady-state pitch and yaw maneuvers, reverse-heading maneuvers, and wind circles and boxes. Theoretically determined constants, based on theory of potential flow over a sphere are also included in the wind calculations. These include attack and sideslip calibration constants and the aircraft upwash factor.

Table 2. Summary of data files.

File	Description	Format	Output from:
mmddhhmn.ORG	raw aircraft data	binary	N3R data acquisition system
mmddhhmn.BIN	Ashtech GPS data	binary	N3R data acquisition system
mmddhhmn.MKR	marker data	ASCII	N3R data acquisition system
ammdd-0x.BIN	Ashtech GPS data	binary	ground station
ammdd-0x.EPH	Ashtech GPS data	binary	ground station
mmddhhmn.DAT	DGPS data	ASCII	<i>flykin</i>
mmddhhmn.NCR	netCDF raw data	binary	<i>bin2nc, filterspike</i>
mmddhhmn.NCP	netCDF processed data	binary	<i>makepod</i>
mmddhhmn.LOG	calibrations, data statistics	ASCII	<i>makepod</i>

mm month

dd day

hh hour

mn minute

a “Ashtech ground station”

x = 1, 2, 3, etc. (if multiple flights are conducted during the same day)

Table 3. Calibration constants and switches used in *makepod*.

Constant	Value	Description
LicorSw	0	switch for LICOR 6262 (0 = off, 1 = on)
LaserSW	1	switch for laser altimeters (0 = off, 1 = on)
RadarSw	1	switch for Ka-band radar scatterometer (0 = off, 1 = on)
EG&GSw	1	switch for EG&G dew point sensor (0 = off, 1 = on)
FlightQ	9	minimum Px for which winds are computed
Pad	50	maximum elements to pad arrays for FFT edge effect reduction
R _T	0.82	temperature recovery factor
" ₀	-0.0663225	angle of attack of DSP at zero lift
K _·	0.24	pitch calibration constant
K _§	0.19	yaw calibration constant
K _{up}	0.101	upwash factor
' _q	1.0175	dynamic pressure correction
' _p	-1.43	pitch offset for relative velocity
' _r	0.0	roll offset for relative velocity
' _h	-0.5	heading offset for relative velocity
A _{pass}	0.75	highest frequency passed by low-pass filter (attitude) highest frequency stopped by high-pass filter (attitude)
A _{stop}	1.333	lowest frequency stopped by low-pass filter (attitude) lowest frequency passed by high-pass filter (attitude)
V _{pass}	0.25	highest frequency passed by low-pass filter (velocity) highest frequency stopped by high-pass filter (velocity)
V _{stop}	0.444	lowest frequency stopped by low-pass filter (velocity) lowest frequency passed by high-pass filter (velocity)
H _{pass}	0.0075	highest frequency passed by low-pass filter (hor. position) highest frequency stopped by high-pass filter (hor. position)
H _{stop}	0.01333	lowest frequency stopped by low-pass filter (hor. position) lowest frequency passed by high-pass filter (hor. position)
W _{pass}	0.0375	highest frequency passed by low-pass filter (vert. position) highest frequency stopped by high-pass filter (vert. position)
W _{stop}	0.0666	lowest frequency stopped by low-pass filter (vert. position) lowest frequency passed by high-pass filter (vert. position)

6 Data

6.1 NCR Files

The NCR file includes only non-calculated quantities (e.g., static pressure, uncorrected temperature, unblended positions and velocities from GPS and accelerometers, etc.). The structure of the NCR files is based on the netCDF file structure (Rew et al. 1997). Further information on these netCDF libraries can be found at www.unidata.ucar.edu/packages/netcdf. Users familiar with the netCDF file type will be able to read these files with tools available for accessing standard netCDF libraries.

The header of the file contains information relating to the data variables, their dimensions, attributes for each variable, and attributes for the entire file. All of the data are stored either as short-word (4-byte) or long-word (8-byte) integers. All variables either contain one or two dimensions. The primary dimension for the NCR variables is *scan* which is equal to the number of seconds contained in the file. Higher rate variables (greater than 1 Hz) have a second dimension. For the present data set, channels were sampled at either 5, 10, 50 Hz, or 150 Hz, depending on the variable. Thus, 5-, 10-, 50- or 150-Hz data have a second dimension of *5HzData*, *10HzData*, *50HzData*, or *150HzData*, respectively.

Table 4 lists all of the variables in the NCR files along with a short description of each. Most of these variables are native N3R data. Three additional variables include information related to good/bad data flags. Native N3R variables have eight attributes. The *scale_factor* and *add_offset* attribute are used to convert the data into floating point numbers in the proper engineering units (as defined by the attribute *units*). The attributes *valid_min* and *valid_max* define the range in which values must fall between for them to be valid. The *fill_value* attribute has value either -1, 0, or 1. For *fill_value* = -1, non-valid data will have values equal to the *valid_min*. For *fill_value* = 1, non-valid data will have values equal to the *valid_max*. For *fill_value* = 0, non-valid data will have values equal to 0. The *long_name* attribute simply furnishes a longer, more detailed name for the variable. Finally, the attribute *cal_coef* is a six- element vector containing 5-degree polynomial coefficients used to convert data from raw voltages into engineering units. This information is already contained within the *scale_factor* and *add_offset*, but is required to change the calibration at a later time, if necessary.

Global attributes (file-wide) include the title and date of the file. The *title* attribute contains the name of the aircraft and the associated experiment or project. The *date* attribute describes the day the file was acquired. All other global attributes are used to describe the names of the processing programs executed on the data. For each program there exists two attributes, one that describes the control version of that program and another describing the date it was executed. For example, each NCR file should have an attribute *filterspike* that is equal to a character string describing the control version of *filterspike* that was run (*i.e.*, *filterspike.c*, v1.2). Each should also have an attribute *filterspike_date* describing the date and time *filterspike* was executed. This attribute is also stored as a character string. Note that quality flag variables PVflag and Angflag are determined in *bin2nc* while the variable Ambiguities is output from *flykin*.

Table 4. Summary of NCR file variables.

Variable	Units	Freq	S/A	Description
GPSTime	s	1	S	Ashtech Time
TTime	s	10	S	TANS-vector Time
NLat	deg	5	S	Ashtech Latitude
NLon	deg	5	S	Ashtech Longitude
NAlt	m	5	S	Ashtech Altitude
Nu	m s ⁻¹	5	S	Ashtech Velocity (east)
Nv	m s ⁻¹	5	S	Ashtech Velocity (north)
Nw	m s ⁻¹	5	S	Ashtech Velocity (vertical)
TPitch	deg	10	S	TANS-vector Pitch
TRoll	deg	10	S	TANS-vector Roll
THdg	deg	10	S	TANS-vector Heading
Px	mb	50	A	Differential Pressure (x-axis)
Py	mb	50	A	Differential Pressure (y-axis)
Pz	mb	50	A	Differential Pressure (z-axis)
Ps	mb	50	A	Static (reference) Pressure
Ax	m s ⁻²	50	A	BAT Probe Acceleration (x-axis)
Ay	m s ⁻²	50	A	BAT Probe Acceleration (y-axis)
Az	m s ⁻²	50	A	BAT Probe Acceleration (z-axis)
Axb	m s ⁻²	50	A	Backseat Acceleration (x-axis)
Ayb	m s ⁻²	50	A	Backseat Acceleration (y-axis)
Azb	m s ⁻²	50	A	Backseat Acceleration (z-axis)
Arol	s ⁻²	50	A	Differential (Roll) Acceleration (normalized)
Tp1	°C	50	A	Fast-Response Microbead Temperature
Fust_mv	: V	50	A	Fast-Response FUST Probe Thermocouple
TBar	°C	1	A	Slow-Response Thermistor Temperature
H2O	g m ⁻³	50	A	IRGA Absolute Humidity
CO2	mg m ⁻³	50	A	IRGA Carbon Dioxide
Tdew	°C	1	A	Chilled Mirror Dew Point Temperature
SfcT	°C	50	A	Sea Surface Temperature
SkyT	°C	1	A	Sky Temperature
Qs_up	W m ⁻²	1	A	Downwelling (Upward Looking) Visible Radiation
Qs_dn	W m ⁻²	1	A	Upwelling (Downward Looking) Visible Radiation
BodyT	°C	1	A	Everest 4000.4GXL (SST) Body Temperature
L1Dist	m	150	S	Distance (left wing)
L2Dist	m	150	S	Distance (instrument pod)
L3Dist	m	150	S	Distance (right wing)
L4Dist	m	150	S	Distance (15° “glint” laser)
L1Retn	counts	150	S	Number of Valid Returns (left wing)
L2Retn	counts	150	S	Number of Valid Returns (instrument pod)
L3Retn	counts	150	S	Number of Valid Returns (right wing)
L4Retn	counts	150	S	Number of Valid Returns (15° “glint” laser)
Ka_Ctl	mV	50	A	Ka-band Scatterometer Control
Ka_Rcv1	mV	50	A	Ka-band Scatterometer Receive Channel 1
Ka_Rcv2	mV	50	A	Ka-band Scatterometer Receive Channel 2
PVflag		5		Position / Velocity Flag
Angflag		10		Angles Flag
Ambiguities		5		Number of Ambiguities for Differential Correction

6.2 NCP Files

The NCP file contains derived quantities such as the wind velocity, corrected air temperature, and dry air density. Like the NCR file, the structure of the NCP is based on netCDF. All of the variables contained within the NCP file are either 1 Hz (dimension *scan*), 50 Hz (dimensions *scan* and *50HzScan*), or 150 Hz (dimensions *scan* and *150HzScan*). Table 5 lists the variables in the NCP files with a short description of each. Also contained in the table are variable dependencies for derived quantities. For example, NAlt (altitude) in the NCP file depends not only on NAlt in the NCR file, but also on the three BAT probe accelerations (A_x , A_y , and A_z) used to augment the 10-Hz GPS data. Note also that NAlt in the NCP file therefore differs from NAlt in the NCR file.

Data in the NCP file are stored as 4-byte or 8-byte integers. Again, the variable attributes *scale_factor* and *add_offset* are used to convert to floating-point values with the proper engineering units given by the attribute *units*. The final variable attribute is *long_name*.

The variable *Dataflag* uses bit settings to flag bad data. The variable attribute *bit_settings* is a vector string describing the bit settings for this variable. A set bit indicates bad data. The first four bits are reserved for flagging bad winds. Bit one indicates the determination of bad data was made in makepod (the values lie outside some predetermined valid minimum or maximum). Bit 2 indicates bad GPS data (most likely due to missing data). Bit 3 indicates bad TANS-vector data (GPS attitude). Bit 4 indicates no differential corrections for the GPS. This is separate from the bit 2 case because it may result from a lack of ground station data or simply too few satellites to provide useful differential corrections. Bit settings are easily checked using the standard C operators AND, OR, AND/OR (or their non-C equivalent).

6.3 MKR Files

The MKR file contains an ASCII listing of specific times and locations during the flight when the pilot toggles the “on/off” switch or presses the “event” button on the control switch box. This file is used to mark the start and end of flux legs, profiles, or other specific maneuvers. When the marker switch is turned “on”, a three-character string of XXX, a value of “-1”, the scan number (i.e., number of elapsed seconds since the start of data acquisition), and current latitude and longitude are written to the MKR file. Similarly, a value of “0” is written with the time and location information when the marker switch is turned off. The event switch is used to mark a specific event during flight (e.g., flying over a buoy, crossing the coastline). An event is recorded in the MKR file with a three-character string of EVT along with the scan number, latitude and longitude. The MKR file is manually edited at the end of the flight. The default character string of XXX is usually replaced with three-character identifiers that are used to describe marker pair. For example, FLX is used to denote flux leg while PRO is used to indicate a profile. Other manually edited notes include a summary of the weather conditions, flight plan, problems encountered, and other remarks that may be helpful during data analysis. Appendix A contains the listings of the marker files from all flights during the CBLAST-Low pilot field study. In addition, a key is provided which identifies each three-character identifier.

Table 5. Summary of NCP file variables.

Variable	Units	Freq	Description	Dependencies
GPSTime	s	1	GPS Time	GPSTime
NLat	deg	50	Latitude	NLat, Ax, Ay, Az
NLon	deg	50	Longitude	NLon, Ax, Ay, Az
NAlt	m	50	Altitude	NAlt, Ax, Ay, Az
GndSpd	m s ⁻¹	1	Ground Speed	Nu, Nv
AirSpd	m s ⁻¹	1	Air Speed	Px, Py, Pz, Ps, Tp1, TBar, H2O, Tdew
TPitch	deg	50	Pitch	TPitch, Ax, Ay, Az, Ayb, Azb, Arol
TRoll	deg	50	Roll	TRoll, Ax, Ay, Az, Ayb, Azb, Arol
THdg	deg	50	Heading	THdg, Ax, Ay, Az, Ayb, Azb, Arol
Axb	m s ⁻²	50	Acceleration (a-axis)	Axb
Ayb	m s ⁻²	50	Acceleration (y-axis)	Ayb
Azb	m s ⁻²	50	Acceleration (z-axis)	Azb
U	m s ⁻¹	50	East Wind Speed	Px, Py, Pz, Ps, Ax, Ay, Az, Ayb, Azb, Arol,
V	m s ⁻¹	50	North Wind Speed	Nu, Nv, Nw, TPitch, TRoll, THdg, TBar, H2O,
W	m s ⁻¹	50	Vertical Wind Speed	Tdew (all three vectors)
Tp1	°C	50	Air Temperature	Px, Py, Pz, Ps, Tp1, TBar
Fust_mv	: V	50	Air Temperature	to be determined
H2O	g m ⁻³	50	Absolute Humidity	H2O, Tdew
CO2	mg m ⁻³	50	Carbon Dioxide	CO2
Tdew	°C	1	Dew Point	Tdew
Ps	mb	50	Static Pressure	Ps, Px, Py, Pz, Tp1, TBar, H2O, Tdew
RhoD	kg m ⁻³	50	Dry Air Density	Ps, Tp1, TBar, H2O, Tdew
SfcT	K	50	Sea Surface Temperature	SfcT
SkyT	K	1	Sky Temperature	SkyT
Qs_up	W m ⁻²	1	Downwelling Visible Radiation	Qs_up
Qs_dn	W m ⁻²	1	Upwelling Visible Radiation	Qs_dn
L1Dist	m	150	Distance (left wing)	L1Dist
L2Dist	m	150	Distance (pod)	L2Dist
L3Dist	m	150	Distance (right wing)	L3Dist
L4Dist	m	150	Distance (glint laser)	L4Dist
L1Retn	counts	150	No. Valid Returns (left wing)	L1Retn
L2Retn	counts	150	No. Valid Returns (pod)	L2Retn
L3Retn	counts	150	No. Valid Returns (right wing)	L3Retn
L4Retn	counts	150	No. Valid Returns (glint laser)	L4Retn
Ka_Ctl	counts	50	Scatterometer Control	Ka_Ctl
Ka_Rcv1	counts	50	Scatterometer Receive Ch. 1	Ka_Rcv1
Ka_Rcv2	counts	50	Scatterometer Receive Ch. 2	Ka_Rcv2
Dataflag		50	Quality Data Flag	

Note: Dependencies are those variables from NCR files that are used in the calculation of *variable*, for specific bit settings, see variable attribute *bit_settings* in NCP files.

6.4 LOG Files

The LOG file contains a listing of input parameters passed through *makepod*. Contained are switches indicating what instruments were on the aircraft and hence what variables exist in the files. Also included are calibration factors for wind calculations. Filter pass and stop bands are recorded in the LOG files. These describe the frequency bands for the high- and low-pass filters used to blend variables (e.g., TANS-vector GPS data and accelerometers). Valid minima and maxima are also defined. Statistics for the raw and processed variables are determined, including minimum, maximum, and moments.

6.5 Known Problems

There were occasional problems with instrument failures during the CBLAST-Low pilot field study. These problems, generally minor, were quickly identified and corrected. The following is a brief synopsis of those problems.

The roll accelerometer in right wing was not functioning properly for the first three flights. This sensor was probably damaged during a microburst event when N3R was parked at small regional airport in Illinois during its transit from Idaho Falls to Martha's Vineyard. The sensor was replaced prior to Flight 4 and functioned properly for the remainder of the experiment. Data from the roll accelerometers is used to augment the 10-Hz TANS-vector GPS roll data to a rate of 50 Hz. The roll accelerometer data is one of many variables used in the calculation of the wind. Its contribution is useful, but not vital.

Data from the 15° glint laser was invalid during the first two flights because of partial blockage of the optical lens due to a fiberglass cover. As a result, the laser reports a "missing" distance with no return pulses. The hole in this cover was enlarged prior to Flight 3. The glint laser worked properly for this flight, however, a few drop outs remained. The opening in the fiberglass cover was enlarged a second time prior to Flight 4. All glint laser data for the remainder of the field study were valid.

Dew point temperature data acquired by the chilled mirror sensor is questionable during Flight 2. Misalignment of the port-hole openings which lead into the mirror chamber are suspected to cause an over aspiration of the sensor which leads to extreme values reported by the instrument. The port-hole alignment problem was corrected prior to Flight 3. Near the end of Flight 4, the dew point temperature data are questionable. In this case where the MABL was very humid and was marked with patches of visible fog, the sensor may have experienced difficulties in "burning off" moisture residing on the mirror (over saturation).

The TANS-vector GPS usually converges on a proper solution of aircraft pitch, roll, and heading within the first several minutes of operation when the unit is turned on. On occasion, this instrument fails to provide a valid solution. This was encountered during Flight 8 where the TANS-vector GPS did not output valid aircraft attitude data. The flight was prematurely terminated and the TANS-vector GPS was manually reinitialized. Approximately 15 min of TANS-vector GPS data

were lost during in the middle of Flight 15. The lack of available satellites may be a possible reason why this instrument failed to provide valid solutions for a short time.

There are several instances where DGPS corrections were not made. The first twenty three minutes of data acquired in Flight 9 could not be differentially corrected because of a brief power outage which shut down the ground station computer. DGPS corrections failed about 15 minutes before the end of Flight 18. DGPS corrections were not available for the first twenty one minutes of Flight 19 because the GPS ground station was started late.

Data from both Everest IR radiometers and the chilled mirror sensor were subject to interference from N3R radio transmissions. As a result, data from these sensors (SfcT, SkyT, Tdew) have occasional spikes which may last up to several seconds. Radio transmissions were avoided during flux legs and other specific maneuvers in order to minimize the spikes in these variables. No attempt was made to remove the spikes.

7 Flight Summaries

The CBLAST-Low pilot study was conducted during a three-week period in July and August 2001 off the south shore of Martha's Vineyard Island, Massachusetts. A total of twenty missions (~ 48 flight hours) were flown by N3R on days with light winds ($< 7 \text{ m s}^{-1}$) under various atmospheric stabilities. Numerous flux legs and MABL profiles were acquired during the course of the study. When possible, N3R flew over other CBLAST-Low "assets", including the R/V *Asterias*, the Air-Sea Interaction Meteorology (ASIMET) buoy ($40^{\circ} 59.5' \text{ N}$, $70^{\circ} 35.9' \text{ W}$), and a three-dimensional SST array ($41^{\circ} 15.0' \text{ N}$, $70^{\circ} 36.0' \text{ W}$).

All N3R flights were based out of the Martha's Vineyard Airport (MVY). Table 6 is a summary listing of flights during the CBLAST-Low pilot study. Included is the flight number, date, filename, start and end times for each file (UTC), number of scans (seconds) for each file, approximate flight hours, and miscellaneous comments. Flight hours were determined by a Hobbs meter, which keeps track of time from when the aircraft engine is started until it is shutdown. Appendix B contains figures of N3R flight tracks. The following is a brief summary of each flight.

7.1 Flight 1 (21 JUL 01)

The region was dominated by high pressure, clear skies, and relatively dry (low humidity) conditions. Winds were initially calm in the early morning hours becoming southwesterly at about 4 m s^{-1} by late morning to early afternoon. The first CBLAST-Low flight (Fig. 19) included roll and pitch radar calibration maneuvers, twelve low-level (~ 10 m) north-south flux legs, and two MABL profiles.

7.2 Flight 2 (22 JUL 01)

The coastal waters of southern New England were dominated by high pressure, clear skies but with a slight increase in humidity. Winds were initially calm around sunrise and became southwesterly at 2 to 3 m s^{-1} by mid-morning. A simple north-south, east-west box pattern (Fig. 20) was flown at about ~ 10 m in the early morning flight to acquire mean wind and turbulent flux data to validate satellite-based synthetic aperture radar (SAR) derived winds. The SAR overpass for waters south of Martha's Vineyard and Nantucket occurred at 1049 UTC. Two MABL profiles were also included in the flight.

7.3 Flight 3 (23 JUL 01)

Thick early morning fog eventually cleared by late morning with southwesterly winds of about 4 to 5 m s^{-1} with gusts up to 8 to 9 m s^{-1} . The early afternoon flight (Fig. 21) included six north-south flux legs over the ASIMET buoy, multiple short altitude profiles (~ 150 m), and roll and pitch radar calibration maneuvers.

Table 6. Summary of N3R flights.

FL	Date	File Name	Start/End Time (UTC)		Scans	FL Hr	Flight Pattern
1	21 JUL 01	07211228	12:58:29	16:29:01	12633	3.4	north-south flux legs, radar calibration maneuvers
2	22 JUL 01	07220953	10:04:45	11:27:42	4978	1.4	SAR intercomparison
3	23 JUL 01	07231646	16:50:15	19:13:14	8580	2.4	north-south flux legs, radar calibration maneuvers
4	25 JUL 01	07251641	16:54:11	18:52:47	7117	2.0	north-south flux legs, IR camera runs
5	27 JUL 01	07271211	12:31:32	16:32:30	14459	4.0	north-south flux legs, IR camera runs
6	27 JUL 01	07272229	22:37:34	23:14:04	2191	0.7	“mowing the lawn” IR camera runs
7	28 JUL 01	07281042	11:02:21	13:59:25	10625	3.0	multi-directional flux legs, IR camera runs
8	29 JUL 01	07290928	09:31:22	10:18:13	2806	1.5	sunrise IR camera runs
9	29 JUL 01	07291112	11:43:54	13:46:36	7363	2.0	“spirograph” flux legs
10	30 JUL 01	07301120	11:43:48	15:10:56	12429	3.5	east-west “bow tie” flux legs, IR camera runs, wind calibration maneuvers
11	31 JUL 01	07310909	09:29:00	11:52:59	8640	2.4	north-south “bow tie” flux legs, sunrise “mowing the lawn” IR camera runs
12	01 AUG 01	08010911	09:40:09	12:54:59	11691	3.3	SAR intercomparison, IR camera runs, “spirograph” flux legs
13	01 AUG 01	08011644	16:54:29	19:40:33	9965	2.8	“bow tie” flux legs over R/V <i>Asterias</i> , “spirograph” flux legs
14	02 AUG 01	08021423	14:47:23	17:12:35	8713	2.4	“spirograph” flux legs, IR camera runs
15	03 AUG 01	08030052	00:58:21	02:22:29	5049	1.9	nighttime “mowing the lawn” IR camera runs
16	05 AUG 01	08051541	15:51:03	16:30:35	2373	0.7	flight terminated due to heavy fog and poor visibility
17	05 AUG 01	08052006	20:11:12	20:55:25	2654	0.8	flight terminated due to heavy fog and poor visibility
18	07 AUG 01	08071320	13:29:19	17:32:00	14558	4.1	“spirograph” and “bow tie” flux legs
19	08 AUG 01	08080955	10:03:04	14:01:50	14327	4.0	SAR intercomparison, “spirograph” flux legs
20	08 AUG 01	08081526	15:37:21	17:06:38	5358	1.5	“bow tie” flux legs over R/V <i>Asterias</i>

7.4 Flight 4 (25 JUL 01)

Moderate southwesterly winds of 5 to 6 m s⁻¹ were present during much of the day with shallow “puffs” of low-level fog moving over the island in the early afternoon. Four north-south flux legs were flown (Fig. 22) from near the coast over the 3D SST array and past the ASIMET buoy. The UW/WHOI camera system was installed on the day before this flight. Several transects were flown at about 400 m for the UW/WHOI camera system. Visibility at this level was poor because of the fog banks under N3R. Because of the poor visibility, visual navigation and reference to surface ships and buoys was difficult.

7.5 Flight 5 (27 JUL 01)

A cold front had moved through the region on the previous evening. A northeasterly wind of 4 to 6 m s⁻¹ created a dry, well-mixed MABL. This flight (Fig. 23) included numerous north-south flux legs extending from near the Martha’s Vineyard Coastal Observatory (MVCO) meteorological tower to the ASIMET buoy. Three MABL profiles and high altitude (~ 400 m) UW/WHOI camera runs were also included.

7.6 Flight 6 (27 JUL 01)

The wind speed decreased by late afternoon and early evening to less than 3 m s⁻¹ for the second flight of the day. For this mission, a “mowing the lawn” or “radiator” pattern was flown by N3R (Fig. 24) at 400 m to map out SST variability by the UW/WHOI camera system. The N3R data acquisition system was manually shut down prior to landing since power was needed for aircraft landing lights.

7.7 Flight 7 (28 JUL 01)

The region continued to enjoy fair weather dominated by high pressure system with light northwesterly winds of 3 m s⁻¹ in early morning. By late morning the wind direction became northeasterly and remained fairly light (~ 3 m s⁻¹). Numerous low-level flux legs were flown by N3R (Fig. 25) over the ASIMET buoy with shallow profiles at the ends of each flux leg. Three MABL profiles were also included in the flight. High level camera runs flown for the UW/WHOI camera system at the beginning of the mission.

7.8 Flight 8 (29 JUL 01)

High pressure continued to dominate the weather with a few mid- and high-level clouds moving into the region. Winds were calm to very light and variable (< 2 m s⁻¹) for this early morning flight which started prior to sunrise. A simple north-south, east-west box pattern was flown (Fig. 26) at 400 m for the UW/WHOI camera system. The box was to be repeated at low levels for a SAR intercomparison, however, the flight was terminated because the TANS-vector GPS was not outputting valid pitch, roll, and heading solutions. It should be noted that the data file begins after take off in an attempt to reinitialize the TANS-vector GPS.

7.9 Flight 9 (29 JUL 01)

Once the TANS-vector GPS was properly reinitialized about an hour after the end of Flight 8, N3R conducted a flux mission utilizing a “spirograph” pattern centered over the ASIMET buoy with multiple short profiles (~ 150 m) at the end of each flux leg (Fig. 27). This pattern has the advantage of quickly mapping the spatial variability of the atmosphere and ocean in about an hour. A MABL profile was also included during this flight. The first twenty three minutes of the data file were not differentially corrected due to a brief power outage which shut down the ground station computer.

7.10 Flight 10 (30 JUL 01)

Fair weather continued to dominate the coastal waters with high clouds to the south from a low pressure system in the mid-Atlantic region. Light winds of about 2 to 3 m s⁻¹ from the northeast were present in the early morning, increasing to about 5 to 6 m s⁻¹ and from the east by late morning. Wind calibration maneuvers were included in this flight, along with three MABL profiles, a box pattern at 400 m for the UW/WHOI camera system, east-west “bow tie” flux legs and shallow profiles over ASIMET buoy, and multiple flux legs and short profiles over the R/V *Asterias*. which surveyed the waters several kilometers off the coast of Martha’s Vineyard (Fig. 28).

7.11 Flight 11 (31 JUL 01)

Fair weather continued to persist with a few high clouds from a low pressure system to the south which was quickly moving to the northeast. Light winds of 2 to 3 m s⁻¹ were from the north. The flight included another “mowing the lawn” pattern prior to and shortly after sunrise for the UW/WHOI camera system, two MABL profiles, and seven northeast-southwest flux legs over the ASIMET buoy (Fig. 29).

7.12 Flight 12 (01 AUG 01)

High pressure continued to dominate the region with very light winds of 2 to 3 m s⁻¹ from the northwest to northeast. N3R flew a simple north-south, east-west box prior to sunrise for the UW/WHOI camera system prior and repeated the same exact flight track at 10 m during a SAR overpass which occurred at 1057 UTC (Fig. 30). A “spirograph” flux pattern was flown over the ASIMET buoy with multiple shallow profiles at the end of each flux leg. Three MABL profiles were also included in this flight.

7.13 Flight 13 (01 AUG 01)

Flight 13 was the second flight of the day. Winds continued to be light and variable under fair weather. Numerous east-west “bow tie” flux legs were flown in the vicinity of the R/V *Asterias* several kilometers off the coast of Martha’s Vineyard (Fig. 31). Another “spirograph” flux pattern was flown again over the ASIMET buoy. Two MABL profiles were included in this flight.

7.14 Flight 14 (02 AUG 01)

Very hazy, hot, and humid conditions were present as a high pressure system slowly moved eastward. Winds were about 4 to 5 m s⁻¹ from the southwest. The late morning flight included a simple north-south, east-west box pattern for the UW/WHOI camera system and a “spirograph” flux pattern over the ASIMET buoy with multiple shallow profiles at the end of each flux leg (Fig. 32). Two MABL profiles were included in this flight.

7.15 Flight 15 (03 AUG 01)

The weather continued to be hazy and humid with steady southwesterly winds of 5 to 6 m s⁻¹ as a high pressure system slowly moved eastward. A “mowing the lawn” pattern was flown at 400 m during this nighttime flight for the UW/WHOI camera system (Fig. 33). The N3R data acquisition system was booted up after takeoff and shut down prior to landing since power was needed for external and internal aircraft lights. Approximately 15 min of TANS-vector GPS data were lost about 40 min into the flight. The lack of available satellites may be a possible reason why this instrument failed to provide valid solutions. The UW/WHOI camera system was removed after the end of this flight.

7.16 Flight 16 (05 AUG 01)

Hazy, hot, and humid conditions prevailed with light southwesterly winds of 2 to 3 m s⁻¹ ahead of a stalled cold front. This flight was terminated shortly after take off because of heavy offshore fog and very poor visibility (Fig. 34).

7.17 Flight 17 (05 AUG 01)

A second N3R mission was attempted later on the same day. The weather continued to be hazy, hot, and humid with light southwesterly of 4 to 5 m s⁻¹. Once again, the flight was terminated shortly after take off because of heavy offshore fog and very poor visibility (Fig. 35). Note that the N3R data acquisition was shut down prior to landing.

7.18 Flight 18 (07 AUG 01)

The weather continued to be hazy, hot, and humid, moderate southwesterly winds of 4 to 6 m s⁻¹ ahead of a stalled cold front. Flight visibility was only about 1 km. Two sets of “spirograph” and “bow tie” flux patterns were flown near the coastline and over the ASIMET buoy (Fig. 36). A single MABL profile was included in this flight. DGPS corrections failed about 15 minutes before the end of the flight.

7.19 Flight 19 (08 AUG 01)

Hazy, very hot, and humid conditions persisted with light and variable winds ahead of a stalled cold front. N3R flew a simple north-south, east-west box during a SAR overpass which

occurred at 1053 UTC (Fig. 37). Two “spirograph” flux patterns were flown near the coastline and over the ASIMET buoy with multiple shallow profiles at the end of each flux leg. Three MABL profiles and various calibration maneuvers were also included in this flight. Note that DGPS corrections were not available for the first twenty one minutes of the flight because the GPS ground station was started late.

7.20 Flight 20 (08 AUG 01)

N3R flew a second time in the early afternoon on the same day. The weather continued to be hazy, very hot, and humid with light and variable winds. This flight was dedicated to numerous low-level north-south flux legs from the coastline over the R/V *Asterias* (Fig. 38). A single MABL profile was included at the end of the flight.

Acknowledgments

This work was supported under a contract from the Office of Naval Research (N00014-01-F-0008). The authors wish to thank our colleagues Sean Burns, Ron Dobosy, Ed Dumas, Rick Eckman, Larry Mahrt, Jielun Sun, Doug Vandemark, and Dean Vickers for their support towards the continued improvement of aircraft-based measurements. We also wish to acknowledge Andy Jessup, Mike Welch, and Chris Zappa for their cooperative effort on making high fidelity SST measurements. Special thanks are extended to ARL engineers Dave Auble, Shane Beard, Eric Egan, and Randy Johnson for their technical assistance on the various sensors and electronics flown by N3R. Finally, the authors would like to thank Ron Dobosy, Jeff West, and Tami Grimmatt for providing a critical review of this document.

References

- Auble, D. L., and T. P. Meyers, 1992: An open path, fast response infrared absorption gas analyzer for H₂O and CO₂. *Bound.-Layer Meteor.*, **59**, 243-256.
- Cannon, M. E., G. LaChapelle, and G. Lu, 1993: Kinematic ambiguity resolution with a high precision C/A code receiver. *J. Surveying Engin.*, **119**, 147-155.
- Crawford, T. L., and R. J. Dobosy, 1992: A sensitive fast-response probe to measure turbulence and heat flux from any airplane. *Bound.-Layer Meteor.*, **59**, 257-278.
- Crawford, T. L., R. T. McMillen, T. P. Meyers, and B. B. Hicks, 1993: Spatial and temporal variability of heat, water vapor, carbon dioxide, and momentum air-sea exchange in a coastal environment. *J. Geophys. Res.*, **98**, 12869-12880.
- Crawford, T. L., R. J. Dobosy, and E. Dumas, 1996: Aircraft wind measurement considering lift-induced upwash. *Boundary-Layer Meteorology*, **80**, 79-94.
- Crescenti, G. H., T. L. Crawford, and E. J. Dumas, 1999: Data report: LongEZ (N3R) participation in the 1999 Shoaling Waves Experiment (SHOWEX) spring pilot study. NOAA Technical Memorandum, ERL ARL-232, Silver Spring, MD, 86 pp.
- Drennan, W. M., K. K. Kahma, and M. A. Donelan, 1999: On momentum flux and velocity spectra over waves. *Bound.-Layer Meteor.*, **92**, 489-515.
- Eckman, R. M., T. L. Crawford, E. J. Dumas, K. R. Birdwell, 1999: Airborne meteorological measurements collected during the Model Validation Program (MVP) field experiments at Cape Canaveral, Florida. NOAA Technical Memorandum OAR ATDD-233, Silver Spring, MD, 54 pp.
- French, J. R., G. H. Crescenti, T. L. Crawford, and E. J. Dumas, 2000: LongEZ (N3R) participation in the 1999 Shoaling Waves Experiment (SHOWEX). NOAA Data Report OAR ARL-20, Silver Spring, MD, 51 pp.
- French, J. R., T. L. Crawford, R. C. Johnson, and O. C. Coté, 2001: A high-resolution temperature probe for airborne measurements. Preprint, *Eleventh Symposium on Meteorological Observations and Instrumentation*, Albuquerque, NM, Amer. Meteor. Soc., 139-144.
- Greischar, L. and R. Stull, 1999: Convective transport theory for surface fluxes tested over the western Pacific warm pool. *J. Atmos. Sci.*, **56**, 2201-2211.
- Hacker, J. M., and T. L. Crawford, 1999: The BAT-probe: the ultimate tool to measure turbulence from any kind of aircraft (or sailplane). *Technical Soaring*, **XXIII(2)**, 43-46.

- Lambert, D., and P. Durand, 1999: The marine atmospheric boundary layer during SEMAPHORE. Part I: Mean vertical structure and non-axisymmetry of turbulence. *Quart. J. Roy. Meteor. Soc.*, **125**, 495-512.
- Leise, J. A., and J. M. Masters, 1991: Wind measurement from aircraft. Unpublished Technical Report, NOAA Aircraft Operations Center, Miami, FL, 182 pp.
- Mahrt, L., D. Vickers, J. Howell, J. Hojstrup, J. Wilczak, J. Edson, and J. Hare, 1996: Sea surface drag coefficients in RASEX. *J. Geophys. Res.*, **101**, 14327-14335.
- Mahrt, L., D. Vickers, J. Sun, T. Crawford, C. Vogel, and E. Dumas, 1999: Coastal zone boundary layers. Preprint, *13th Symposium on Boundary Layers and Turbulence*, Dallas, TX, Amer. Meteor. Soc., 403-406.
- Mahrt, L., D. Vickers, J. Sun, T. L. Crawford, G. H. Crescenti, and P. Frederickson, 2001: Surface stress in offshore flow and quasi-frictional decoupling. *J. Geophys. Res.*, **106**, in press.
- Mourad, P. D., 1999: Footprints of atmospheric phenomena in synthetic aperture radar images of the ocean surface: a review. *Air-Sea Exchange: Physics, Chemistry and Dynamics*, G. L. Geernaert, Ed., Kluwer Academic Publishers, 269-290.
- Mourad, P. D., D. R. Thompson, and D. C. Vandemark, 2000: Extracting fine-scale wind fields from synthetic aperture radar images of the ocean surface. *John Hopkins APL Tech. Digest*, **21**, 108-115.
- Ramage, C. S., 1984: Can shipboard measurements reveal secular changes in tropical air-sea heat flux? *J. Climate Appl. Meteor.*, **23**, 187-193.
- Rew, R., G. Davis, S. Emmerson, and H. Davies, 1997: NetCDF User's Guide for C: An Access Interface for Self-Describing, Portable Data, Version 3. Unidata Program Center, University Corporation for Atmospheric Research, Boulder CO.
- Serra, Y. L., D. P. Rogers, D. E. Hagan, C. A. Friehe, R. L. Grossman, R. A. Weller, and S. Anderson, 1997: Atmospheric boundary layer over the central and western equatorial Pacific Ocean observed during COARE and CEPEX. *J. Geophys. Res.*, **102**, 23217-23237.
- Showstack, R., 2000: U. S. unscrambles GPS signals, making them more accurate for scientific and public use. *EOS Trans.*, **81**, 222.
- Sun, J., J. F. Howell, S. K. Esbensen, L. Mahrt, C. M. Greb, R. Grossman, and M. A. LeMone, 1996: Scale dependence of air-sea fluxes over the western equatorial Pacific. *J. Atmos. Sci.*, **53**, 2997-3012.

- Sun, J., L. Mahrt, D. Vickers, J. Wong, T. Crawford, C. Vogel, E. Dumas, P. Mourad, and D. Vandemark, 1999: Air-sea interaction in the coastal shoaling zone. Preprint, *13th Symposium on Boundary Layers and Turbulence*, Dallas, TX, Amer. Meteor. Soc., 343-346.
- Sun, J., D. Vandemark, L. Mahrt, D. Vickers, T. Crawford, and C. Vogel, 2001: Momentum transfer over the coastal zone. *J. Geophys. Res.*, **106**, 12437-12448
- Vandemark, D., T. Crawford, R. Dobosy, T. Elfouhaily, and B. Chapron, 1999a: Sea surface slope statistics from a low-altitude aircraft. Proc., *International Geoscience and Remote Sensing Symposium*, Hamburg, Germany, 28 Jun.-2 Jul., IEEE.
- Vandemark, D., P. Mourad, T. Crawford, C. Vogel, and J. Sun, 1999b: Measured correlations between roll-vortex signatures and radar-inferred sea surface roughness. Proc., *International Geoscience and Remote Sensing Symposium*, Hamburg, Germany, 28 Jun.-2 Jul., IEEE.
- Vandemark, D., P. D. Mourad, S. A. Bailey, T. L. Crawford, C. A. Vogel, J. Sun, and B. Chapron, 2001: Measured changes in ocean surface roughness due to atmospheric boundary layer rolls. *J. Geophys. Res.*, **106**, 4639-4654.
- Vogel, C. A., and T. L. Crawford, 1997: Dissipation measurements in the marine atmospheric surface layer. Preprint, *12th Symposium on Boundary Layers and Turbulence*, Vancouver, BC, Amer. Meteor. Soc., 310-311.
- Vogel, C. A., and T. L. Crawford, 1999: Exchange measurements above the air-sea interface using an aircraft. *Air-Sea Exchange: Physics, Chemistry and Dynamics*, G. L. Geernaert, Ed., Kluwer Academic Publishers, 231-245.
- Vogel, C. A., T. L. Crawford, J. Sun, and L. Mahrt, 1999: Spatial variation of the atmospheric surface drag coefficient within a coastal shoaling zone. Preprint, *13th Symposium on Boundary Layers and Turbulence*, Dallas, TX, Amer. Meteor. Soc., 347-348.
- Vickers, D., L. Mahrt, J. Sun, and T. Crawford, 2000: Momentum flux in off-shore flow. Preprint, *14th Symposium on Boundary Layers and Turbulence*, Aspen, CO, Amer. Meteor. Soc., paper P6A.6.
- Vickers, D., L. Mahrt, J. Sun, and T. Crawford, 2001: Structure of offshore flow. *Mon. Wea. Rev.*, **129**, 1251-1258.

Appendix A: Marker Files

The MKR file contains an ASCII listing of specific times and locations during the flight when the pilot toggles the “on/off” switch or presses the “event” buttons on the control switch box. This file is used to mark the start and end of flux legs, profiles, or other specific maneuvers. When the marker switch is turned “on”, a three-character string of XXX, a value of “-1”, the scan number (i.e., number of elapsed seconds since the start of data acquisition), and current latitude and longitude are written to the MKR file. Similarly, a value of “0” is written with the time and location information when the marker switch is turned off. The event switch is used to mark a specific event during flight (e.g., flying over a buoy, crossing the coastline). An event is recorded in the MKR file with a three-character string of EVT along with the scan number, latitude and longitude. The MKR file is manually edited at the end of the flight. The default character string of XXX is usually replaced with three-character identifiers that are used to describe the marker pair. For example, FLX is used to denote a flux leg while PRO is used to indicate a profile. Other manually edited notes include a summary of the weather conditions, flight plan, problems encountered, and other remarks that may be helpful during data analysis. Listed below are three-character identifiers which describe these marker pairs for CBLAST-Low.

ACC	Acceleration Calibration Maneuver	PRO	Profile Sounding
ERR	Error	PTC	Pitch Calibration Maneuver
EVT	Event	STC	Static
FLX	Flux Leg	WAG	Wag (Roll) Calibration Maneuver
FRY	Ferry	WCL	Wind Circle Left (counterclockwise)
IRC	Infrared Camera Run	WCR	Wind Circle Right (clockwise)
MSG	Message	YAW	Yaw Calibration Maneuver

CBLAST-Low Pilot Study - Summer 2001

Flight: 01
Date: 21 JUL 01 (Saturday)
Duration: 3.4 hr
Pilot: Timothy L. Crawford

Summary: First flight, roll and pitch calibrations, profile, 12 north-south flux legs, and profile. Flux legs centered over 41/ 11' N, 70/ 35' W, headings of 20/ and 200/.

Weather: Region dominated by high pressure, clear skies, relatively dry conditions, winds initially calm, increasing to 8 kts from the SW.

MVY ATIS: 1053 UTC calm 10V clear 12//11/ 30.08
MVY ATIS: 1153 UTC calm 10V clear 18//13/ 30.09
MVY ATIS: 1353 UTC 200/05 10V clear 22//13/ 30.07
MVY ATIS: 1453 UTC 220/08 10V clear 21//14/ 30.08
MVY ATIS: 1553 UTC 220/08 10V clear 22//13/ 30.08

Instrumentation Notes & Comments:

IRGA #2 installed
Five Riegl laser altimeters installed
NASA Ka-band radar scatterometer installed

Roll accelerometer in right wing not functioning properly
L4 "glint" laser not functioning because of partial lens blockage

Marker for D:07211228.ORG OPENED at 565109

STC	-1	00017	12:58:45	41	23.3	-70	36.8	all systems on
	0	00183	13:01:31	41	23.3	-70	36.8	
WAG	-1	00688	13:09:56	41	18.1	-70	37.8	roll wag cal for radar
	0	00768	13:11:16	41	15.8	-70	37.3	
PTC	-1	00789	13:11:37	41	15.2	-70	37.2	pitch up/dn cal for radar
	0	00844	13:12:32	41	13.7	-70	37.0	
PRO	-1	00905	13:13:33	41	11.9	-70	36.5	profile up to 3700' (1130 m)
	0	01340	13:20:48	41	11.3	-70	37.0	
PRO	-1	01340	13:20:48	41	11.3	-70	37.0	profile down from 3700' (1130 m)
	0	01721	13:27:09	41	09.6	-70	36.1	
FLX	-1	02146	13:34:14	41	19.8	-70	33.9	flux leg south (185/)
	0	02763	13:44:31	41	02.7	-70	35.9	
FLX	-1	02955	13:47:43	41	01.2	-70	36.4	flux leg north (005/)
	0	03547	13:57:35	41	19.1	-70	34.0	
FLX	-1	03714	14:00:22	41	20.1	-70	33.8	flux leg south (185/)
	0	04359	14:11:07	41	02.8	-70	35.9	
FLX	-1	04505	14:13:33	41	01.6	-70	36.2	flux leg north (005/)
	0	05106	14:23:34	41	19.9	-70	33.8	
FLX	-1	05292	14:26:40	41	20.2	-70	33.7	flux leg south (185/)
	0	05923	14:37:11	41	03.0	-70	35.8	
FLX	-1	06235	14:42:23	41	04.9	-70	36.0	flux leg north (005/)
	0	06689	14:49:57	41	19.2	-70	33.9	
FLX	-1	06911	14:53:39	41	19.6	-70	34.3	flux leg south (185/)
	0	07520	15:03:48	41	02.9	-70	35.9	
FLX	-1	07709	15:06:57	41	01.8	-70	36.2	flux leg north (005/)
	0	08270	15:16:18	41	19.0	-70	34.0	
FLX	-1	08430	15:18:58	41	20.3	-70	33.7	flux leg south (185/)
	0	09075	15:29:43	41	02.8	-70	35.9	
FLX	-1	09298	15:33:26	41	00.9	-70	36.1	flux leg north (005/)
	0	09908	15:43:36	41	19.0	-70	34.0	
FLX	-1	10041	15:45:49	41	20.2	-70	33.8	flux leg south (185/)
	0	10692	15:56:40	41	02.5	-70	35.9	
FLX	-1	10870	15:59:38	41	00.5	-70	36.7	flux leg north (005/)
	0	11469	16:09:37	41	19.3	-70	33.9	
MSG		11472	16:09:40					BAT 0 frequency slow: Freq=49
MSG		11472	16:09:40					BAT 1 frequency slow: Freq=49
PRO	-1	11678	16:13:06	41	15.1	-70	35.6	profile up to 1300' (400 m)
	0	12097	16:20:05	41	16.0	-70	34.6	

Marker for D:07211228.ORG CLOSED at 577742

Total scans: 12633
Missed Ints: 00000
BAT A: 0631649 of 0631650 000.000% Dropouts
BAT B: 0631649 of 0631650 000.000% Dropouts
ASH: 0063165 of 0063165 000.000% Dropouts
TAN: 0123702 of 0126330 002.080% Dropouts

CBLAST-Low Pilot Study - Summer 2001

Flight: 02
Date: 22 JUL 01 (Sunday)
Duration: 1.4 hr
Pilot: Timothy L. Crawford

Summary: Early morning SAR flight, overpass at 1049 UTC. Profile, simple box pattern, profile.

Weather: Region dominated by high pressure, clear skies, slight increase in

humidity. Winds initially calm, increasing to 5 kts from the SW.

MVY ATIS: 0943 UTC calm 10V clear 16//16/ 30.04
MVY ATIS: 0953 UTC calm 10V clear 16//16/ 30.04
MVY ATIS: 1053 UTC 240/05 09V clear 18//17/ 30.04

Instrumentation Notes & Comments:

Roll accelerometer in right wing not functioning properly
L4 "glint" laser not functioning because of partial lens blockage
Chilled mirror dew point sensor was over-aspirated resulting in bad data

Marker for D:07220953.ORG OPENED at 036285

STC -1 00012 10:04:56 41 23.3 -70 36.8 all systems on
0 00072 10:05:56 41 23.3 -70 36.8
PRO -1 00483 10:12:47 41 18.8 -70 35.0 profile down from 2600' (800 m)
0 00632 10:15:16 41 14.3 -70 34.0
FLX -1 00633 10:15:17 41 14.3 -70 34.0 SAR flux leg south (185/)
0 01334 10:26:58 40 54.5 -70 36.2
FLX -1 01371 10:27:35 40 53.8 -70 35.3 SAR flux leg east (100/)
0 02227 10:41:51 40 50.2 -70 00.6
FLX -1 02281 10:42:45 40 51.2 -69 59.4 SAR flux leg north (000/)
EVT 02491 10:46:15 40 58.0 -70 00.1 visible surface discontinuity
EVT 02622 10:48:26 41 02.3 -70 00.3 visible surface discontinuity
0 02845 10:52:09 41 09.6 -70 00.0
FLX -1 02888 10:52:52 41 10.4 -70 01.2 SAR flux leg west (275/)
0 03787 11:07:51 41 15.3 -70 36.0
PRO -1 03793 11:07:57 41 15.3 -70 36.2 profile up to 3000' (900 m)
0 04388 11:17:52 41 14.4 -70 32.8
STC -1 04915 11:26:39 41 23.3 -70 36.8 preparing to shut down all systems
0 04976 11:27:40 41 23.3 -70 36.8

Marker for D:07220953.ORG CLOSED at 041263

Total scans: 04978
Missed Ints: 00000
BAT A: 0248900 of 0248900 000.000% Dropouts
BAT B: 0248900 of 0248900 000.000% Dropouts
ASH: 0024890 of 0024890 000.000% Dropouts
TAN: 0048768 of 0049780 002.033% Dropouts

CBLAST-Low Pilot Study - Summer 2001

Flight: 03
Date: 23 JUL 01 (Monday)
Duration: 2.4 hr
Pilot: Timothy L. Crawford

Summary: Early afternoon flight, six north-south flux legs, multiple short altitude profiles, roll and pitch calibrations.

Weather: Thick early morning fog, clearing by late morning, SW winds.

MVY ATIS: 1552 UTC 220/02 10V scat 24//20/ 30.04
MVY ATIS: 1752 UTC 240/09/G18 10V clear 25//21/ 30.02
MYV ATIS: 1852 UTC 240/10/G18 10V clear 25//21/ 29.99

Instrumentation Notes & Comments:

Roll accelerometer in right wing not functioning properly
L4 "glint" laser now functioning properly, however with a few drop outs
Aspiration on chilled mirror dew point sensor fixed

Marker for D:07231646.ORG OPENED at 147015

```
STC -1 00004 16:50:18 41 23.3 -70 36.8 all systems on
      0 00060 16:51:14 41 23.3 -70 36.8
PRO -1 00643 17:00:57 41 16.5 -70 35.9 profile up/dn to 3500' (1050 m)
      0 01105 17:08:39 41 17.0 -70 32.9
PRO -1 01105 17:08:39 41 17.0 -70 32.9 profile down from 3500' (1050 m)
      0 01375 17:13:09 41 17.2 -70 31.6
FLX -1 01410 17:13:44 41 16.5 -70 32.6 flux leg south (180/)
      0 02250 17:27:44 40 54.4 -70 35.9
PRO -1 02250 17:27:44 40 54.4 -70 35.9 profile up/dn to 500' (150 m)
      0 02438 17:30:52 40 52.7 -70 36.3
FLX -1 02438 17:30:52 40 52.7 -70 36.3 flux leg north (000/)
      0 03212 17:43:46 41 17.9 -70 35.2
PRO -1 03212 17:43:46 41 17.9 -70 35.2 profile up/dn to 500' (150 m)
      0 03369 17:46:23 41 20.0 -70 35.7
FLX -1 03369 17:46:23 41 20.0 -70 35.7 flux leg south (180/)
      0 04310 18:02:04 40 54.5 -70 35.9
PRO -1 04310 18:02:04 40 54.5 -70 35.9 profile up/dn to 500' (150 m)
      0 04466 18:04:40 40 51.8 -70 35.3
FLX -1 04466 18:04:40 40 51.8 -70 35.3 flux leg north (000/)
      0 05302 18:18:36 41 19.3 -70 34.0
PRO -1 05302 18:18:36 41 19.3 -70 34.3 profile up/dn to 500' (150 m)
      0 05451 18:21:05 41 19.8 -70 33.3
FLX -1 05453 18:21:07 41 19.8 -70 33.3 flux leg south (180/)
      0 06373 18:36:27 40 54.3 -70 35.9
PRO -1 06373 18:36:27 40 54.3 -70 35.9 profile up/dn to 500' (150 m)
      0 06603 18:40:17 40 52.9 -70 35.4
FLX -1 06603 18:40:17 40 52.9 -70 35.4 flux leg north (000/)
      0 07389 18:53:23 41 19.3 -70 36.2
PRO -1 07389 18:53:23 41 19.3 -70 36.2 profile up/dn to 500' (150 m)
      0 07539 18:55:53 41 19.2 -70 36.6
PTC -1 07539 18:55:53 41 19.2 -70 36.6 pitch up/dn cal for radar
      0 07664 18:57:58 41 16.6 -70 39.4
PRO -1 07697 18:58:31 41 16.0 -70 40.2 profile up to 3000' (930 m)
      0 08064 19:04:38 41 17.1 -70 40.6
PRO -1 08069 19:04:43 41 17.2 -70 40.8 descent into MVY
      0 08514 19:12:08 41 23.3 -70 36.8
STC -1 08518 19:12:12 41 23.3 -70 36.8 preparing to shut down all systems
      0 08575 19:13:09 41 23.3 -70 36.8
```

Marker for D:07231646.ORG CLOSED at 155595

```
Total scans: 08580
Missed Ints: 00000
      BAT A: 0429000 of 0429000 000.000% Dropouts
      BAT B: 0429000 of 0429000 000.000% Dropouts
      ASH: 0042900 of 0042900 000.000% Dropouts
      TAN: 0085572 of 0085800 000.266% Dropouts
```

CBLAST-Low Pilot Study - Summer 2001

```
Flight: 04
Date: 25 JUL 01 (Wednesday)
Duration: 2.0 hr
Pilot: Timothy L. Crawford
```

Summary: Four north-south flux legs from near the coast over the 3D SST array to the ASIMET buoy plus another 5 nm. Several transects at 1250' for the infrared/visible cameras.

Weather: Moderate SW winds with shallow "puffs" of fog moving over the region in the early afternoon at several hundred feet. Visibility at 1250' was poor due to elevated fog. Because of the poor visibility, visual

navigation and reference to surface ships and buoys was difficult.

MVY ATIS: 1552 UTC 270/10 10V clear 30//23/ 29.86
MVY ATIS: 1753 UTC 240/12 9V clear 26//23/ 29.85

Instrumentation Notes & Comments:

Roll accelerometer in right wing fixed
Chilled mirror dew point sensor questionable near end of flight (oversaturation)
University of Washington/WHOI infrared/visible camera system installed

Marker for D:07251641.ORG OPENED at 320051

STC	-1	00052	16:55:02	41	23.3	-70	36.8	all systems on
		0	00126	16:56:16	41	23.3	-70	36.8
IRC	-1	00497	17:02:27	41	20.7	-70	37.2	focus run for IR camera @ 1500' (460 m)
		0	00501	17:02:31	41	20.6	-70	37.2
EVT		00628	17:04:38	41	16.9	-70	34.6	over R/V Nobska @ 300' (90 m)
PRO	-1	00683	17:05:33	41	15.7	-70	34.5	profile up to 3300' (1000 m)
		0	01097	17:12:27	41	17.1	-70	35.5
FLX	-1	01245	17:14:55	41	20.3	-70	35.4	flux leg south (180/)
EVT		01455	17:18:25	41	15.2	-70	35.4	east of 3D SST array
		0	02228	17:31:18	40	54.4	-70	36.1
PRO	-1	02228	17:31:18	40	54.4	-70	36.1	profile up/dn to 500' (150 m)
		0	02416	17:34:26	40	52.6	-70	35.6
FLX	-1	02416	17:34:26	40	52.6	-70	35.6	flux profile north (000/)
EVT		02626	17:37:56	40	59.5	-70	35.8	over ASIMET buoy
EVT		03103	17:45:53	41	15.3	-70	35.5	over 3D SST array
		0	03244	17:48:14	41	19.9	-70	35.4
PRO	-1	03244	17:48:14	41	19.9	-70	35.4	profile up/dn to 500' (150 m)
		0	03376	17:50:26	41	19.8	-70	34.0
FLX	-1	03376	17:50:26	41	19.8	-70	34.0	flux profile south (180/)
		0	04357	18:06:47	40	55.3	-70	36.0
PRO	-1	04357	18:06:47	40	55.3	-70	36.0	profile up/dn to 500' (150 m)
		0	04553	18:10:03	40	54.5	-70	35.0
FLX	-1	04553	18:10:03	40	54.5	-70	35.0	flux profile north (000/)
EVT		04705	18:12:35	40	59.5	-70	35.8	over ASIMET buoy
EVT		05188	18:20:38	41	15.3	-70	35.5	over 3D SST array
		0	05317	18:22:47	41	19.5	-70	35.4
PRO	-1	05317	18:22:47	41	19.5	-70	35.4	profile up to 3300' (1000 m)
EVT		05424	18:24:34	41	18.1	-70	34.1	over R/V Nobska
EVT		05574	18:27:04	41	14.5	-70	35.8	over 3D SST array
		0	05611	18:27:41	41	13.7	-70	36.5
IRC	-1	05857	18:31:47	41	11.1	-70	38.5	IR camera run @ 1280' (390 m)
EVT		05992	18:34:02	41	15.4	-70	35.6	over 3D SST array
		0	06036	18:34:46	41	16.8	-70	34.6
IRC	-1	06156	18:36:46	41	16.0	-70	32.6	IR camera run @ 1280' (390 m)
EVT		06256	18:38:26	41	15.3	-70	35.8	over 3D SST array
		0	06327	18:39:37	41	15.6	-70	38.3
EVT		06507	18:42:37	41	15.7	-70	35.2	over 3D SST array
EVT		06621	18:44:31	41	19.4	-70	33.9	over R/V Nobska

Marker for D:07251641.ORG CLOSED at 327168

Total scans: 07117
Missed Ints: 00000
BAT A: 0355850 of 0355850 000.000% Dropouts
BAT B: 0355850 of 0355850 000.000% Dropouts
ASH: 0035585 of 0035585 000.000% Dropouts
TAN: 0069897 of 0071170 001.789% Dropouts

CBLAST-Low Pilot Study - Summer 2001

Flight: 05

Date: 27 JUL 01 (Friday)
Duration: 4.0 hr
Pilot: Timothy L. Crawford

Summary: Profile, four north-south flux legs from Katama to ASIMET buoy,
profile, four upwind/downwind flux legs, profile, and infrared
camera runs.

Weather: Cold front moved through previous evening, northeasterly
flow creating a well mixed, unstable marine atmospheric boundary
layer, strong winds off shore in the morning.

MVY ATIS: 0924 UTC 020/08 10V clear 13//11/ 30.17
MVY ATIS: 0952 UTC 020/08 10V clear 13//11/ 30.19
MVY ATIS: 1052 UTC 020/11 10V clear 16//10/ 30.20
MVY ATIS: 1152 UTC 030/11 10V clear 16//10/ 30.22
MVY ATIS: 1452 UTC 040/12 10V clear 19//09/ 30.22
MVY ATIS: 1555 UTC 040/08 10V clear 19//08/ 30.23

Instrumentation Notes & Comments: None

Marker for D:07271211.ORG OPENED at 477092

STC	-1	00023	12:31:54	41	23.3	-70	36.8	all systems on
	0	00084	12:32:55	41	23.3	-70	36.8	
PRO	-1	00606	12:41:37	41	24.9	-70	29.7	profile up to 4600' (1400 m)
	0	01160	12:50:51	41	21.8	-70	24.3	
PRO	-1	01162	12:50:53	41	21.8	-70	24.3	profile dn from 4600' (1400 m)
	0	01345	12:53:56	41	20.6	-70	32.1	
FLX	-1	01351	12:54:02	41	20.5	-70	32.3	flux leg south (190/)
	0	02141	13:07:12	40	53.7	-70	37.1	
PRO	-1	02141	13:07:12	40	53.7	-70	37.1	profile up/dn to 500' (150 m)
	0	02347	13:10:38	40	50.7	-70	38.5	
FLX	-1	02347	13:10:38	40	50.7	-70	38.5	flux leg north (010/)
	0	03573	13:31:04	41	20.7	-70	31.7	
FLX	-1	03610	13:31:41	41	20.3	-70	32.3	flux leg south (185/)
	0	04382	13:44:33	40	53.5	-70	37.4	
PRO	-1	04382	13:44:33	40	53.5	-70	37.4	profile up/dn to 500' (150 m)
	0	04597	13:48:08	40	50.3	-70	38.7	
FLX	-1	04597	13:48:08	40	50.3	-70	38.7	flux leg north (010/)
	0	05793	14:08:04	41	20.6	-70	31.9	
FLX	-1	05853	14:09:04	41	19.7	-70	32.8	flux leg south (185/)
	0	06613	14:21:44	40	53.8	-70	37.1	
PRO	-1	06619	14:21:50	40	53.6	-70	37.1	profile up/dn to 4600' (1400 m)
EVT		07055	14:29:06	41	01.6	-70	35.0	top of profile
	0	07337	14:33:48	41	07.1	-70	28.0	
FLX	-1	07394	14:34:45	41	07.2	-70	28.9	flux leg southwest (215/)
	0	07954	14:44:05	40	50.9	-70	43.9	
FLX	-1	08005	14:44:56	40	50.4	-70	43.2	flux leg northeast (030/)
	0	08807	14:58:18	41	08.2	-70	29.6	
FLX	-1	08852	14:59:03	41	08.2	-70	30.5	flux leg southwest (210/)
	0	09426	15:08:37	40	50.5	-70	42.0	
FLX	-1	09481	15:09:32	40	50.9	-70	42.9	flux leg northeast (030/)
	0	10242	15:22:13	41	08.2	-70	29.2	
PRO	-1	10283	15:22:54	41	08.2	-70	30.3	profile up/dn to 4900' (1500 m)
EVT		10695	15:29:46	40	56.1	-70	41.5	top of profile
	0	10942	15:33:53	40	55.1	-70	50.9	
IRC	-1	11042	15:35:33	40	57.2	-70	50.6	IR camera run @ 1280' (390 m)
	0	11783	15:47:54	41	02.6	-70	23.9	
IRC	-1	11849	15:49:00	41	01.4	-70	24.2	IR camera run @ 1280' (390 m)
	0	12413	15:58:24	40	56.9	-70	48.7	
IRC	-1	12510	16:00:01	40	54.4	-70	48.9	IR camera run @ 1280' (390 m)
	0	12907	16:06:38	40	48.4	-70	34.4	
IRC	-1	12988	16:07:59	40	49.6	-70	32.7	IR camera run @ 1250' (390 m)
	0	13839	16:22:10	41	12.8	-70	40.0	

IRC -1 13865 16:22:36 41 13.5 -70 40.1 IR camera run @ 1250' (390 m)
 0 14156 16:27:27 41 21.2 -70 39.0
 FRY -1 14157 16:27:28 41 21.2 -70 39.0 ferry and descent to MVY
 0 14264 16:29:15 41 23.2 -70 37.1
 STC -1 14410 16:31:41 41 23.3 -70 36.8 preparing to shut down all systems
 MSG 14452 16:32:23 BAT 0 frequency slow: Freq=36
 0 14456 16:32:27 41 23.3 -70 36.8

Marker for D:07271211.ORG CLOSED at 491551

Total scans: 14459
 Missed Ints: 00000
 BAT A: 0722936 of 0722950 000.002% Dropouts
 BAT B: 0722950 of 0722950 000.000% Dropouts
 ASH: 0072295 of 0072295 000.000% Dropouts
 TAN: 0143421 of 0144590 000.808% Dropouts

CBLAST-Low Pilot Study - Summer 2001

Flight: 06
 Date: 27 JUL 01 (Friday)
 Duration: 0.7 hr
 Pilot: Timothy L. Crawford

Summary: Infrared camera runs using the "mowing the lawn" flight plan.

Weather: Cold front moved through previous evening, northeasterly flow creating a well mixed, unstable marine atmospheric boundary layer, winds decreasing in magnitude by late afternoon.

MVY ATIS: 2152 UTC 090/07 10V clear 19//09/ 30.20
 MVY ATIS: 2252 UTC calm 10V clear 18//11/ 30.23

Instrumentation Notes & Comments:

Data acquisition system manually shut down prior to landing for landing lights

Marker for D:07272229.ORG OPENED at 513454

STC -1 00003 22:37:36 41 23.3 -70 36.8 all systems on
 0 00093 22:39:06 41 23.3 -70 36.8
 IRC -1 00585 22:47:18 41 19.9 -70 35.5 W IR camera run @ 1280' (390 m)
 0 00730 22:49:43 41 18.5 -70 41.6
 IRC -1 00785 22:50:38 41 17.5 -70 41.4 E IR camera run @ 1280' (390 m)
 0 00959 22:53:32 41 19.0 -70 34.5
 IRC -1 01026 22:54:39 41 17.9 -70 34.2 W IR camera run @ 1280' (390 m)
 0 01118 22:56:11 41 17.1 -70 38.1
 IRC -1 01195 22:57:28 41 16.6 -70 36.8 E IR camera run @ 1280' (390 m)
 0 01289 22:59:02 41 16.9 -70 32.9
 IRC -1 01359 23:00:12 41 15.6 -70 33.3 W IR camera run @ 1280' (390 m)
 0 01491 23:02:24 41 14.2 -70 38.7
 IRC -1 01543 23:03:16 41 13.2 -70 38.3 E IR camera run @ 1280' (390 m)
 0 01630 23:04:43 41 13.9 -70 35.1
 EVT 01852 23:08:25 41 10.5 -70 41.4 fishing ship

Marker for D:07272229.ORG CLOSED at 515645

Total scans: 02191
 Missed Ints: 00000
 BAT A: 0109550 of 0109550 000.000% Dropouts
 BAT B: 0109550 of 0109550 000.000% Dropouts
 ASH: 0010955 of 0010955 000.000% Dropouts
 TAN: 0021906 of 0021910 000.018% Dropouts

CBLAST-Low Pilot Study - Summer 2001

Flight: 07
Date: 28 JUL 01 (Saturday)
Duration: 3.0 hr
Pilot: Timothy L. Crawford

Summary: Infrared camera run, profile, northeast-southwest flux legs,
profile, northwest-southeast flux legs, several more flux leg
of various headings, multiple short profiles.

Weather: Region dominated by high pressure system, light northwesterly
winds in early morning, becoming northeasterly by late
morning.

MVY ATIS: 0939 UTC 330/05 08V clear 09//08/ 30.27
MVY ATIS: 0951 UTC 320/06 10V clear 11//10/ 30.27
MVY ATIS: 1053 UTC 330/06 10V clear 15//13/ 30.28
MVY ATIS: 1253 UTC 020/06 10V clear 19//11/ 30.29

Instrumentation Notes & Comments: None

Marker for D:07281042.ORG OPENED at 558141

STC	-1	00004	11:02:24	41	23.3	-70	36.8	all systems on
		0	00051	11:03:11	41	23.3	-70	36.8
IRC	-1	00568	11:11:48	41	18.2	-70	35.5	S IR camera run @ 1280' (390 m)
		0	01367	11:25:07	40	51.9	-70	35.0
IRC	-1	01474	11:26:54	40	52.3	-70	36.9	N IR camera run @ 1280' (390 m)
		0	01904	11:34:04	41	04.6	-70	35.3
IRC	-1	02015	11:35:55	41	03.2	-70	33.5	SW IR camera run @ 1250' (390 m)
		0	02300	11:40:40	40	55.1	-70	39.6
PRO	-1	02510	11:44:10	40	57.5	-70	40.2	profile down from 3600' (1100 m)
		0	02884	11:50:24	41	06.7	-70	31.9
FLX	-1	02967	11:51:47	41	05.8	-70	30.6	flux leg southwest (215/)
		0	03445	11:59:45	40	52.6	-70	40.6
PRO	-1	03445	11:59:45	40	52.6	-70	40.6	profile up/dn to 500' (150 m)
		0	03614	12:02:34	40	51.6	-70	41.6
FLX	-1	03614	12:02:34	40	51.6	-70	41.6	flux leg northeast (025/)
		0	04183	12:12:03	41	06.1	-70	30.7
PRO	-1	04183	12:12:03	41	06.1	-70	30.7	profile up/dn to 500' (150 m)
		0	04370	12:15:10	41	07.3	-70	29.5
FLX	-1	04370	12:15:10	41	07.3	-70	29.5	flux leg southwest (215/)
EVT		04654	12:19:54	40	59.4	-70	35.9	over ASIMET buoy
		0	04894	12:23:54	40	53.1	-70	41.4
PRO	-1	04900	12:24:00	40	52.9	-70	41.5	profile up to 3600' (1100 m)
		0	05275	12:30:15	41	00.6	-70	50.1
PRO	-1	05275	12:30:15	41	00.6	-70	50.1	profile down from 3600' (1100 m)
		0	05574	12:35:14	41	02.8	-70	43.3
FLX	-1	05577	12:35:17	41	02.8	-70	43.2	flux leg southeast (120/)
		0	05997	12:42:17	40	55.6	-70	27.2
PRO	-1	05997	12:42:17	40	55.6	-70	27.2	profile up/dn to 500' (150 m)
		0	06181	12:45:21	40	54.3	-70	25.2
FLX	-1	06181	12:45:21	40	54.3	-70	25.2	flux leg northwest (300/)
		0	06774	12:55:14	41	03.3	-70	44.7
PRO	-1	06774	12:55:14	41	03.3	-70	44.7	profile up/dn to 500' (150 m)
		0	06959	12:58:19	41	03.7	-70	46.3
FLX	-1	06959	12:58:19	41	03.7	-70	46.3	flux leg southeast (115/)
		0	07485	13:07:05	40	55.6	-70	27.1
PRO	-1	07485	13:07:05	40	55.6	-70	27.1	profile up/dn to 500' (150 m)
		0	07654	13:09:54	40	55.6	-70	30.7
FLX	-1	07654	13:09:54	40	55.6	-70	30.7	flux leg northwest (315/)
		0	08005	13:15:45	41	02.7	-70	39.9
PRO	-1	08005	13:15:45	41	02.7	-70	39.9	profile up/dn to 500' (150 m)
		0	08120	13:17:40	41	02.7	-70	37.8

FLX	-1	08120	13:17:40	41	02.7	-70	37.8	flux leg southeast (155/)
EVT		08227	13:19:27	40	59.5	-70	35.9	over ASIMET buoy
	0	08383	13:22:03	40	54.8	-70	33.2	
PRO	-1	08383	13:22:03	40	54.8	-70	33.2	profile up/dn to 500' (150 m)
	0	08507	13:24:07	40	55.0	-70	35.1	
FLX	-1	08507	13:24:07	40	55.0	-70	35.1	flux leg north (350/)
EVT		08658	13:26:38	40	59.4	-70	35.9	over ASIMET buoy
	0	08841	13:29:41	41	04.5	-70	37.2	
PRO	-1	08841	13:29:41	41	04.5	-70	37.2	profile up/dn to 500' (150 m)
	0	08948	13:31:28	41	03.8	-70	35.1	
FLX	-1	08948	13:31:28	41	03.8	-70	35.1	flux leg south (190/)
EVT		09080	13:33:40	40	59.5	-70	35.9	over ASIMET buoy
	0	09236	13:36:16	40	54.4	-70	37.1	
PRO	-1	09236	13:36:16	40	54.4	-70	37.1	profile up/dn to 500' (150 m)
	0	09358	13:38:18	40	55.9	-70	38.4	
FLX	-1	09358	13:38:18	40	55.9	-70	38.4	flux leg northeast (025/)
EVT		09495	13:40:35	40	59.5	-70	35.8	over ASIMET buoy
	0	09680	13:43:40	41	04.2	-70	32.6	
PRO	-1	09690	13:43:50	41	04.5	-70	32.5	profile up to 3600' (1100 m)
	0	10044	13:49:44	41	14.7	-70	35.3	
PRO	-1	10044	13:49:44	41	14.7	-70	35.3	profile down from 3600' (1100 m)
	0	10370	13:55:10	41	23.7	-70	36.6	
STC	-1	10567	13:58:27	41	23.3	-70	36.8	preparing to shut down all systems
	0	10621	13:59:21	41	23.3	-70	36.8	

Marker for D:07281042.ORG CLOSED at 568766

Total scans: 10625
Missed Ints: 00000
BAT A: 0531250 of 0531250 000.000% Dropouts
BAT B: 0531250 of 0531250 000.000% Dropouts
ASH: 0053125 of 0053125 000.000% Dropouts
TAN: 0105729 of 0106250 000.490% Dropouts

CBLAST-Low Pilot Study - Summer 2001

Flight: 08
Date: 29 JUL 01 (Sunday)
Duration: 1.5 hr
Pilot: Timothy L. Crawford

Summary: Infrared camera run prior to sunrise, simple north-south, east-west box pattern at 1280' (390 m) for SAR overpass.

Weather: Region dominated by high pressure system, mid and high level clouds moving into region, calm to very light and variable winds.

MVY ATIS: 0818 UTC calm 10V clear 12//11/ 30.22
MVY ATIS: 0916 UTC calm 10v clear 12//11/ 30.23
MVY ATIS: 0953 UTC calm 10v clear 12//11/ 30.23
MVY ATIS: 1053 UTC calm 10v clear 17//15/ 30.23
MVY ATIS: 1253 UTC calm 10v clear 20//16/ 30.23

Instrumentation Notes & Comments:

Data file was started after takeoff because of difficulty with the TANS not functioning properly and was terminated early before the overpass.

Marker for D:07290928.ORG OPENED at 034282

IRC	-1	00005	09:31:26	41	19.2	-70	36.2	S IR camera run @ 1280' (390 m)
	0	00266	09:35:47	41	10.8	-70	35.6	
IRC	-1	00507	09:39:48	41	10.4	-70	32.7	S IR camera run @ 1280' (390 m)

```

    0 00985 09:47:46 40 55.7 -70 35.5
IRC -1 01032 09:48:39 40 54.5 -70 34.2 E IR camera run @ 1280' (390 m)
    0 01584 09:57:51 40 55.1 -70 10.1
IRC -1 01637 09:58:44 40 56.2 -70 08.9 N IR camera run @ 1280' (390 m)
    0 02075 10:06:02 41 09.2 -70 09.3
IRC -1 02132 10:06:59 41 10.1 -70 10.7 W IR camera run @ 1280' (390 m)
    0 02800 10:18:07 41 09.9 -70 35.8

```

Marker for D:07290928.ORG CLOSED at 037094

```

Total scans: 02806
Missed Ints: 00006
    BAT A: 0140232 of 0140300 000.048% Dropouts
    BAT B: 0140232 of 0140300 000.048% Dropouts
    ASH: 0013994 of 0014030 000.257% Dropouts
    TAN: 0000000 of 0028060 100.000% Dropouts

```

CBLAST-Low Pilot Study - Summer 2001

```

Flight: 09
Date: 29 JUL 01 (Sunday)
Duration: 2.0 hr
Pilot: Timothy L. Crawford

```

Summary: "Spirograph" flux legs over the ASIMET buoy with multiple short altitude profiles and a deep boundary layer profile.

Weather: Region dominated by high pressure system, mid and high level clouds moving into region, calm to very light and variable winds.

```

MVY ATIS: 0818 UTC calm 10V clear 12//11/ 30.22
MVY ATIS: 0916 UTC calm 10v clear 12//11/ 30.23
MVY ATIS: 0953 UTC calm 10v clear 12//11/ 30.23
MVY ATIS: 1053 UTC calm 10v clear 17//15/ 30.23
MVY ATIS: 1253 UTC calm 10v clear 20//16/ 30.23

```

Instrumentation Notes & Comments:

TANS functioning after manually- and velocity-aided search reset
Data not differentially corrected prior to scan 01400, ground station off

Marker for D:07291112.ORG OPENED at 042234

```

FLX -1 01400 12:07:14 40 55.1 -70 37.3 flux leg north (010/)
    0 01730 12:12:43 41 04.8 -70 36.1
PRO -1 01730 12:12:43 41 04.8 -70 36.1 profile up/dn to 500' (150 m)
    0 01843 12:14:36 41 04.2 -70 38.2
FLX -1 01843 12:14:36 41 04.2 -70 38.2 flux leg southeast (155/)
    0 02190 12:20:23 40 55.2 -70 32.9
PRO -1 02190 12:20:23 40 55.2 -70 32.9 profile up/dn to 500' (150 m)
    0 02281 12:21:54 40 56.2 -70 30.9
FLX -1 02281 12:21:54 40 56.2 -70 30.9 flux leg northwest (305/)
    0 02616 12:27:29 41 02.8 -70 41.0
PRO -1 02616 12:27:29 41 02.8 -70 41.0 profile up/dn to 500' (150 m)
    0 02742 12:29:35 41 01.0 -70 41.0
FLX -1 02742 12:29:35 41 01.0 -70 41.0 flux leg east (110/)
    0 03034 12:34:27 40 58.7 -70 29.5
PRO -1 03034 12:34:27 40 58.7 -70 29.5 profile up/dn to 500' (150 m)
    0 03154 12:36:27 41 00.5 -70 29.7
FLX -1 03154 12:36:27 41 00.5 -70 29.7 flux profile west (255/)
    0 03473 12:41:46 40 58.2 -70 42.4
PRO -1 03473 12:41:46 40 58.2 -70 42.4 profile up/dn to 500' (150 m)
    0 03578 12:43:31 40 56.6 -70 41.2

```

FLX	-1	03578	12:43:31	40	56.6	-70	41.2	flux leg northeast (060/)
		0	03896	12:48:49	41	02.3	-70	30.2
PRO	-1	03896	12:48:49	41	02.3	-70	30.2	profile up/dn to 500' (150 m)
		0	04005	12:50:38	41	03.5	-70	31.9
FLX	-1	04005	12:50:38	41	03.5	-70	31.9	flux leg southwest (215/)
		0	04358	12:56:31	40	55.6	-70	40.1
PRO	-1	04358	12:56:31	40	55.6	-70	40.1	profile up/dn to 500' (150 m)
		0	04475	12:58:28	40	55.2	-70	37.6
FLX	-1	04475	12:58:28	40	55.2	-70	37.6	flux leg north (020/)
		0	04772	13:03:25	40	04.2	-70	34.2
PRO	-1	04772	13:03:25	40	04.2	-70	34.2	profile up/dn to 500' (150 m)
		0	04888	13:05:21	41	04.2	-70	36.7
FLX	-1	04888	13:05:21	41	04.2	-70	36.7	flux leg south (170/)
		0	05222	13:10:55	40	54.3	-70	34.8
PRO	-1	05222	13:10:55	40	54.3	-70	34.8	profile up/dn to 500' (150 m)
		0	05336	13:12:49	40	55.3	-70	32.8
FLX	-1	05336	13:12:49	40	55.3	-70	32.8	flux leg northwest (330/)
		0	05652	13:18:05	41	03.9	-70	39.3
PRO	-1	05652	13:18:05	41	03.9	-70	39.3	profile up/dn to 500' (150 m)
		0	05754	13:19:47	41	02.9	-70	41.2
FLX	-1	05754	13:19:47	41	02.9	-70	41.2	flux leg southeast (130/)
		0	06105	13:25:38	40	56.3	-70	30.5
PRO	-1	06116	13:25:49	40	56.1	-70	30.1	profile up to 4900' (1500 m)
		0	06657	13:34:50	41	11.8	-70	35.2
PRO	-1	06661	13:34:54	41	11.9	-70	35.2	profile down to MVY
		0	07197	13:43:50	41	23.6	-70	36.7
STC	-1	07314	13:45:47	41	23.3	-70	36.8	preparing to shut down all systems
		0	07357	13:46:30	41	23.3	-70	36.8

Marker for D:07291112.ORG CLOSED at 049597

Total scans: 07363

Missed Ints: 00000

BAT A: 0368150 of 0368150 000.000% Dropouts

BAT B: 0368150 of 0368150 000.000% Dropouts

ASH: 0036815 of 0036815 000.000% Dropouts

TAN: 0071765 of 0073630 002.533% Dropouts

CBLAST-Low Pilot Study - Summer 2001

Flight: 10

Date: 30 JUL 01 (Monday)

Duration: 3.5 hr

Pilot: Timothy L. Crawford

Summary: Wind calibrations, infrared camera run (box pattern), east-west "bow tie" flux legs and short profiles over ASIMET buoy, profile, multiple flux legs and short profiles over the R/V Asterias.

Weather: Fair weather with high clouds to the south from a low pressure system in the mid-Atlantic region. Light winds from the northeast and east.

MVY ATIS: 0953 UTC 060/04 10V clear 30.16

MVY ATIS: 1053 UTC 060/03 10V clear 14//12/ 30.17

MVY ATIS: 1153 UTC 110/07 10V clear 19//13/ 30.18

MVY ATIS: 1402 UTC 090/12 10V clear 21//14/ 30.18

MVY ATIS: 1453 UTC 090/11 10V clear 22//14/ 30.17

Instrumentation Notes & Comments: None

Marker for D:07301120.ORG OPENED at 128628

STC -1 00005 11:43:52 41 23.3 -70 36.8 all systems on

	0	00057	11:44:44	41	23.3	-70	36.8	
PTC	-1	00687	11:55:14	41	18.6	-70	35.0	pitch up/dn calibration
	0	00810	11:57:17	41	14.9	-70	34.7	
YAW	-1	00815	11:57:22	41	14.7	-70	34.7	yaw calibration
	0	01003	12:00:30	41	08.9	-70	34.6	
ACC	-1	01009	12:00:36	41	08.8	-70	34.6	acceleration run calibration
	0	01253	12:04:40	41	01.7	-70	35.7	
WCR	-1	01481	12:08:28	41	01.0	-70	36.3	wind circle right
	0	01709	12:12:16	41	01.2	-70	36.6	
WCL	-1	01791	12:13:38	40	59.7	-70	34.3	wind circle left
	0	01994	12:17:01	40	60.0	-70	34.2	
PRO	-1	02053	12:18:00	41	01.5	-70	32.7	profile down from 3800' (1150 m)
	0	02393	12:23:40	41	02.8	-70	27.1	
IRC	-1	02456	12:24:43	41	02.9	-70	30.0	W IR camera run @ 1280' (390 m)
	0	02690	12:28:37	41	02.6	-70	41.0	
IRC	-1	02690	12:28:37	41	02.6	-70	41.0	S IR camera run @ 1280' (390 m)
	0	02957	12:33:04	40	54.6	-70	42.0	
IRC	-1	02957	12:33:04	40	54.6	-70	42.0	E IR camera run @ 1280' (390 m)
	0	03358	12:39:45	40	54.6	-70	28.	
IRC	-1	03358	12:39:45	40	54.6	-70	28.8	N IR camera run @ 1280' (390 m)
	0	03722	12:45:49	41	05.1	-70	28.6	
FLX	-1	04001	12:50:28	41	01.5	-70	28.0	flux leg west (250/)
	0	04348	12:56:15	40	57.8	-70	42.4	
PRO	-1	04348	12:56:15	40	57.8	-70	42.4	profile up/dn to 500' (150 m)
	0	04438	12:57:45	40	59.0	-70	42.8	
FLX	-1	04438	12:57:45	40	59.0	-70	42.8	flux leg east (085/)
	0	04835	13:04:22	40	59.7	-70	29.2	
PRO	-1	04835	13:04:22	40	59.7	-70	29.2	profile up/dn to 500' (150 m)
	0	04959	13:06:26	41	01.5	-70	31.1	
FLX	-1	04959	13:06:26	41	01.5	-70	31.1	flux leg southwest (240/)
	0	05256	13:11:23	40	56.9	-70	43.4	
PRO	-1	05256	13:11:23	40	56.9	-70	43.4	profile up/dn to 500' (150 m)
	0	05360	13:13:07	40	58.4	-70	43.8	
FLX	-1	05360	13:13:07	40	58.4	-70	43.8	flux leg east (080/)
	0	05784	13:20:11	41	00.2	-70	29.2	
PRO	-1	05784	13:20:11	41	00.2	-70	29.2	profile up/dn to 500' (150 m)
	0	05906	13:22:13	41	01.7	-70	31.3	
FLX	-1	05906	13:22:13	41	01.7	-70	31.3	flux leg southwest (240/)
	0	06168	13:26:35	40	57.8	-70	42.4	
PRO	-1	06168	13:26:35	40	57.8	-70	42.4	profile up/dn to 500' (150 m)
	0	06264	13:28:11	40	59.3	-70	42.9	
FLX	-1	06264	13:28:11	40	59.3	-70	42.9	flux leg east (085/)
	0	06632	13:34:19	40	59.8	-70	28.9	
PRO	-1	06632	13:34:19	40	59.8	-70	28.9	profile up/dn to 500' (150 m)
	0	06756	13:36:23	41	01.5	-70	31.1	
FLX	-1	06756	13:36:23	41	01.5	-70	31.1	flux leg southwest (245/)
	0	07028	13:40:55	40	57.5	-70	42.6	
PRO	-1	07097	13:42:04	40	58.6	-70	44.5	profile up to 4100' (1250 m)
	0	07393	13:47:00	41	07.2	-70	42.9	
PRO	-1	07399	13:47:06	41	07.4	-70	42.8	profile down from 4100' (1250 m)
	0	07711	13:52:18	41	16.7	-70	39.2	
FLX	-1	07824	13:54:11	41	16.1	-70	35.7	flux leg southeast (145/)
	0	07953	13:56:20	41	12.4	-70	33.1	
PRO	-1	07953	13:56:20	41	12.4	-70	33.1	profile up/dn to 500' (150 m)
	0	08050	13:57:57	41	11.1	-70	35.2	
FLX	-1	08050	13:57:57	41	11.1	-70	35.2	flux leg north (340/)
	0	08266	14:01:33	41	17.4	-70	40.0	
PRO	-1	08266	14:01:33	41	17.4	-70	40.0	profile up/dn to 500' (150 m)
	0	08379	14:03:26	41	18.0	-70	37.7	
FLX	-1	08379	14:03:26	41	18.0	-70	37.7	flux leg southeast (135/)
	0	08618	14:07:25	41	12.2	-70	31.4	
PRO	-1	08618	14:07:25	41	12.2	-70	31.4	profile up/dn to 500' (150 m)
	0	08730	14:09:17	41	11.1	-70	34.0	
FLX	-1	08730	14:09:17	41	11.1	-70	34.0	flux leg northwest (350/)
	0	08990	14:11:37	41	18.9	-70	36.9	

PRO -1 08990 14:11:37 41 18.9 -70 36.9 profile up/dn to 500' (150 m)
 0 09093 14:15:20 41 18.8 -70 34.4
 FLX -1 09093 14:15:20 41 18.8 -70 34.4 flux leg south (180/)
 0 09329 14:19:16 41 11.1 -70 35.6
 PRO -1 09329 14:19:16 41 11.1 -70 35.6 profile up/dn to 500' (150 m)
 0 09460 14:21:27 41 12.0 -70 38.3
 FLX -1 09460 14:21:27 41 12.0 -70 38.3 flux leg northeast (040/)
 0 09724 14:25:51 41 17.9 -70 32.9
 PRO -1 09724 14:25:51 41 17.9 -70 32.9 profile up/dn to 500' (150 m)
 0 09841 14:27:48 41 16.2 -70 32.0
 FLX -1 09841 14:27:48 41 16.2 -70 32.0 flux leg west (250/)
 0 10034 14:31:01 41 14.2 -70 40.3
 PRO -1 10034 14:31:01 41 14.2 -70 40.3 profile up/dn to 500' (150 m)
 0 10145 14:32:52 41 15.9 -70 41.0
 FLX -1 10145 14:32:52 41 15.9 -70 41.0 flux leg east (090/)
 0 10426 14:37:33 41 15.3 -70 30.8
 PRO -1 10426 14:37:33 41 15.3 -70 30.8 profile up/dn to 500' (150 m)
 0 10562 14:39:49 41 13.8 -70 33.0
 FLX -1 10562 14:39:49 41 13.8 -70 33.0 flux leg northwest (320/)
 0 10742 14:42:49 41 17.7 -70 38.7
 PRO -1 10742 14:42:49 41 17.7 -70 38.7 profile up/dn to 500' (150 m)
 0 10862 14:44:49 41 18.6 -70 37.2
 FLX -1 10862 14:44:49 41 18.6 -70 37.2 flux leg southeast (145/)
 0 11128 14:49:15 41 12.0 -70 32.3
 PRO -1 11140 14:49:27 41 11.7 -70 32.0 profile up to 4600' (1400 m)
 0 11708 14:58:55 41 12.6 -70 32.4
 PRO -1 11712 14:58:59 41 12.7 -70 32.5 profile down to MVY
 0 12295 15:08:42 41 23.6 -70 36.6
 STC -1 12400 15:10:27 41 23.3 -70 36.8 preparing to shut down all systems
 0 12420 15:10:47 41 23.3 -70 36.8

Marker for D:07301120.ORG CLOSED at 141057

Total scans: 12429
 Missed Ints: 00000
 BAT A: 0621450 of 0621450 000.000% Dropouts
 BAT B: 0621450 of 0621450 000.000% Dropouts
 ASH: 0062145 of 0062145 000.000% Dropouts
 TAN: 0123243 of 0124290 000.842% Dropouts

CBLAST-Low Pilot Study - Summer 2001

Flight: 11
 Date: 31 JUL 01 (Tuesday)
 Duration: 2.4 hr
 Pilot: Timothy L. Crawford

Summary: Infrared camera runs using the "mowing the lawn" flight plan just prior to and shortly after sunrise, profile, several north/south (040//220/) flux legs over ASIMET buoy with short altitude profiles.

Weather: Fair weather with a few high clouds from a low pressure system to the south quickly moving to the north and east. Light winds from the north with a confused wave state.

MVY ATIS: 0745 UTC 020/07 10V clear 15//13/ 30.15
 MVY ATIS: 0911 UTC 020/05 10V scat 440 scat 5000 17//15/ 30.19
 MVY ATIS: 0953 UTC 010/05 10V clear 13//12/ 30.18
 MVY ATIS: 1052 UTC 020/04 10V clear 17//15/ 30.19

Instrumentation Notes & Comments: None

Marker for D:07310909.ORG OPENED at 206940

STC	-1	00004	09:29:03	41	23.3	-70	36.8	all systems on
	0	00067	09:30:06	41	23.3	-70	36.8	
IRC	-1	00582	09:38:41	41	17.4	-70	32.2	W IR camera run @ 1280' (390 m)
	0	00756	09:41:35	41	16.7	-70	40.1	
IRC	-1	00846	09:43:05	41	15.0	-70	40.6	E IR camera run @ 1280' (390 m)
	0	01148	09:48:07	41	15.0	-70	29.9	
IRC	-1	01262	09:50:01	41	12.7	-70	30.2	W IR camera run @ 1280' (390 m)
	0	01484	09:53:43	41	12.7	-70	40.2	
IRC	-1	01582	09:55:21	41	11.0	-70	40.2	E IR camera run @ 1280' (390 m)
	0	01876	10:00:15	41	11.3	-70	29.9	
IRC	-1	01995	10:02:14	41	08.9	-70	30.0	W IR camera run @ 1280' (390 m)
	0	02233	10:06:12	41	08.7	-70	40.7	
IRC	-1	02333	10:07:52	41	07.0	-70	41.0	E IR camera run @ 1280' (390 m)
	0	02643	10:13:02	41	07.1	-70	29.9	
IRC	-1	02769	10:15:08	41	04.7	-70	30.4	W IR camera run @ 1280' (390 m)
	0	02987	10:18:46	41	04.7	-70	40.2	
IRC	-1	03080	10:20:19	41	02.9	-70	40.5	E IR camera run @ 1250' (390 m)
	0	03383	10:25:22	41	02.8	-70	29.8	
PRO	-1	03603	10:29:02	40	58.5	-70	33.8	profile down from 3900' (1200 m)
	0	04071	10:36:50	40	58.0	-70	39.0	
FLX	-1	04393	10:42:12	41	02.5	-70	34.4	flux leg south (200/)
	0	04632	10:46:11	40	54.7	-70	38.2	
PRO	-1	04632	10:46:11	40	54.7	-70	38.2	profile up/dn to 500' (150 m)
	0	04748	10:48:07	40	55.4	-70	40.5	
FLX	-1	04748	10:48:07	40	55.4	-70	40.5	flux leg northeast (040/)
	0	05112	10:54:11	41	03.6	-70	31.6	
PRO	-1	05112	10:54:11	41	03.6	-70	31.6	profile up/dn to 500' (150 m)
	0	05233	10:56:12	41	03.7	-70	34.4	
FLX	-1	05233	10:56:12	41	03.7	-70	34.4	flux leg south (200/)
	0	05517	11:00:56	40	54.7	-70	38.3	
PRO	-1	05517	11:00:56	40	54.7	-70	38.3	profile up/dn to 500' (150 m)
	0	05608	11:02:27	40	55.3	-70	40.2	
FLX	-1	05608	11:02:27	40	55.3	-70	40.2	flux leg northeast (040/)
	0	05983	11:08:42	41	03.4	-70	31.5	
PRO	-1	05983	11:08:42	41	03.4	-70	31.5	profile up/dn to 500' (150 m)
	0	06100	11:10:39	41	03.5	-70	34.1	
FLX	-1	06100	11:10:39	41	03.5	-70	34.1	flux leg south (200/)
	0	06389	11:15:28	40	54.5	-70	38.4	
PRO	-1	06389	11:15:28	40	54.5	-70	38.4	profile up/dn to 500' (150 m)
	0	06509	11:17:28	40	55.4	-70	38.9	
FLX	-1	06509	11:17:28	40	55.4	-70	38.9	flux leg northeast (030/)
	0	06866	11:23:25	41	03.8	-70	32.1	
PRO	-1	06866	11:23:25	41	03.8	-70	32.1	profile up/dn to 500' (150 m)
	0	06963	11:25:02	41	04.0	-70	34.0	
FLX	-1	06963	11:25:02	41	04.0	-70	34.0	flux leg south (200/)
	0	07271	11:30:10	40	54.3	-70	38.4	
PRO	-1	07345	11:31:24	40	54.3	-70	40.7	profile up to 4900'(1500 m)
	0	07766	11:38:25	41	06.2	-70	39.9	
PRO	-1	07766	11:38:25	41	06.2	-70	39.9	profile down to MVY
	0	08235	11:46:14	41	19.7	-70	39.1	
STC	-1	08574	11:51:53	41	23.3	-70	36.8	preparing to shut down all systems
	0	08635	11:52:54	41	23.3	-70	36.8	

Marker for D:07310909.ORG CLOSED at 215580

Total scans: 08640
Missed Ints: 00000
BAT A: 0432000 of 0432000 000.000% Dropouts
BAT B: 0432000 of 0432000 000.000% Dropouts
ASH: 0043200 of 0043200 000.000% Dropouts
TAN: 0085324 of 0086400 001.245% Dropouts

CBLAST-Low Pilot Study - Summer 2001

Flight: 12
Date: 01 AUG 01 (Wednesday)
Duration: 3.3 hr
Pilot: Timothy L. Crawford

Summary: Infrared camera run prior to sunrise, simple north-south, east-west box pattern at 1280' (390 m) prior to SAR overpass. Same box pattern flow at 10 m for SAR intercomparison at 1057 UTC. "Spirograph" flux legs over the ASIMET buoy with multiple short altitude profiles and a deep boundary layer profile.

Weather: Region dominated by high pressure with very light winds from the northwest to northeast. Wave state somewhat confused.

MVY ATIS: 0803 UTC calm 10V clear 14//14/ 30.23
MVY ATIS: 0835 UTC 320/03 10V clear 14//13/ 30.24
MVY ATIS: 0854 UTC 310/04 10V clear 14//13/ 30.24
MVY ATIS: 0937 UTC 330/03 08V clear 16//15/ 30.26
MVY ATIS: 0953 UTC calm 07V clear 16//15/ 30.37
MVY ATIS: 1153 UTC 020/06 10V clear 22//17/ 30.29

Instrumentation Notes & Comments: None

Marker for D:08010911.ORG OPENED at 294009

STC	-1	00004	09:40:12	41	23.3	-70	36.8	all systems on
	0	00065	09:41:13	41	23.3	-70	36.8	
IRC	-1	00354	09:46:02	41	21.1	-70	34.5	S IR camera run @ 1280' (390 m)
	0	00699	09:51:47	41	10.0	-70	35.5	
IRC	-1	00703	09:51:51	41	09.9	-70	35.5	S IR camera run @ 1280' (390 m)
	0	01121	09:58:49	40	55.8	-70	35.6	
IRC	-1	01173	09:59:41	40	55.0	-70	34.0	E IR camera run @ 1280' (390 m)
	0	01701	10:08:29	40	55.0	-70	10.5	
MSG		01741	10:09:09					BAT 0 frequency slow: Freq=49
MSG		01741	10:09:09					BAT 1 frequency slow: Freq=49
IRC	-1	01748	10:09:16	40	55.9	-70	09.4	N IR camera run @ 1280' (390 m)
	0	02188	10:16:36	41	08.9	-70	09.2	
FLX	-1	02249	10:17:37	41	09.5	-70	10.9	W IR camera run @ 1280' (390 m)
EVT		02666	10:24:34	41	09.9	-70	26.9	ship wake
	0	02883	10:28:11	41	09.9	-70	35.2	
PRO	-1	03025	10:30:33	41	13.2	-70	36.8	profile down from 3600' (1100 m)
	0	03452	10:37:40	41	13.0	-70	33.0	
FLX	-1	03585	10:39:53	41	10.1	-70	35.2	SAR flux leg south (180/)
	0	04058	10:47:46	40	55.9	-70	35.5	
FLX	-1	04110	10:48:38	40	55.0	-70	34.0	SAR flux leg east (090/)
	0	04688	10:58:16	40	55.0	-70	10.5	
FLX	-1	04739	10:59:07	40	55.9	-70	09.3	SAR flux leg north (000/)
	0	05208	11:06:56	41	09.0	-70	09.1	
FLX	-1	05259	11:07:47	41	09.7	-70	10.3	SAR flux leg west (270/)
	0	05961	11:19:29	41	09.9	-70	35.5	
PRO	-1	05965	11:19:33	41	09.9	-70	35.6	profile up to 3100' (950 m)
	0	06270	11:24:38	40	59.6	-70	36.0	
PRO	-1	06270	11:24:38	40	59.6	-70	36.0	profile down from 3100' (950 m)
	0	06531	11:28:59	40	54.6	-70	34.0	
FLX	-1	06534	11:29:02	40	54.7	-70	34.0	flux leg north (340/)
	0	06909	11:35:17	41	04.3	-70	38.2	
PRO	-1	06909	11:35:17	41	04.3	-70	38.2	profile up/dn to 500' (150 m)
	0	07008	11:36:56	41	02.9	-70	39.5	
FLX	-1	07008	11:36:56	41	02.9	-70	39.5	flux leg southeast (140/)
	0	07291	11:41:39	40	55.6	-70	31.5	
PRO	-1	07291	11:41:39	40	55.6	-70	31.5	profile up/dn to 500' (150 m)
	0	07401	11:43:29	40	56.8	-70	29.9	
FLX	-1	07401	11:43:29	40	56.8	-70	29.9	flux leg northwest (300/)
	0	07766	11:49:34	41	02.1	-70	41.8	

PRO -1 07766 11:49:34 41 02.1 -70 41.8 profile up/dn to 500' (150 m)
 0 07874 11:51:22 41 00.2 -70 42.0
 FLX -1 07874 11:51:22 41 00.2 -70 42.0 flux leg east (100/)
 0 08196 11:56:44 40 58.5 -70 28.4
 PRO -1 08196 11:56:44 40 58.5 -70 28.4 profile up/dn to 500' (150 m)
 0 08311 11:58:39 41 00.0 -70 28.7
 FLX -1 08311 11:58:39 41 00.0 -70 28.7 flux leg west (265/)
 0 08684 12:04:52 40 58.6 -70 42.5
 PRO -1 08684 12:04:52 40 58.6 -70 42.5 profile up/dn to 500' (150 m)
 0 08801 12:06:49 40 56.7 -70 41.2
 FLX -1 08801 12:06:49 40 56.7 -70 41.2 flux leg northeast (055/)
 0 09133 12:12:21 41 02.0 -70 30.1
 PRO -1 09133 12:12:21 41 02.0 -70 30.1 profile up/dn to 500' (150 m)
 0 09245 12:14:13 41 02.9 -70 31.7
 FLX -1 09245 12:14:13 41 02.9 -70 31.7 flux leg southwest (225/)
 0 09580 12:19:48 40 55.5 -70 40.4
 PRO -1 09580 12:19:48 40 55.5 -70 40.4 profile up/dn to 500' (150 m)
 0 09697 12:21:45 40 54.6 -70 38.3
 FLX -1 09697 12:21:45 40 54.6 -70 38.3 flux leg north (015/)
 0 10058 12:27:46 41 04.3 -70 33.6
 PRO -1 10058 12:27:46 41 04.3 -70 33.6 profile up/dn to 500' (150 m)
 0 10160 12:29:28 41 23.2 -70 33.5
 FLX -1 10160 12:29:28 41 23.2 -70 33.5 flux leg south (180/)
 0 10467 12:34:35 40 54.9 -70 35.7
 PRO -1 10550 12:35:58 40 54.9 -70 35.0 profile up to 4600' (1400 m)
 0 11002 12:43:30 41 08.5 -70 37.2
 FRY -1 11010 12:43:38 41 08.8 -70 37.3 return to MVY
 0 11531 12:52:19 41 23.7 -70 36.6

Marker for D:08010911.ORG CLOSED at 305700

Total scans: 11691

Missed Ints: 00000

BAT A: 0584549 of 0584550 000.000% Dropouts

BAT B: 0584549 of 0584550 000.000% Dropouts

ASH: 0058455 of 0058455 000.000% Dropouts

TAN: 0115974 of 0116910 000.801% Dropouts

CBLAST-Low Pilot Study - Summer 2001

Flight: 13

Date: 01 AUG 01 (Wednesday)

Duration: 2.8 hr

Pilot: Timothy L. Crawford

Summary: East-west "bow tie" flux runs near and over the R/V Asterias
 and "spirograph" flux runs over the ASIMET buoy, profiles.

Weather: Region dominated by high pressure with light and variable
 winds. Wave state somewhat confused.

MVY ATIS: 1553 UTC 080/06 10V clear 26//18/ 30.29

MVY ATIS: 1852 UTC 210/06 10V clear 26// 30.30

Instrumentation Notes & Comments: None

Marker for D:08011644.ORG OPENED at 320069

PRO -1 00361 17:00:29 41 20.1 -70 32.2 profile down from 1000' (300 m)
 0 00547 17:03:35 41 18.8 -70 29.4
 FLX -1 00622 17:04:50 41 18.5 -70 32.7 flux leg west (255/)
 0 00842 17:08:30 41 16.9 -70 41.3
 PRO -1 00842 17:08:30 41 16.9 -70 41.3 profile up/dn to 500' (150 m)
 0 00947 17:10:15 41 18.5 -70 41.0

FLX	-1	00947	17:10:15	41	18.5	-70	41.0	flux leg east (100/)
	0	01292	17:16:00	41	16.6	-70	27.7	
PRO	-1	01292	17:16:00	41	16.6	-70	27.7	profile up/dn to 500' (150 m)
	0	01419	17:18:07	41	18.2	-70	28.3	
FLX	-1	01419	17:18:07	41	18.2	-70	28.3	flux leg west (260/)
	0	01740	17:23:28	41	16.6	-70	41.4	
PRO	-1	01740	17:23:28	41	16.6	-70	41.4	profile up/dn to 500' (150 m)
	0	01845	17:25:13	41	18.1	-70	41.1	
FLX	-1	01845	17:25:13	41	18.1	-70	41.1	flux leg east (100/)
	0	02188	17:30:56	41	16.7	-70	27.9	
PRO	-1	02188	17:30:56	41	16.7	-70	27.9	profile up/dn to 500' (150 m)
	0	02292	17:32:40	41	18.3	-70	27.9	
FLX	-1	02292	17:32:40	41	18.3	-70	27.9	flux leg west (260/)
	0	02615	17:38:03	41	16.8	-70	41.1	
PRO	-1	02615	17:38:03	41	16.8	-70	41.1	profile up/dn to 500' (150 m)
	0	02716	17:39:44	41	16.2	-70	39.8	
FLX	-1	02716	17:39:44	41	16.2	-70	39.8	flux leg east (090/)
	0	03028	17:44:56	41	16.8	-70	27.5	
PRO	-1	03028	17:44:56	41	16.8	-70	27.5	profile up/dn to 500' (150 m)
	0	03142	17:46:50	41	15.4	-70	28.5	
FLX	-1	03142	17:46:50	41	15.4	-70	28.5	flux leg west (270/)
	0	03456	17:52:04	41	16.2	-70	41.5	
PRO	-1	03456	17:52:04	41	16.2	-70	41.5	profile up/dn to 500' (150 m)
	0	03540	17:53:28	41	15.6	-70	41.6	
FLX	-1	03540	17:53:28	41	15.6	-70	41.6	flux leg east (090/)
	0	03883	17:59:11	41	16.0	-70	27.7	
PRO	-1	03883	17:59:11	41	16.0	-70	27.7	profile up/dn to 500' (150 m)
	0	03962	18:00:30	41	14.6	-70	27.8	
FLX	-1	03962	18:00:30	41	14.6	-70	27.8	flux leg west (275/)
	0	04299	18:06:07	41	16.2	-70	40.9	
PRO	-1	04299	18:06:07	41	16.2	-70	40.9	profile up/dn to 500' (150 m)
	0	04379	18:07:37	41	15.4	-70	39.6	
FLX	-1	04379	18:07:37	41	15.4	-70	39.6	flux leg east (095/)
	0	04662	18:12:10	41	15.3	-70	28.0	
PRO	-1	04662	18:12:10	41	15.3	-70	28.0	profile up to 1600' (500 m)
	0	04823	18:14:51	41	10.7	-70	29.0	
PRO	-1	04823	18:14:51	41	10.7	-70	29.0	profile down from 1600' (500 m)
	0	04960	18:17:08	41	07.2	-70	32.2	
FLX	-1	04963	18:17:11	41	07.1	-70	32.3	flux leg south (200/)
	0	05426	18:24:54	40	54.7	-70	38.3	
PRO	-1	05426	18:24:54	40	54.7	-70	38.3	profile up/dn to 500' (150 m)
	0	05544	18:26:52	40	54.6	-70	35.8	
FLX	-1	05544	18:26:52	40	54.6	-70	35.8	flux leg north (355/)
	0	05872	18:32:20	41	04.7	-70	36.0	
PRO	-1	05872	18:32:20	41	04.7	-70	36.0	profile up/dn to 500' (150 m)
	0	05979	18:34:07	41	04.3	-70	38.0	
FLX	-1	05979	18:34:07	41	04.3	-70	38.0	flux leg south (165/)
	0	06315	18:39:43	40	54.7	-70	33.7	
PRO	-1	06315	18:39:43	40	54.7	-70	33.7	profile up/dn to 500' (150 m)
	0	06431	18:41:39	40	55.6	-70	31.6	
FLX	-1	06431	18:41:39	40	55.6	-70	31.6	flux leg northwest (315/)
	0	06775	18:47:23	41	03.4	-70	40.2	
PRO	-1	06775	18:47:23	41	03.4	-70	40.2	profile up/dn to 500' (150 m)
	0	06891	18:49:19	41	02.0	-70	41.3	
FLX	-1	06891	18:49:19	41	02.0	-70	41.3	flux leg southeast (125/)
	0	07206	18:54:34	40	57.0	-70	30.0	
PRO	-1	07206	18:54:34	40	57.0	-70	30.0	profile up/dn to 500' (150 m)
	0	07324	18:56:32	40	58.7	-70	29.3	
FLX	-1	07324	18:56:32	40	58.7	-70	29.3	flux leg west (280/)
	0	07683	19:02:31	41	00.3	-70	42.8	
PRO	-1	07683	19:02:31	41	00.3	-70	42.8	profile up/dn to 500' (150 m)
	0	07788	19:04:16	40	58.6	-70	42.7	
FLX	-1	07788	19:04:16	40	58.6	-70	42.7	flux leg east (080/)
	0	08105	19:09:33	41	00.3	-70	29.2	
PRO	-1	08105	19:09:33	41	00.3	-70	29.2	profile up/dn to 500' (150 m)

```

    0 08225 19:11:33 41 02.1 -70 29.8
FLX -1 08225 19:11:33 41 02.1 -70 29.8 flux leg southwest (245/)
    0 08588 19:17:36 40 57.1 -70 41.8
PRO -1 08588 19:17:36 40 57.1 -70 41.8 profile up/dn to 500' (150 m)
    0 08704 19:19:32 40 55.7 -70 40.1
FLX -1 08704 19:19:32 40 55.7 -70 40.1 flux leg northeast (040/)
    0 09034 19:25:02 41 03.4 -70 31.5
PRO -1 09038 19:25:06 41 03.5 -70 31.4 profile up to 3600' (1100 m)
MSG 09319 19:29:47 BAT 0 frequency slow: Freq=49
MSG 09319 19:29:47 BAT 1 frequency slow: Freq=49
    0 09405 19:31:13 41 14.2 -70 34.6
PRO -1 09407 19:31:15 41 14.3 -70 34.6 profile down to MVY
    0 09833 19:38:21 41 23.3 -70 37.0
STC -1 09908 19:39:36 41 23.3 -70 36.8 preparing to shut down all systems
    0 09960 19:40:28 41 23.3 -70 36.8

```

Marker for D:08011644.ORG CLOSED at 330034

```

Total scans: 09965
Missed Ints: 00000
    BAT A: 0498249 of 0498250 000.000% Dropouts
    BAT B: 0498249 of 0498250 000.000% Dropouts
    ASH: 0049825 of 0049825 000.000% Dropouts
    TAN: 0099041 of 0099650 000.611% Dropouts

```

CBLAST-Low Pilot Study - Summer 2001

```

Flight: 14
Date: 02 AUG 01 (Thursday)
Duration: 2.4 hr
Pilot: Timothy L. Crawford

```

Summary: Late morning flight, IR camera run with simple box pattern around ASIMET buoy, "spirograph" flux legs with short profiles over ASIMET buoy, profiles.

Weather: Very hazy, hot, and humid, light southwesterly winds as a high pressure system slowly moves eastward.

```

MVY ATIS: 1352 UTC 230/08 10V clear 25//20/ 30.25
MVY ATIS: 1652 UTC 220/09 10V clear 26//20/ 30.21

```

Instrumentation Notes & Comments: None

Marker for D:08021423.ORG OPENED at 398843

```

STC -1 00006 14:47:28 41 23.3 -70 36.8 all systems on
    0 00062 14:48:24 41 23.3 -70 36.8
PRO -1 00521 14:56:03 41 17.1 -70 35.6 profile up to 4000' (1200 m)
    0 00877 15:01:59 41 06.6 -70 35.5
PRO -1 00882 15:02:04 41 06.4 -70 35.5 profile down from 4000' (1200 m)
    0 01362 15:10:04 40 54.1 -70 43.4
IRC -1 01606 15:14:08 40 49.3 -70 46.9 E IR camera run @ 1280' (390 m)
    0 02098 15:22:20 40 49.3 -70 25.1
IRC -1 02145 15:23:07 40 50.3 -70 23.8 N IR camera run @ 1280' (390 m)
    0 02727 15:32:49 41 09.0 -70 23.9
IRC -1 02773 15:33:35 41 09.7 -70 25.0 W IR camera run @ 1280' (390 m)
    0 03329 15:42:51 41 09.7 -70 44.7
IRC -1 03376 15:43:38 41 08.8 -70 45.5 S IR camera run @ 1280' (390 m)
    0 03702 15:49:04 40 59.7 -70 45.1
FLX -1 03802 15:50:44 40 59.0 -70 41.4 flux leg east (085/)
EVT 04036 15:54:38 41 00.2 -70 31.7 wake
    0 04097 15:55:39 41 00.4 -70 29.2
FLX -1 04226 15:57:48 41 02.2 -70 29.8 flux leg southwest (240/)

```

	0	04604	16:04:06	40	57.0	-70	41.8	
PRO	-1	04604	16:04:06	40	57.0	-70	41.8	profile up/dn to 500' (150 m)
	0	04704	16:05:46	40	55.6	-70	40.0	
FLX	-1	04704	16:05:46	40	55.6	-70	40.0	flux leg northeast (040/)
	0	05012	16:10:54	41	03.6	-70	31.6	
PRO	-1	05012	16:10:54	41	03.6	-70	31.6	profile up/dn to 500' (150 m)
	0	05140	16:13:02	41	04.2	-70	33.6	
FLX	-1	05140	16:13:02	41	04.2	-70	33.6	flux leg southwest (205/)
	0	05511	16:19:13	40	54.6	-70	38.5	
PRO	-1	05511	16:19:13	40	54.6	-70	38.5	profile up/dn to 500' (150 m)
	0	05623	16:21:05	40	54.1	-70	35.8	
FLX	-1	05623	16:21:05	40	54.1	-70	35.8	flux leg north (355/)
	0	05944	16:26:26	41	04.7	-70	35.9	
PRO	-1	05944	16:26:26	41	04.7	-70	35.9	profile up/dn to 500' (150 m)
	0	06057	16:28:19	41	04.6	-70	37.9	
FLX	-1	06057	16:28:19	41	04.6	-70	37.9	flux leg south (165/)
EVT		06126	16:29:28	41	02.7	-70	37.0	visible surface change
	0	06428	16:34:30	40	54.4	-70	33.3	
PRO	-1	06428	16:34:30	40	54.4	-70	33.3	profile up/dn to 500' (150 m)
	0	06533	16:36:15	40	55.4	-70	30.8	
FLX	-1	06533	16:36:15	40	55.4	-70	30.8	flux leg northwest (315/)
	0	06886	16:42:08	41	03.5	-70	40.2	
PRO	-1	06886	16:42:08	41	03.5	-70	40.2	profile up/dn to 500' (150 m)
	0	06995	16:43:57	41	02.2	-70	41.2	
FLX	-1	06995	16:43:57	41	02.2	-70	41.2	flux leg southeast (130/)
	0	07322	16:49:24	40	57.0	-70	29.9	
PRO	-1	07322	16:49:24	40	57.0	-70	29.9	profile up/dn to 500' (150 m)
	0	07426	16:51:08	40	58.7	-70	28.4	
FLX	-1	07426	16:51:08	40	58.7	-70	28.4	flux leg west (275/)
	0	07804	16:57:26	41	00.4	-70	42.5	
PRO	-1	07854	16:58:16	41	01.6	-70	42.7	profile up to 4300' (1300 m)
	0	08233	17:04:35	41	14.6	-70	38.0	
PRO	-1	08236	17:04:38	41	14.7	-70	37.9	profile down to MVY
	0	08595	17:10:37	41	23.4	-70	36.8	
STC	-1	08669	17:11:51	41	23.3	-70	36.8	preparing to shut down all systems
	0	08709	17:12:31	41	23.3	-70	36.8	

Marker for D:08021423.ORG CLOSED at 407556

Total scans: 08713
Missed Ints: 00000
BAT A: 0435650 of 0435650 000.000% Dropouts
BAT B: 0435650 of 0435650 000.000% Dropouts
ASH: 0043565 of 0043565 000.000% Dropouts
TAN: 0086800 of 0087130 000.379% Dropouts

CBLAST-Low Pilot Study - Summer 2001

Flight: 15
Date: 03 AUG 01 (Friday)
Duration: 1.9 hr
Pilot: Timothy L. Crawford

Summary: Nighttime flight for infrared camera runs using the "mowing the lawn" flight plan after sunset.

Weather: Hazy and humid, steady southwesterly winds as a high pressure system slowly moves eastward.

MVY ATIS: 2252 UTC 240/10 10V clear 23//18/ 30.11
MVY ATIS: 2357 UTC 250/11 10V clear 22//17/ 30.11
MVY ATIS: 0213 UTC 260/10/G18 10V clear 22//17/ 30.11

Instrumentation Notes & Comments:

Data acquisition system booted up after takeoff and shut down prior to landing for this nighttime flight (power needed for landing lights).

Marker for D:08030052.ORG OPENED at 435501

IRC	-1	00001	00:58:21	41	17.0	-70	33.0	W	IR camera run @ 1280' (390 m)
		0	00241	01:02:21	41	17.0	-70	39.6	
IRC	-1	00333	01:03:53	41	15.8	-70	39.0	E	IR camera run @ 1280' (390 m)
		0	00551	01:07:31	41	15.9	-70	27.1	
IRC	-1	00668	01:09:28	41	14.2	-70	26.0	W	IR camera run @ 1280' (390 m)
		0	01166	01:17:46	41	14.3	-70	40.1	
IRC	-1	01240	01:19:00	41	13.1	-70	39.1	E	IR camera run @ 1280' (390 m)
		0	01415	01:21:55	41	13.3	-70	29.8	
IRC	-1	01521	01:23:41	41	11.6	-70	28.6	W	IR camera run @ 1280' (390 m)
		0	01925	01:30:25	41	11.5	-70	40.4	
IRC	-1	01995	01:31:35	41	10.2	-70	39.0	E	IR camera run @ 1280' (390 m)
		0	02165	01:34:25	41	10.4	-70	29.8	
IRC	-1	02255	01:35:55	41	08.7	-70	28.2	W	IR camera run @ 1280' (390 m)
		0	02630	01:42:10	41	08.5	-70	40.2	
IRC	-1	02714	01:43:34	41	07.2	-70	38.7	E	IR camera run @ 1280' (390 m)
		0	02875	01:46:15	41	07.5	-70	29.6	
IRC	-1	02959	01:47:39	41	09.5	-70	28.7	W	IR camera run @ 1280' (390 m)
		0	03321	01:53:41	41	09.5	-70	40.1	
IRC	-1	03438	01:55:38	41	12.1	-70	38.5	E	IR camera run @ 1280' (390 m)
		0	03593	01:58:13	41	12.5	-70	29.6	
IRC	-1	03682	01:59:42	41	14.5	-70	28.6	W	IR camera run @ 1280' (390 m)
		0	04059	02:05:59	41	14.3	-70	40.2	
IRC	-1	04178	02:07:58	41	17.0	-70	38.7	E	IR camera run @ 1280' (390 m)
		0	04334	02:10:34	41	17.2	-70	29.7	
IRC	-1	04422	02:12:02	41	19.2	-70	28.7	W	IR camera run @ 1280' (390 m)
		0	04782	02:18:02	41	19.1	-70	39.9	
IRC	-1	04876	02:19:36	41	20.8	-70	39.1	E	IR camera run @ 1280' (390 m)
		0	05022	02:22:02	41	21.2	-70	30.6	

Marker for D:08030052.ORG CLOSED at 440550

Total scans: 05049

Missed Ints: 00000

BAT A: 0252450 of 0252450 000.000% Dropouts

BAT B: 0252450 of 0252450 000.000% Dropouts

ASH: 0025245 of 0025245 000.000% Dropouts

TAN: 0039478 of 0050490 021.810% Dropouts

CBLAST-Low Pilot Study - Summer 2001

Flight: 16

Date: 05 AUG 01 (Sunday)

Duration: 0.7 hr

Pilot: Timothy L. Crawford

Summary: Flight terminated because of heavy offshore fog and poor visibility.

Weather: Hazy, hot, and humid, light southwesterly winds ahead of a stalled cold front.

MVY ATIS: 1453 UTC calm 05V haze 1,200' broken 25//22/ 30.14

MVY ATIS: 1553 UTC calm 03V haze 1,900' broken 26//22/ 30.14

Instrumentation Notes & Comments:

University of Washington/WHOI infrared/visible camera system removed

Marker for D:08051541.ORG OPENED at 057063

STC -1 00005 15:51:07 41 23.3 -70 36.8 all systems on
0 00063 15:52:05 41 23.3 -70 36.8
PRO -1 00635 16:01:37 41 19.6 -70 34.6 profile up to 3300' (1000 m)
0 00944 16:06:46 41 10.3 -70 30.7
PRO -1 00946 16:06:48 41 10.2 -70 30.7 profile down from 3300' (1000 m)
0 01581 16:17:23 41 00.8 -70 36.5

Marker for D:08051541.ORG CLOSED at 059436

Total scans: 02373
Missed Ints: 00000
BAT A: 0118650 of 0118650 000.000% Dropouts
BAT B: 0118650 of 0118650 000.000% Dropouts
ASH: 0011865 of 0011865 000.000% Dropouts
TAN: 0023636 of 0023730 000.396% Dropouts

CBLAST-Low Pilot Study - Summer 2001

Flight: 17
Date: 05 AUG 01 (Sunday)
Duration: 0.8 hr
Pilot: Timothy L. Crawford

Summary: Flight terminated because of heavy offshore fog and poor visibility.

Weather: Hazy, hot, and humid, light southwesterly winds ahead of a stalled cold front.

MVY ATIS: 1952 UTC 220/10 05V haze 1800' broken 24//21/ 30.15

Instrumentation Notes & Comments: None

Marker for D:08052006.ORG OPENED at 072672

STC -1 00002 20:11:13 41 23.3 -70 36.8 all systems on
0 00202 20:14:33 41 23.5 -70 36.8
PRO -1 00624 20:21:35 41 19.2 -70 37.7 profile down from 1400' (440 m)
0 00836 20:25:07 41 20.4 -70 37.6

Marker for D:08052006.ORG CLOSED at 075326

Total scans: 02654
Missed Ints: 00000
BAT A: 0132700 of 0132700 000.000% Dropouts
BAT B: 0132700 of 0132700 000.000% Dropouts
ASH: 0013270 of 0013270 000.000% Dropouts
TAN: 0026529 of 0026540 000.041% Dropouts

CBLAST-Low Pilot Study - Summer 2001

Flight: 18
Date: 07 AUG 01 (Tuesday)
Duration: 4.1 hr
Pilot: Timothy L. Crawford

Summary: "Spirograph" and "bow tie" flux legs with short profiles over ASIMET and near-shore buoy, profiles. Flight visibility about half a of mile.

Weather: Hazy, hot, and humid, moderate southwesterly winds ahead of a stalled cold front.

MVY ATIS: 1252 UTC 270/07 03V mist clear 26//23/ 29.96
MVY ATIS: 1455 UTC 210/12 04V haze clear 27//23/ 29.95
MVY ATIS: 1652 UTC 230/09 04V haze clear 28//23/ 29.91

Instrumentation Notes & Comments:

DGPS corrections unavailable after scan 13635 (flykin solution fails)

Marker for D:08071320.ORG OPENED at 221359

STC	-1	00003	13:29:21	41	23.3	-70	36.8	all systems on
		0	00076	13:30:34	41	23.3	-70	36.9
FLX	-1	00535	13:38:13	41	19.7	-70	35.7	flux leg south (180/)
		0	00871	13:43:49	41	10.2	-70	34.7
PRO	-1	00871	13:43:49	41	10.2	-70	34.7	profile up/dn to 500' (150 m)
		0	01101	13:47:39	41	13.7	-70	35.4
FLX	-1	01101	13:47:39	41	13.7	-70	35.4	flux leg northwest (335/)
		0	01329	13:51:27	41	20.0	-70	38.2
PRO	-1	01329	13:51:27	41	20.0	-70	38.2	profile up/dn to 500' (150 m)
		0	01464	13:53:42	41	18.3	-70	38.1
FLX	-1	01464	13:53:42	41	18.3	-70	38.1	flux leg southeast (150/)
		0	01766	13:58:44	41	11.2	-70	31.0
PRO	-1	01766	13:58:44	41	11.2	-70	31.0	profile up/dn to 500' (150 m)
		0	01866	14:00:24	41	12.5	-70	29.6
FLX	-1	01866	14:00:24	41	12.5	-70	29.6	flux leg northwest (295/)
		0	02228	14:06:26	41	17.8	-70	41.5
PRO	-1	02228	14:06:26	41	17.8	-70	41.5	profile up/dn to 500' (150 m)
		0	02324	14:08:02	41	16.8	-70	41.1
FLX	-1	02324	14:08:02	41	16.8	-70	41.1	flux leg east (110/)
		0	02627	14:13:05	41	14.7	-70	28.8
PRO	-1	02627	14:13:05	41	14.7	-70	28.8	profile up/dn to 500' (150 m)
		0	02732	14:14:50	41	16.4	-70	27.8
FLX	-1	02732	14:14:50	41	16.4	-70	27.8	flux leg west (255/)
		0	03149	14:21:47	41	14.4	-70	42.2
PRO	-1	03149	14:21:47	41	14.4	-70	42.2	profile up/dn to 500' (150 m)
		0	03253	14:23:31	41	13.0	-70	41.0
FLX	-1	03253	14:23:31	41	13.0	-70	41.0	flux leg northeast (060/)
		0	03545	14:28:23	41	18.1	-70	29.7
PRO	-1	03545	14:28:23	41	18.1	-70	29.7	profile up/dn to 500' (150 m)
		0	03645	14:30:03	41	19.7	-70	30.2
FLX	-1	03645	14:30:03	41	19.7	-70	30.2	flux leg southwest (220/)
		0	04060	14:36:58	41	11.4	-70	40.0
PRO	-1	04060	14:36:58	41	11.4	-70	40.0	profile up/dn to 500' (150 m)
		0	04177	14:38:55	41	11.2	-70	37.3
FLX	-1	04177	14:38:55	41	11.2	-70	37.3	flux leg north (015/)
		0	04477	14:43:55	41	20.5	-70	33.1
PRO	-1	04477	14:43:55	41	20.5	-70	33.1	profile up/dn to 500' (150 m)
		0	04570	14:45:28	41	19.6	-70	32.0
FLX	-1	04570	14:45:28	41	19.6	-70	32.0	flux leg southwest (220/)
		0	04944	14:51:42	41	11.1	-70	39.5
PRO	-1	04944	14:51:42	41	11.1	-70	39.5	profile up/dn to 500' (150 m)
		0	05032	14:53:10	41	12.3	-70	40.4
FLX	-1	05032	14:53:10	41	12.3	-70	40.4	flux leg northeast (050/)
		0	05318	14:57:56	41	18.5	-70	30.1
PRO	-1	05318	14:57:56	41	18.5	-70	30.1	profile up/dn to 500' (150 m)
		0	05412	14:59:30	41	19.7	-70	31.3
FLX	-1	05412	14:59:30	41	19.7	-70	31.3	flux leg southwest (215/)
		0	05801	15:05:59	41	11.1	-70	39.6
PRO	-1	05801	15:05:59	41	11.1	-70	39.6	profile up/dn to 500' (150 m)
		0	05896	15:07:34	41	12.8	-70	39.9
FLX	-1	05896	15:07:34	41	12.8	-70	39.9	flux leg northeast (060/)
		0	06164	15:12:02	41	18.0	-70	29.5
PRO	-1	06164	15:12:02	41	18.0	-70	29.5	profile up/dn to 500' (150 m)
		0	06272	15:13:50	41	19.3	-70	30.4
FLX	-1	06272	15:13:50	41	19.3	-70	30.4	flux leg southwest (220/)

0	06674	15:20:32	41	11.1	-70	39.4	
PRO	-1	06701	15:20:59	41	10.5	-70	40.0 profile up to 3300' (1000 m)
0	06987	15:25:45	41	02.0	-70	34.7	
PRO	-1	06989	15:25:47	41	02.0	-70	34.7 profile down from 3300' (1000 m)
0	07318	15:31:16	40	54.4	-70	36.0	
FLX	-1	07322	15:31:20	40	54.6	-70	36.0 flux leg north (355/)
0	07625	15:36:23	41	04.7	-70	36.1	
PRO	-1	07625	15:36:23	41	04.7	-70	36.1 profile up/dn to 500' (150 m)
0	07728	15:38:06	41	04.4	-70	37.9	
FLX	-1	07728	15:38:06	41	04.4	-70	37.9 flux leg south (170/)
0	08092	15:44:10	40	54.4	-70	33.8	
PRO	-1	08092	15:44:10	40	54.4	-70	33.8 profile up/dn to 500' (150 m)
0	08194	15:45:52	40	55.8	-70	31.9	
FLX	-1	08194	15:45:52	40	55.8	-70	31.9 flux leg northwest (310/)
0	08518	15:51:16	41	03.3	-70	40.3	
PRO	-1	08518	15:51:16	41	03.3	-70	40.3 profile up/dn to 500' (150 m)
0	08625	15:53:03	41	02.0	-70	40.9	
FLX	-1	08625	15:53:03	41	02.0	-70	40.9 flux leg southeast (130/)
0	08940	15:58:18	40	56.7	-70	29.7	
PRO	-1	08940	15:58:18	40	56.7	-70	29.7 profile up/dn to 500' (150 m)
0	09065	16:00:23	40	58.9	-70	28.3	
FLX	-1	09065	16:00:23	40	58.9	-70	28.3 flux leg west (270/)
0	09454	16:06:52	41	00.3	-70	42.7	
PRO	-1	09454	16:06:52	41	00.3	-70	42.7 profile up/dn to 500' (150 m)
0	09556	16:08:34	40	58.7	-70	41.9	
FLX	-1	09556	16:08:34	40	58.7	-70	41.9 flux leg east (085/)
0	09895	16:14:13	41	01.1	-70	27.1	
PRO	-1	09895	16:14:13	41	01.1	-70	27.1 profile up/dn to 500' (150 m)
0	10013	16:16:11	41	02.6	-70	28.0	
FLX	-1	10013	16:16:11	41	02.6	-70	28.0 flux leg southwest (240/)
0	10475	16:23:53	40	56.9	-70	41.9	
PRO	-1	10475	16:23:53	40	56.9	-70	41.9 profile up/dn to 500' (150 m)
0	10584	16:25:42	40	55.8	-70	39.7	
FLX	-1	10584	16:25:42	40	55.8	-70	39.7 flux leg northeast (040/)
0	10866	16:30:24	41	03.6	-70	31.7	
PRO	-1	10866	16:30:24	41	03.6	-70	31.7 profile up/dn to 500' (150 m)
0	10986	16:32:24	41	04.7	-70	33.5	
FLX	-1	10986	16:32:24	41	04.7	-70	33.5 flux leg south (200/)
0	11400	16:39:18	40	54.3	-70	38.4	
PRO	-1	11400	16:39:18	40	54.3	-70	38.4 profile up/dn to 500' (150 m)
0	11526	16:41:24	40	54.9	-70	39.8	
FLX	-1	11526	16:41:24	40	54.9	-70	39.8 flux leg northeast (040/)
0	11824	16:46:22	41	02.9	-70	30.8	
PRO	-1	11824	16:46:22	41	02.9	-70	30.8 profile up/dn to 500' (150 m)
0	11921	16:47:59	41	01.9	-70	29.4	
FLX	-1	11921	16:47:59	41	01.9	-70	29.4 flux leg southwest (240/)
0	12318	16:54:36	40	57.1	-70	42.0	
PRO	-1	12318	16:54:36	40	57.1	-70	42.0 profile up/dn to 500' (150 m)
0	12422	16:56:20	40	55.8	-70	40.0	
FLX	-1	12422	16:56:20	40	55.8	-70	40.0 flux leg northeast (040/)
0	12713	17:01:11	41	03.7	-70	31.6	
PRO	-1	12713	17:01:11	41	03.7	-70	31.6 profile up/dn to 500' (150 m)
0	12818	17:02:56	41	02.6	-70	30.4	
FLX	-1	12818	17:02:56	41	02.6	-70	30.4 flux leg southwest (235/)
0	13229	17:09:38	40	56.7	-70	42.3	
PRO	-1	13229	17:09:38	40	56.7	-70	42.3 profile up/dn to 500' (150 m)
0	13332	17:11:30	40	56.4	-70	38.9	
FLX	-1	13332	17:11:30	40	56.4	-70	38.9 flux leg northeast (040/)
0	13589	17:15:47	41	03.4	-70	31.3	

Marker for D:08071320.ORG CLOSED at 235921

Total scans: 14558

Missed Ints: 00004

BAT A: 0727898 of 0727900 000.000% Dropouts

BAT B: 0727898 of 0727900 000.000% Dropouts
ASH: 0072750 of 0072790 000.055% Dropouts
TAN: 0145105 of 0145580 000.326% Dropouts

CBLAST-Low Pilot Study - Summer 2001

Flight: 19
Date: 08 AUG 01 (Wednesday)
Duration: 4.0 hr
Pilot: Timothy L. Crawford

Summary: SAR overpass, "spirograph" and "bow tie" flux legs with short profiles over ASIMET and near-shore buoy, profiles.

Weather: Hazy, very hot, and humid, very light northwesterly winds ahead of a stalled cold front.

MVY ATIS: 0921 UTC calm 04V mist clear 20//19/ 29.86
MVY ATIS: 0953 UTC 190/06 03V clear 20//19/ 29.87
MVY ATIS: 1301 UTC 010/03 07V clear 28//22/ 29.88

Instrumentation Notes & Comments:

Data not differentially corrected prior to 01275, ground station off

Marker for D:08080955.ORG OPENED at 295384

FLX	-1	01640	10:30:23	41	12.8	-70	36.0	SAR flux leg south (180/)
		0	02192	10:39:35	40	56.1	-70	35.6
FLX	-1	02249	10:40:32	40	55.1	-70	34.1	SAR flux leg east (090/)
		0	02800	10:49:43	40	55.1	-70	10.6
FLX	-1	02855	10:50:38	40	56.2	-70	09.1	SAR flux leg north (000/)
		0	03263	10:57:26	41	08.9	-70	09.2
FLX	-1	03313	10:58:16	41	09.7	-70	10.5	SAR flux leg west (270/)
		0	03994	11:09:37	41	10.1	-70	36.2
PRO	-1	04005	11:09:48	41	10.1	-70	36.6	profile up to 4000' (1200 m)
		0	04350	11:15:33	40	59.3	-70	36.2
PRO	-1	04353	11:15:36	40	59.2	-70	36.2	profile down from 4000' (1200 m)
		0	04544	11:18:47	40	52.9	-70	36.6
FLX	-1	04610	11:19:53	40	53.1	-70	35.1	flux leg north (355/)
		0	04986	11:26:09	41	04.6	-70	35.9
PRO	-1	04986	11:26:09	41	04.6	-70	35.9	profile up/dn to 500' (150 m)
		0	05100	11:28:03	41	03.9	-70	37.9
FLX	-1	05100	11:28:03	41	03.9	-70	37.9	flux leg south (165/)
		0	05418	11:33:21	40	54.7	-70	33.9
PRO	-1	05418	11:33:21	40	54.7	-70	33.9	profile up/dn to 500' (150 m)
		0	05524	11:35:07	40	55.3	-70	31.3
FLX	-1	05524	11:35:07	40	55.3	-70	31.3	flux leg northwest (315/)
		0	05877	11:41:00	41	03.4	-70	40.3
PRO	-1	05877	11:41:00	41	03.4	-70	40.3	profile up/dn to 500' (150 m)
		0	05986	11:42:49	41	01.8	-70	41.2
FLX	-1	05986	11:42:49	41	01.8	-70	41.2	flux leg southeast (125/)
		0	06282	11:47:45	40	57.0	-70	29.9
PRO	-1	06282	11:47:45	40	57.0	-70	29.9	profile up/dn to 500' (150 m)
		0	06391	11:49:34	40	58.8	-70	28.7
FLX	-1	06391	11:49:34	40	58.8	-70	28.7	flux leg west (275/)
		0	06743	11:55:26	41	00.3	-70	42.5
PRO	-1	06743	11:55:26	41	00.3	-70	42.5	profile up/dn to 500' (150 m)
		0	06846	11:57:09	40	58.5	-70	41.9
FLX	-1	06846	11:57:09	40	58.5	-70	41.9	flux leg east (080/)
		0	07143	12:02:06	41	00.4	-70	29.2
PRO	-1	07143	12:02:06	41	00.4	-70	29.2	profile up/dn to 500' (150 m)
		0	07246	12:03:49	41	01.8	-70	30.1
FLX	-1	07246	12:03:49	41	01.8	-70	30.1	flux leg southwest (240/)

0	07584	12:09:27	40	56.9	-70	41.7	
PRO	-1	07584	12:09:27	40	56.9	-70	41.7 profile up/dn to 500' (150 m)
0	07682	12:11:05	40	55.7	-70	40.2	
FLX	-1	07682	12:11:05	40	55.7	-70	40.2 flux leg northeast (040/)
0	07988	12:16:11	41	03.5	-70	31.5	
PRO	-1	07988	12:16:11	41	03.5	-70	31.5 profile up/dn to 500' (150 m)
0	08107	12:18:10	41	04.1	-70	33.4	
FLX	-1	08107	12:18:10	41	04.1	-70	33.4 flux leg southwest (205/)
0	08433	12:23:36	40	54.7	-70	38.2	
PRO	-1	08437	12:23:40	40	54.6	-70	38.2 profile up to 4000' (1200 m)
0	08783	12:29:26	41	02.1	-70	38.7	
PRO	-1	08785	12:29:28	41	02.2	-70	38.7 profile down from 4000' (1200 m)
0	09030	12:33:33	41	10.0	-70	36.8	
FLX	-1	09044	12:33:47	41	10.4	-70	36.7 flux leg north (000/)
0	09347	12:38:50	41	20.1	-70	35.6	
PRO	-1	09347	12:38:50	41	20.1	-70	35.6 profile up/dn to 500' (150 m)
0	09435	12:40:18	41	19.4	-70	37.1	
FLX	-1	09435	12:40:18	41	19.4	-70	37.1 flux leg south (170/)
0	09723	12:45:06	41	10.5	-70	33.4	
PRO	-1	09723	12:45:06	41	10.5	-70	33.4 profile up/dn to 500' (150 m)
0	09840	12:47:03	41	11.3	-70	31.2	
FLX	-1	09840	12:47:03	41	11.3	-70	31.2 flux leg northwest (320/)
0	10171	12:52:34	41	19.2	-70	39.8	
PRO	-1	10171	12:52:34	41	19.2	-70	39.8 profile up/dn to 500' (150 m)
0	10284	12:54:27	41	17.5	-70	41.0	
FLX	-1	10284	12:54:27	41	17.5	-70	41.0 flux leg southeast (120/)
0	10572	12:59:15	41	12.8	-70	29.6	
PRO	-1	10572	12:59:15	41	12.8	-70	29.6 profile up/dn to 500' (150 m)
0	10687	13:01:10	41	14.5	-70	28.7	
FLX	-1	10687	13:01:10	41	14.5	-70	28.7 flux leg west (280/)
0	11032	13:06:55	41	16.2	-70	42.3	
PRO	-1	11032	13:06:55	41	16.2	-70	42.3 profile up/dn to 500' (150 m)
0	11146	13:08:49	41	14.2	-70	41.8	
FLX	-1	11146	13:08:49	41	14.2	-70	41.8 flux leg east (080/)
0	11439	13:13:42	41	16.1	-70	28.9	
PRO	-1	11439	13:13:42	41	16.1	-70	28.9 profile up/dn to 500' (150 m)
0	11549	13:15:32	41	17.7	-70	29.7	
FLX	-1	11549	13:15:32	41	17.7	-70	29.7 flux leg southwest (240/)
0	11898	13:21:21	41	12.6	-70	41.7	
PRO	-1	11898	13:21:21	41	12.6	-70	41.7 profile up/dn to 500' (150 m)
0	12008	13:23:11	41	11.0	-70	39.9	
FLX	-1	12008	13:23:11	41	11.0	-70	39.9 flux leg northeast (035/)
0	12329	13:28:32	41	19.3	-70	31.3	
PRO	-1	12329	13:28:32	41	19.3	-70	31.3 profile up/dn to 500' (150 m)
0	12437	13:30:20	41	19.9	-70	33.7	
FLX	-1	12437	13:30:20	41	19.9	-70	33.7 flux leg south (205/)
0	12768	13:35:51	41	10.6	-70	38.1	
WAG	-1	12778	13:36:01	41	10.3	-70	38.3 roll wag cal for radar
0	12848	13:37:11	41	08.3	-70	38.9	
PTC	-1	12864	13:37:27	41	07.9	-70	39.0 pitch up/dn cal for radar
0	12949	13:38:52	41	05.6	-70	40.1	
PRO	-1	12968	13:39:11	41	05.0	-70	40.4 profile up to 3300' (1000 m)
0	13173	13:42:36	41	05.9	-70	43.9	
WCR	-1	13238	13:43:41	41	06.9	-70	43.1 wind circle right
0	13418	13:46:41	41	06.9	-70	41.8	
WCL	-1	13425	13:46:48	41	07.1	-70	41.0 wind circle left
0	13560	13:49:03	41	07.2	-70	40.2	
STC	-1	14286	14:01:09	41	23.3	-70	36.8 preparing to shut down all systems
0	14323	14:01:46	41	23.3	-70	36.8	

Marker for D:08080955.ORG CLOSED at 309711

Total scans: 14327

Missed Ints: 00000

BAT A: 0716350 of 0716350 000.000% Dropouts

BAT B: 0716350 of 0716350 000.000% Dropouts
ASH: 0071635 of 0071635 000.000% Dropouts
TAN: 0141766 of 0143270 001.050% Dropouts

CBLAST-Low Pilot Study - Summer 2001

Flight: 20
Date: 08 AUG 01 (Wednesday)
Duration: 1.5 hr
Pilot: Timothy L. Crawford

Summary: Flux leg intercomparisons with R/V Asterias.

Weather: Hazy, very hot, and humid, very light northwesterly winds ahead of a stalled cold front.

MVY ATIS: 1452 UTC 340/05 07V clear 30//23/ 29.88
MVY ATIS: 1652 UTC 290/06 09V clear 31//23/ 29.87

Instrumentation Notes & Comments: None

Marker for D:08081526.ORG OPENED at 315441

STC	-1	00002	15:37:22	41	23.3	-70	36.8	all systems on
		0	00034	15:37:54	41	23.3	-70	36.8
FLX	-1	00468	15:45:08	41	19.2	-70	33.7	flux leg south (200/)
		0	00615	15:47:35	41	15.0	-70	35.2
PRO	-1	00615	15:47:35	41	15.0	-70	35.2	profile up/dn to 500' (150 m)
		0	00795	15:50:35	41	12.9	-70	36.2
FLX	-1	00795	15:50:35	41	12.9	-70	36.2	flux leg north (010/)
		0	00993	15:53:53	41	18.9	-70	34.1
FLX	-1	01094	15:55:34	41	19.9	-70	33.6	flux leg south (200/)
		0	01265	15:58:25	41	14.9	-70	35.7
PRO	-1	01265	15:58:25	41	14.9	-70	35.7	profile up/dn to 500' (150 m)
		0	01430	16:01:10	41	13.1	-70	36.4
FLX	-1	01430	16:01:10	41	13.1	-70	36.4	flux leg north (010/)
		0	01627	16:04:27	41	18.8	-70	34.1
FLX	-1	01734	16:06:14	41	20.1	-70	33.2	flux leg south (200/)
		0	01926	16:09:26	41	14.6	-70	35.3
PRO	-1	01926	16:09:26	41	14.6	-70	35.3	profile up/dn to 500' (150 m)
		0	02075	16:11:55	41	12.7	-70	36.5
FLX	-1	02075	16:11:55	41	12.7	-70	36.5	flux leg north (010/)
		0	02286	16:15:26	41	18.9	-70	34.1
FLX	-1	02389	16:17:09	41	19.8	-70	33.3	flux leg south (200/)
		0	02579	16:20:19	41	14.7	-70	35.8
PRO	-1	02579	16:20:19	41	14.7	-70	35.8	profile up/dn to 500' (150 m)
		0	02749	16:23:09	41	12.6	-70	36.5
FLX	-1	02749	16:23:09	41	12.6	-70	36.5	flux leg north (010/)
		0	02965	16:26:45	41	18.9	-70	34.1
FLX	-1	03077	16:28:37	41	19.9	-70	33.2	flux leg southwest (220/)
		0	03282	16:32:02	41	14.8	-70	36.5
PRO	-1	03282	16:32:02	41	14.8	-70	36.5	profile up/dn to 500' (150 m)
		0	03431	16:34:31	41	13.7	-70	36.8
FLX	-1	03431	16:34:31	41	13.7	-70	36.8	flux leg north (020/)
		0	03630	16:37:50	41	19.1	-70	33.0
FLX	-1	03746	16:39:46	41	19.9	-70	32.2	flux leg southwest (210/)
		0	03971	16:43:31	41	14.4	-70	36.1
PRO	-1	03971	16:43:31	41	14.4	-70	36.1	profile up/dn to 500' (150 m)
		0	04124	16:46:04	41	12.5	-70	36.1
FLX	-1	04124	16:46:04	41	12.5	-70	36.1	flux leg north (010/)
		0	04346	16:49:46	41	19.1	-70	33.5
FLX	-1	04426	16:51:06	41	19.7	-70	33.4	flux leg southwest (210/)
		0	04636	16:54:36	41	14.3	-70	36.2
PRO	-1	04639	16:54:39	41	14.2	-70	36.2	profile up to 3000' (1000 m)

0 04970 17:00:10 41 14.7 -70 40.5

Marker for D:08081526.ORG CLOSED at 320799

Total scans: 05358

Missed Ints: 00000

BAT A: 0267900 of 0267900 000.000% Dropouts

BAT B: 0267900 of 0267900 000.000% Dropouts

ASH: 0026790 of 0026790 000.000% Dropouts

TAN: 0053153 of 0053580 000.797% Dropouts

Appendix B: N3R Flight Tracks

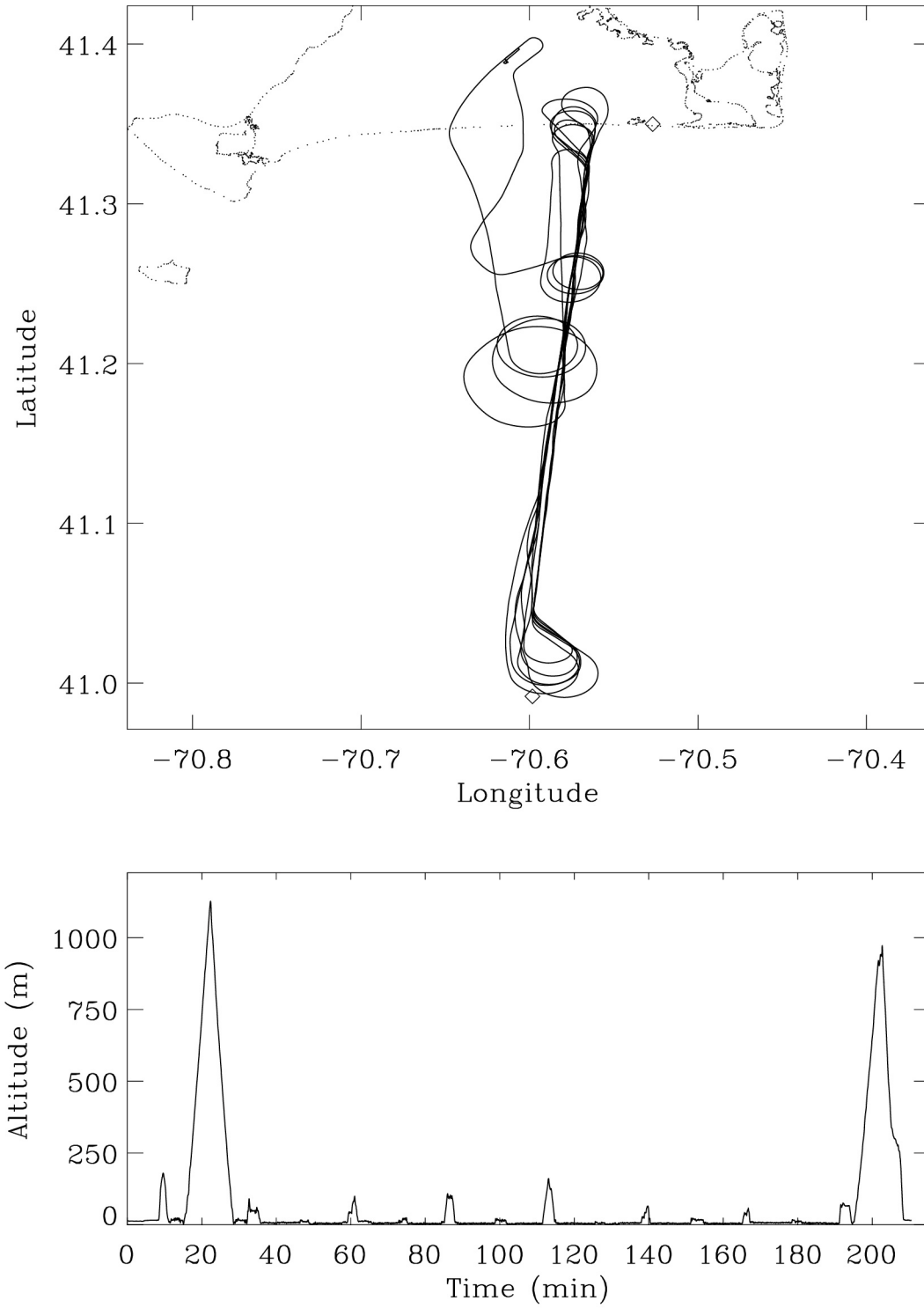


Fig. 19. N3R track for Flight 1 (21 JUL 01).

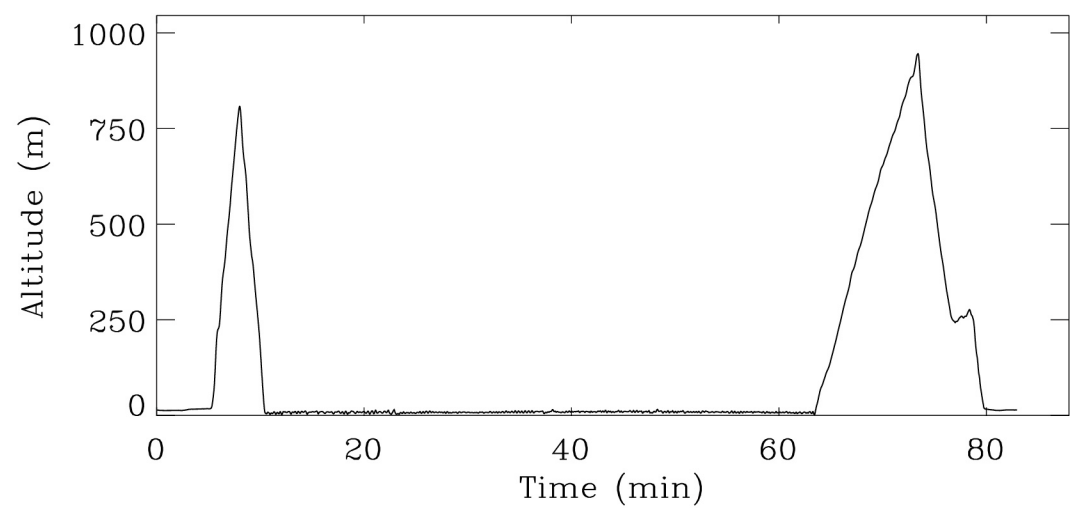
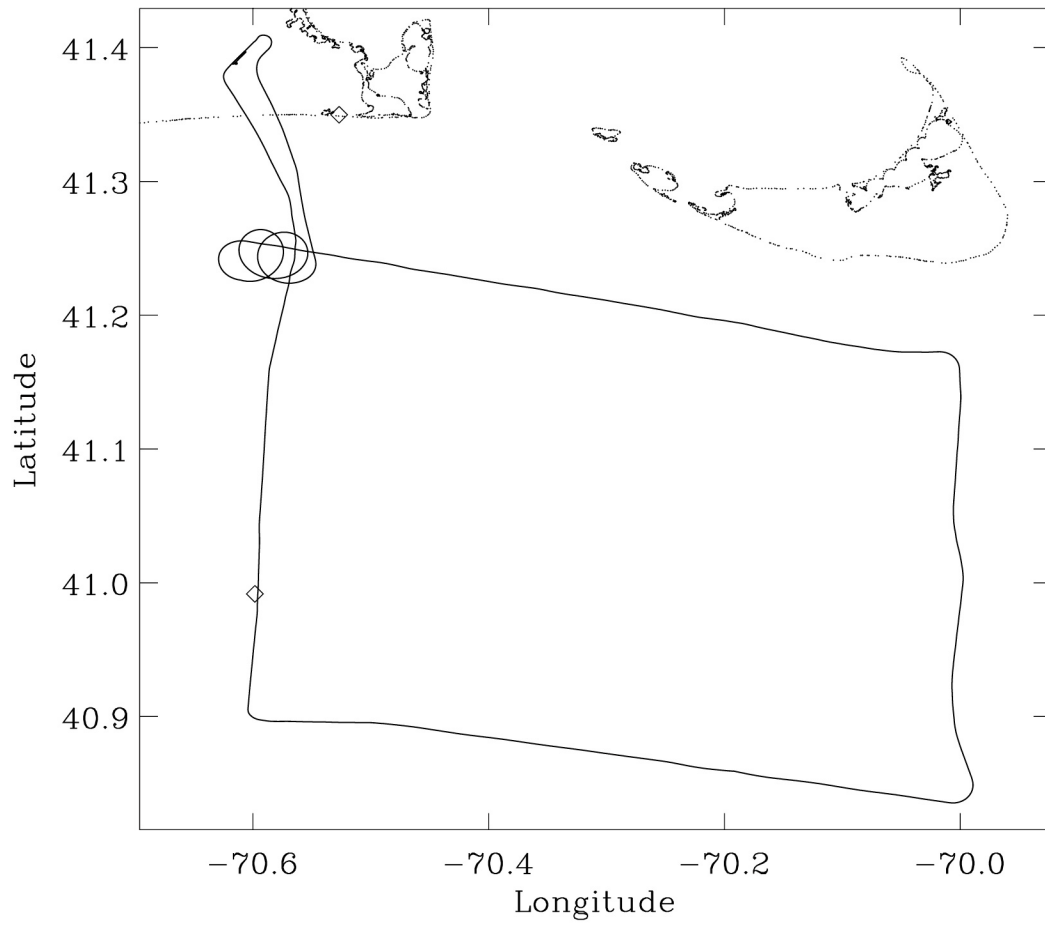


Fig. 20. N3R track for Flight 2 (22 JUL 01).

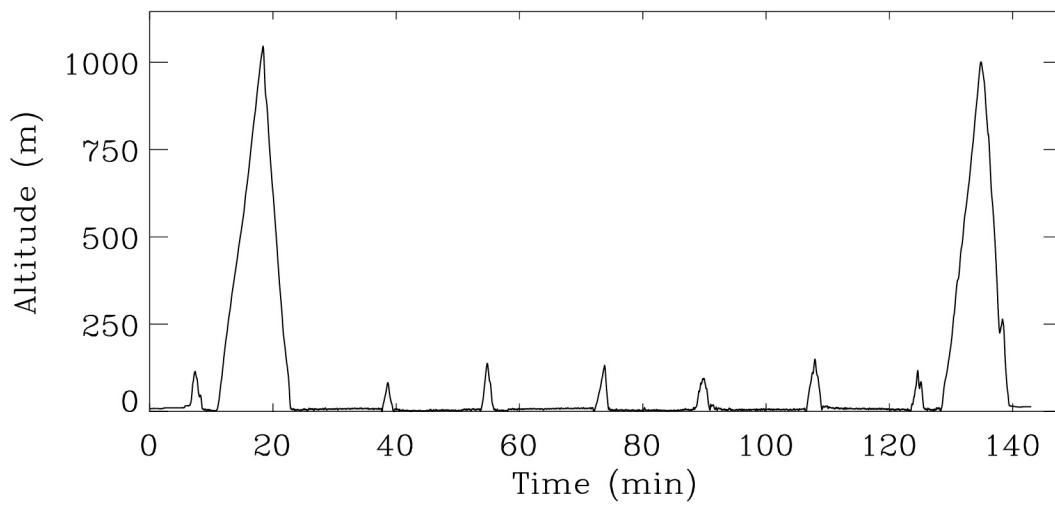
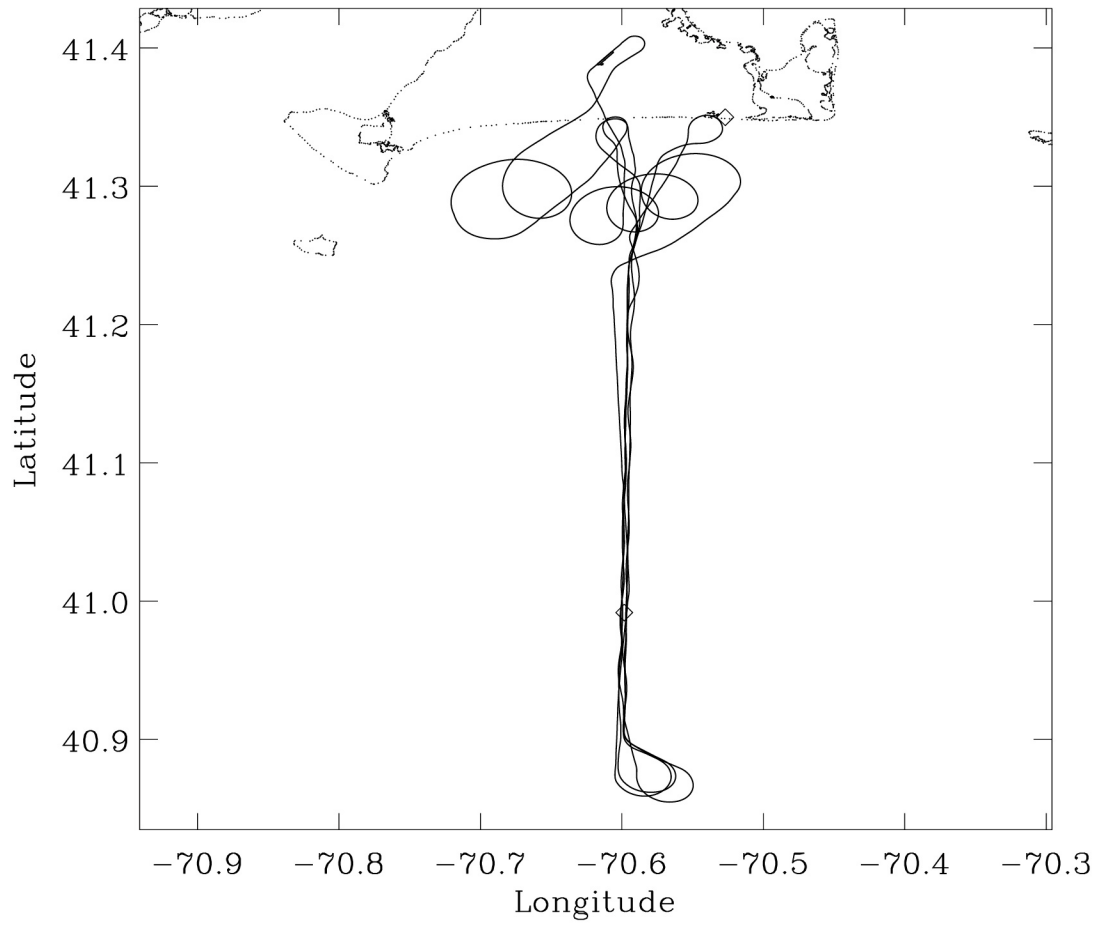


Fig. 21. N3R track for Flight 3 (23 JUL 01).

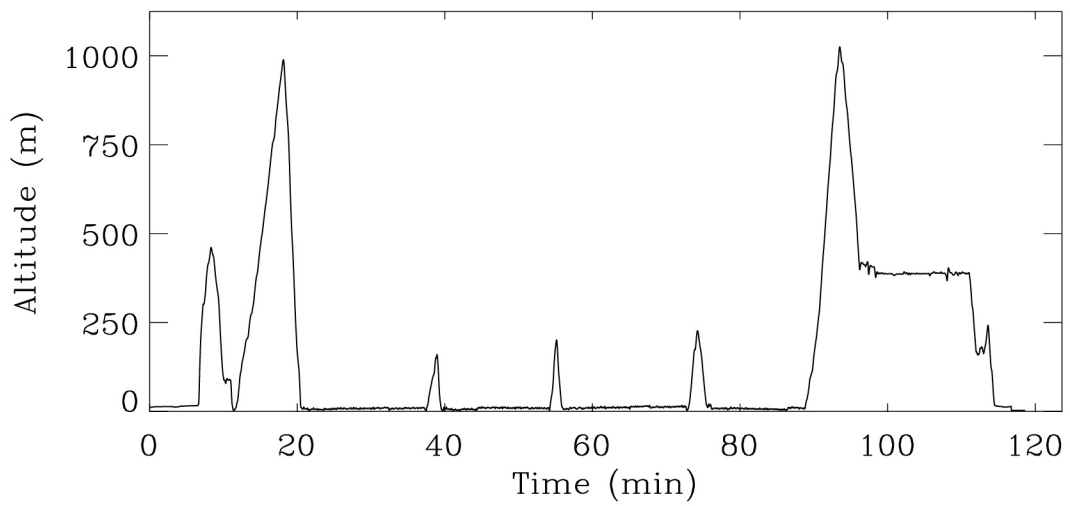
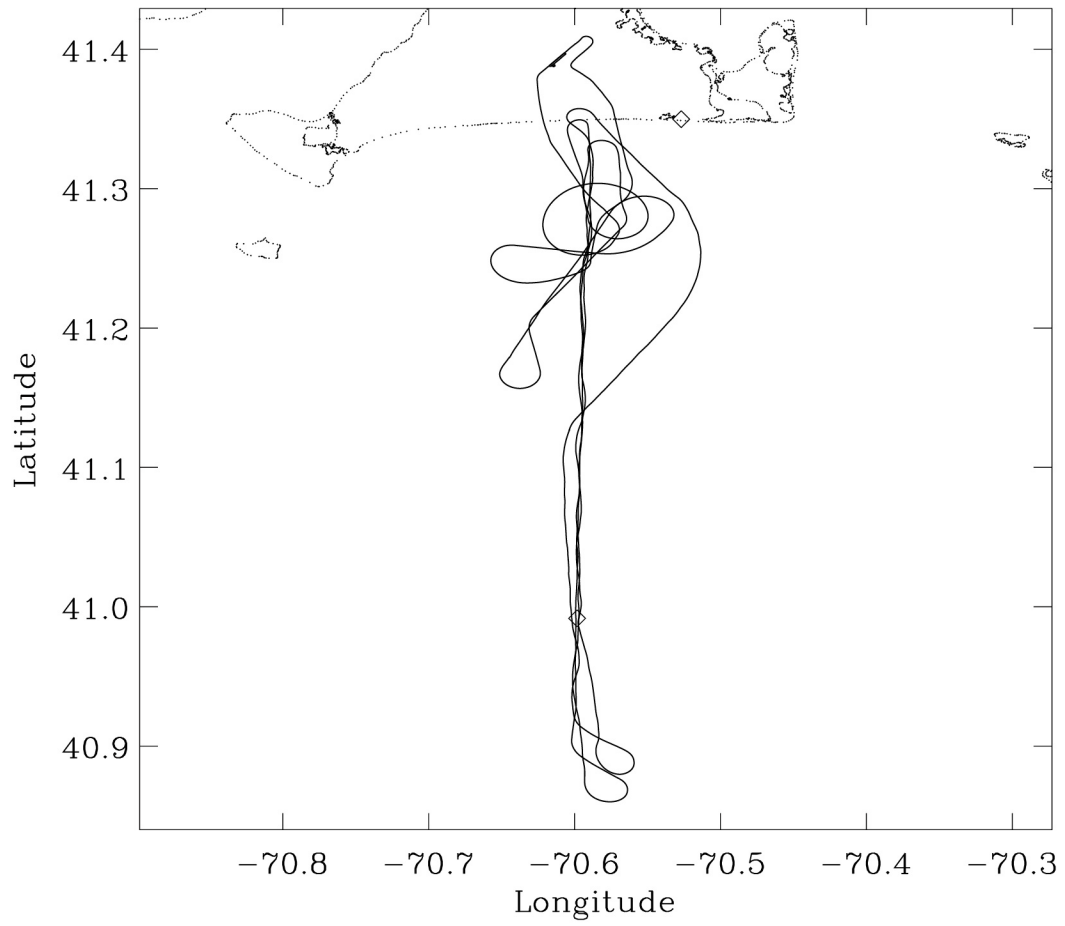


Fig. 22. N3R track for Flight 4 (25 JUL 01).

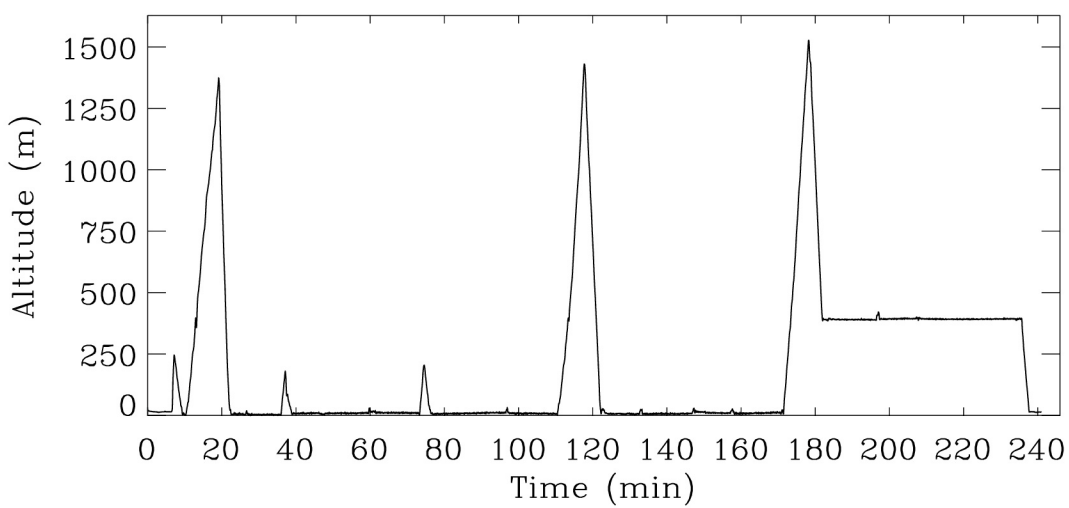
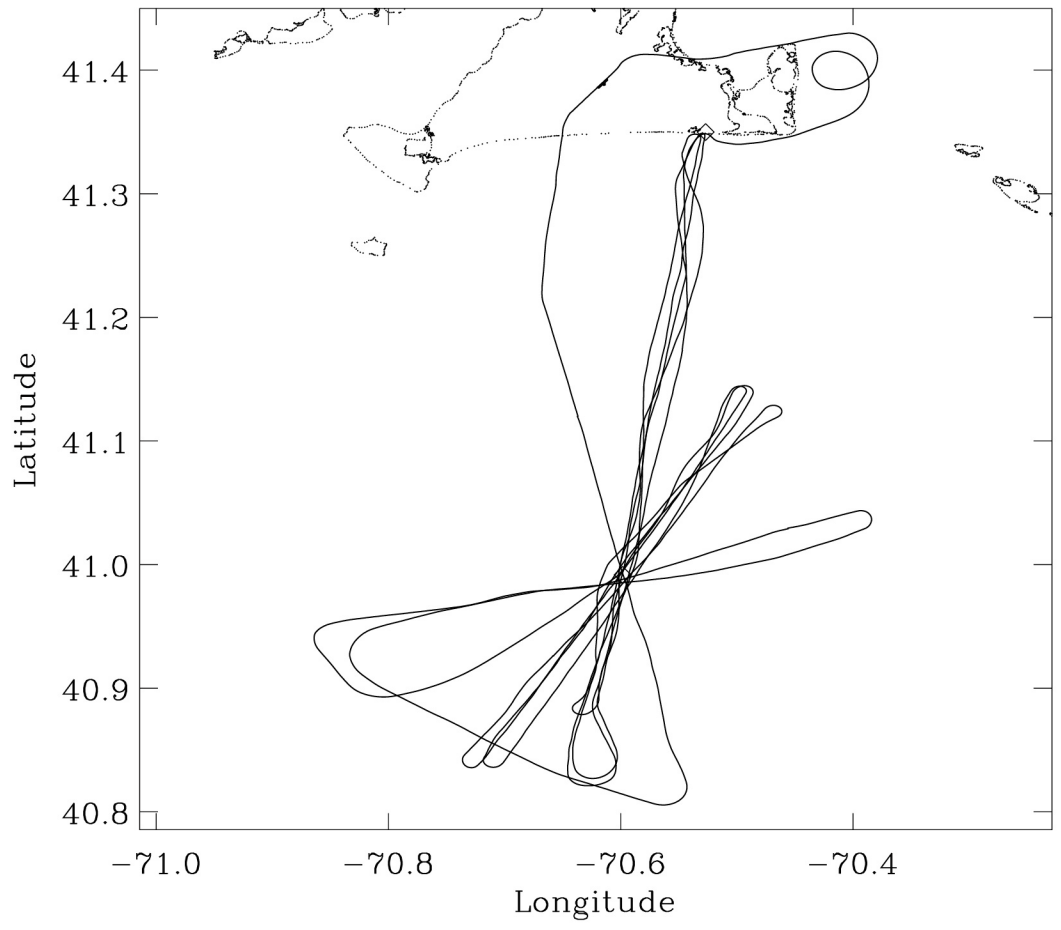


Fig. 23. N3R track for Flight 5 (27 JUL 01).

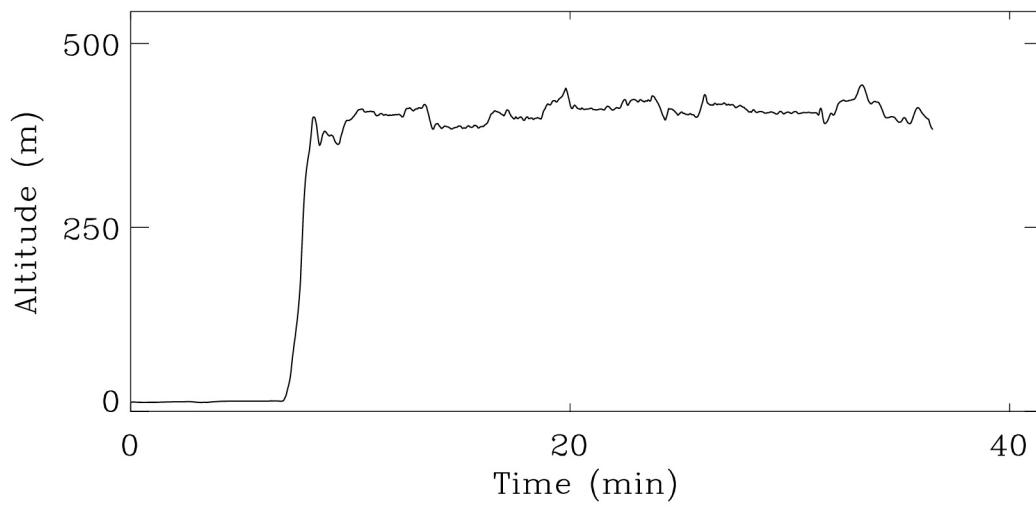
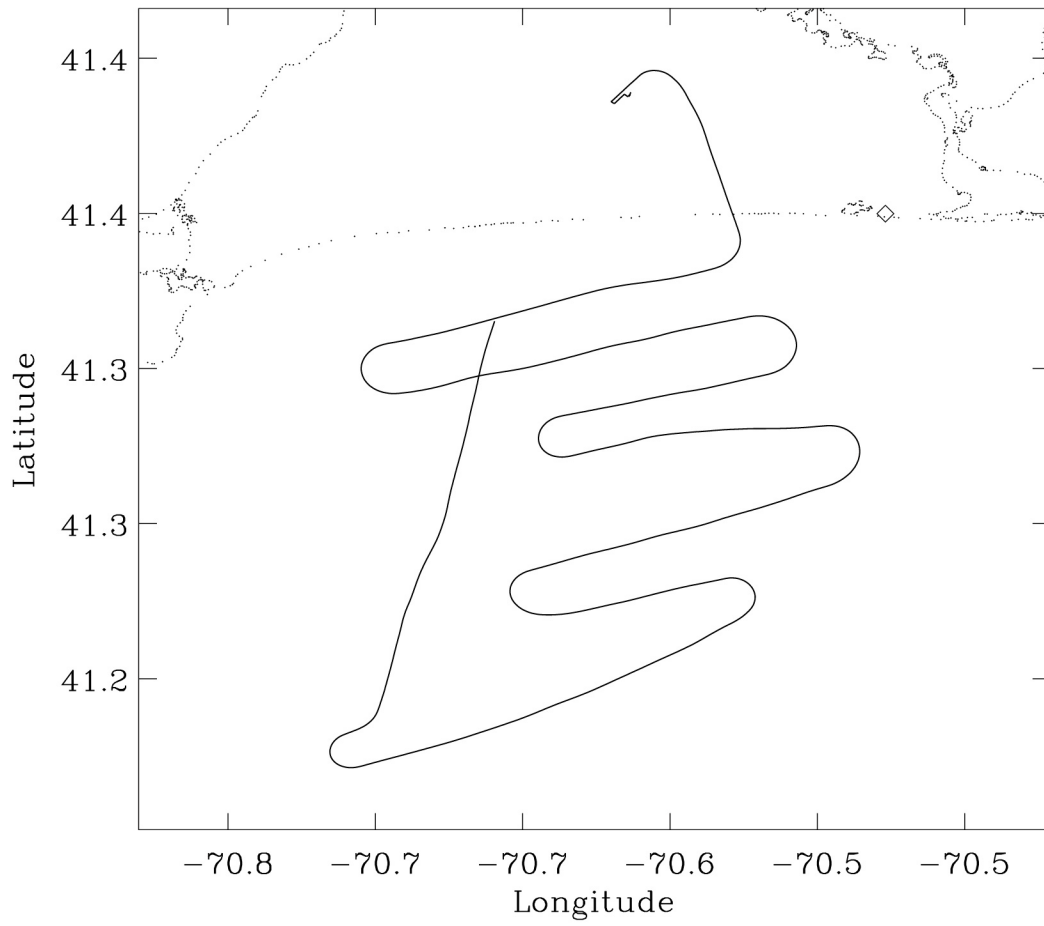


Fig. 24. N3R track for Flight 6 (27 JUL 01).

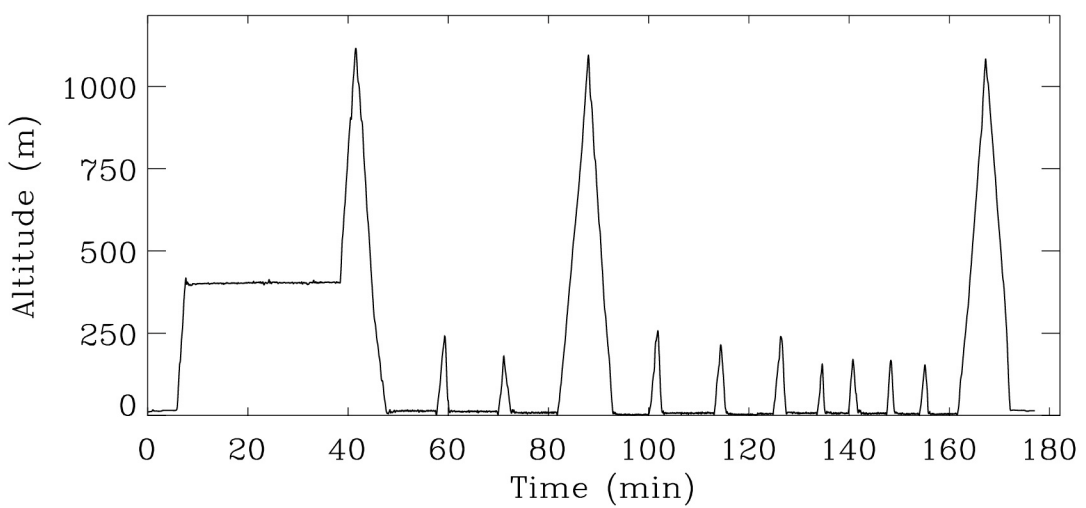
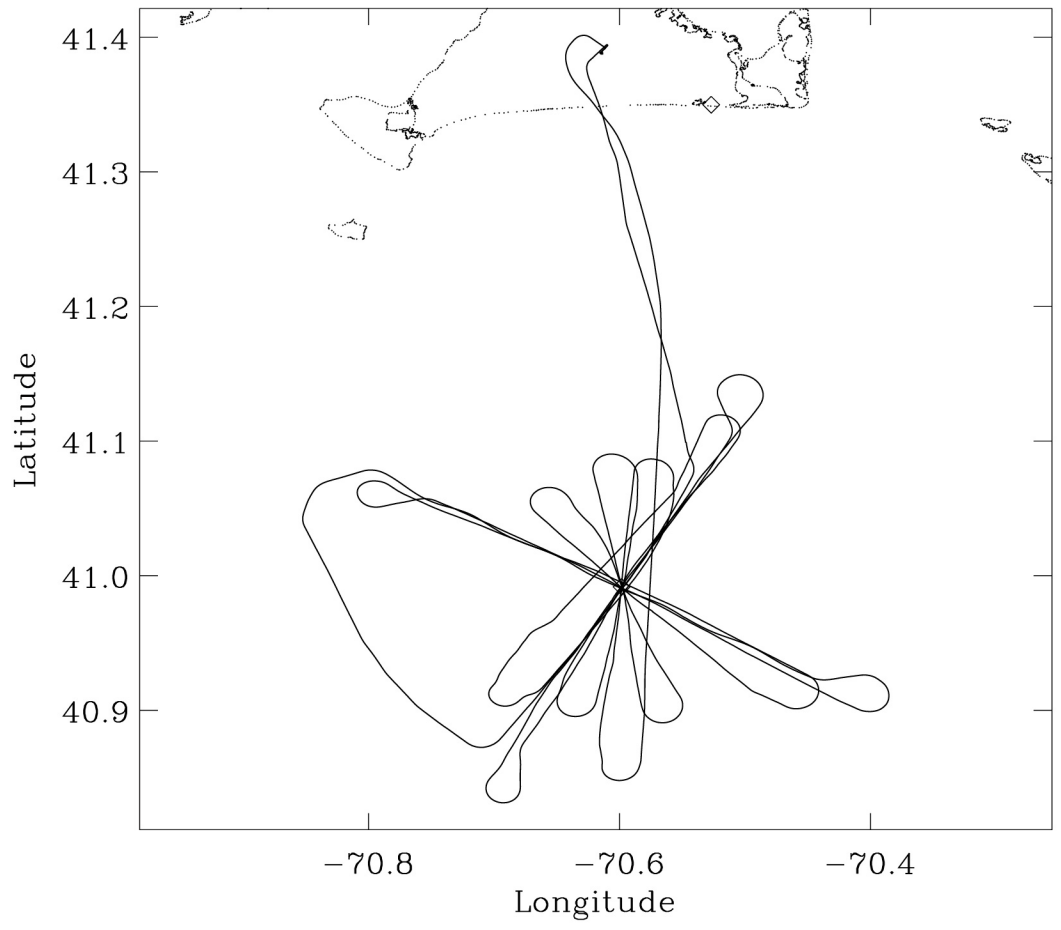


Fig. 25. N3R track for Flight 7 (28 JUL 01).

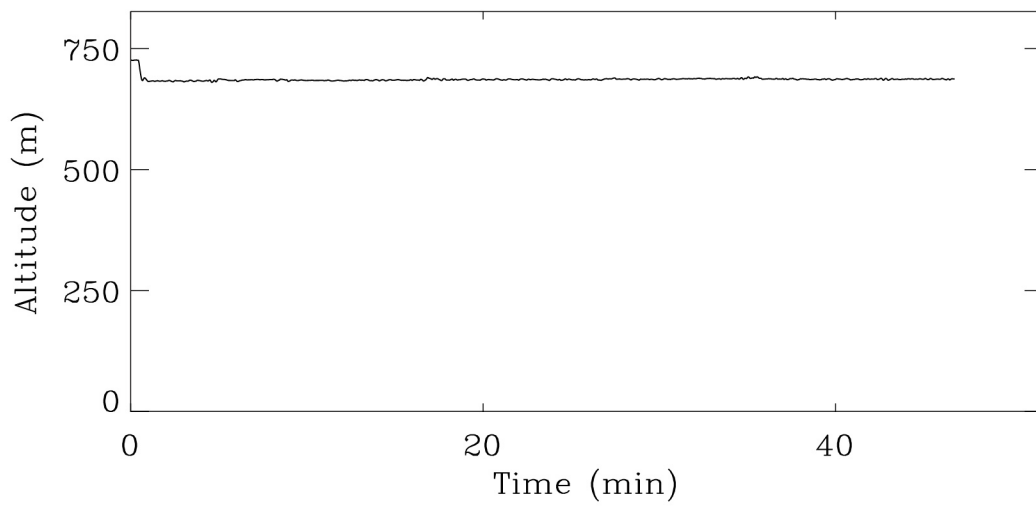
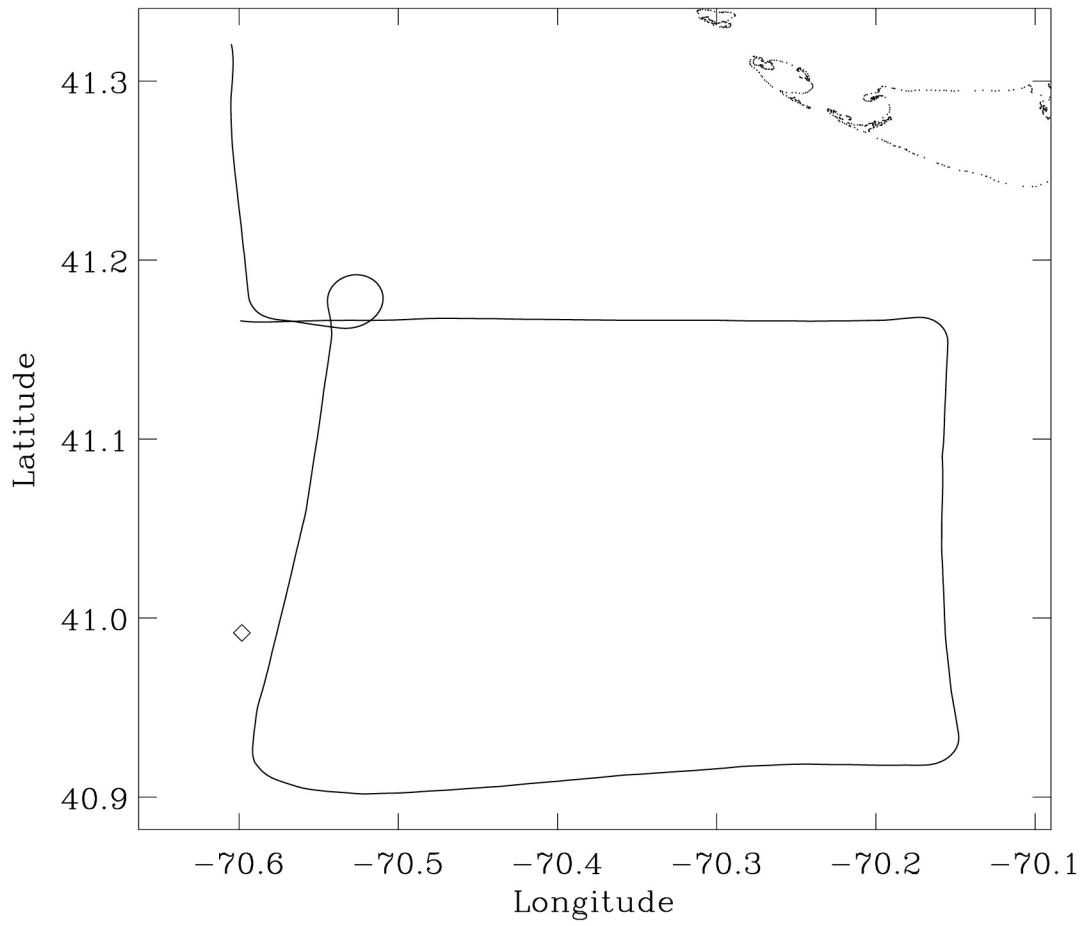


Fig. 26. N3R track for Flight 8 (29 JUL 01).

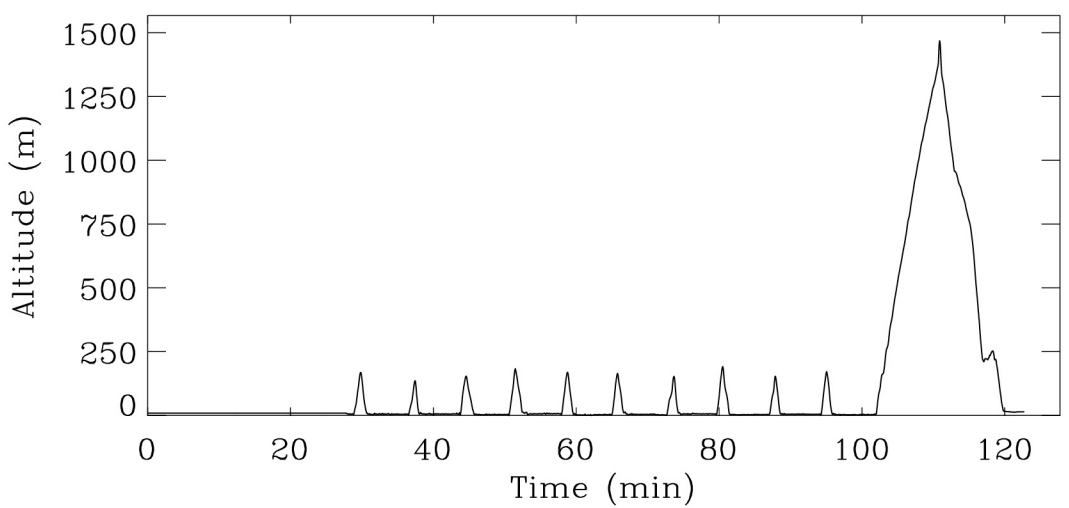
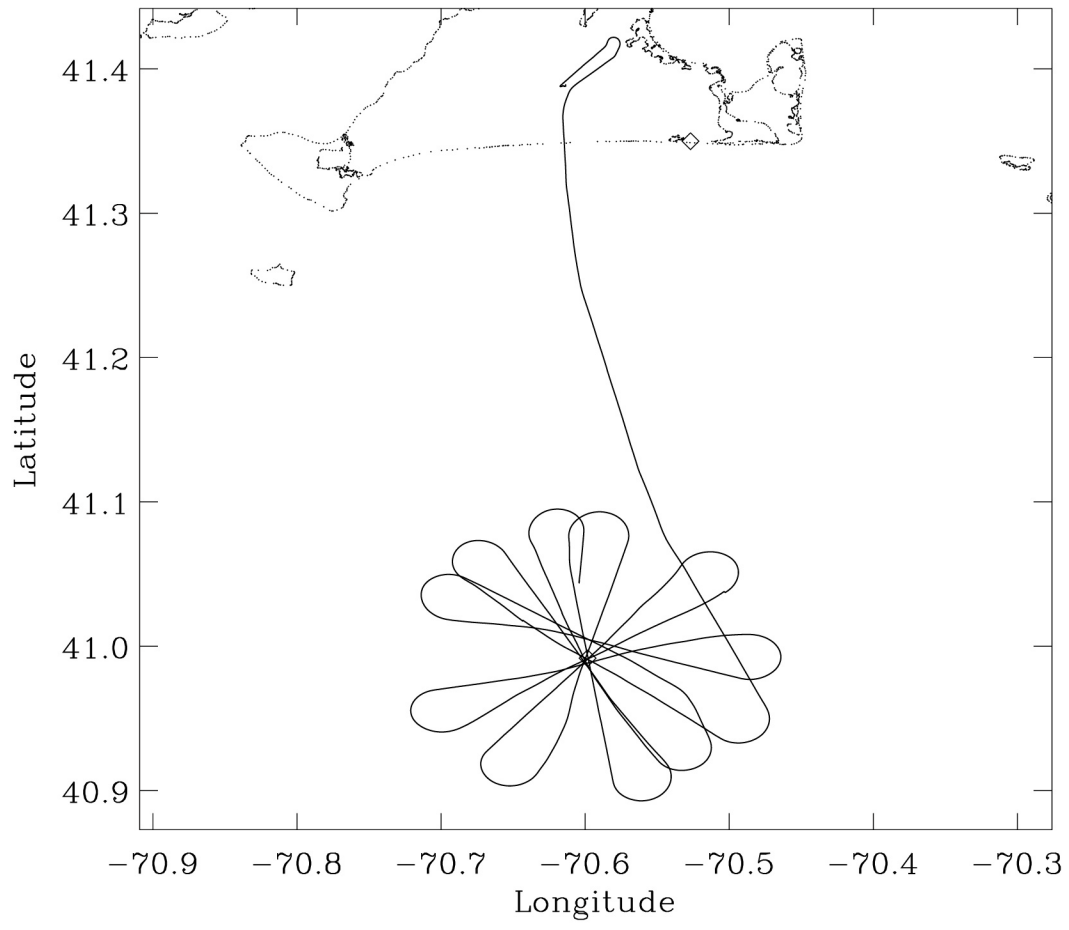


Fig. 27. N3R track for Flight 9 (29 JUL 01).

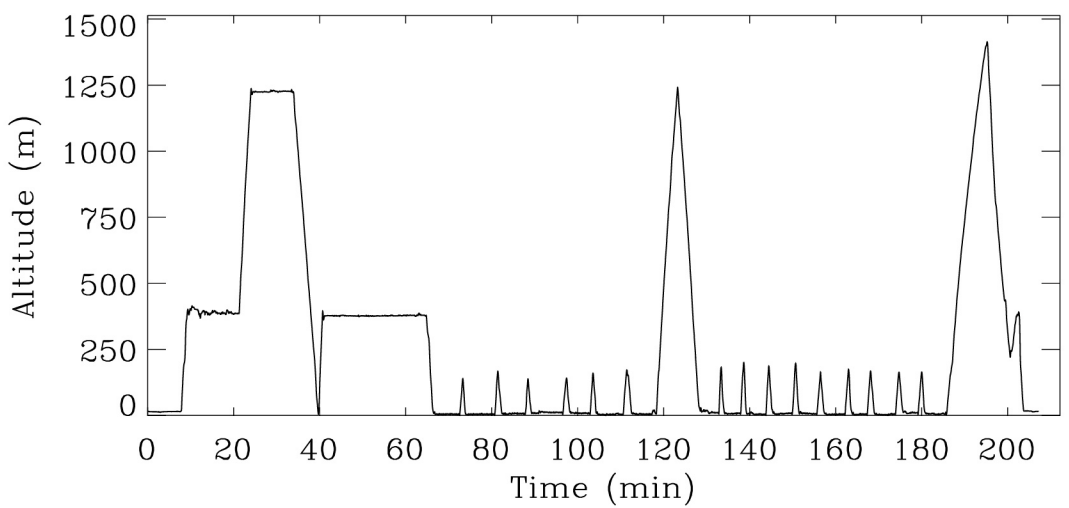
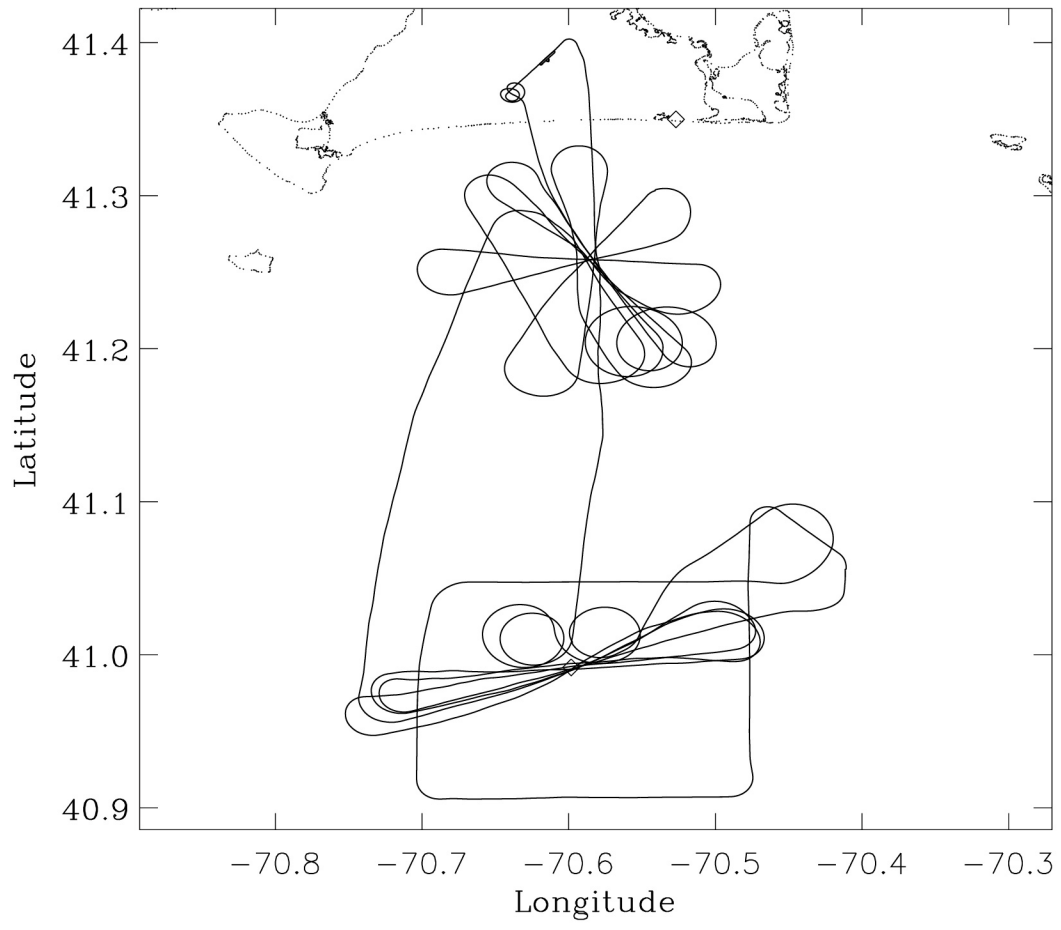


Fig. 28. N3R track for Flight 10 (30 JUL 01).

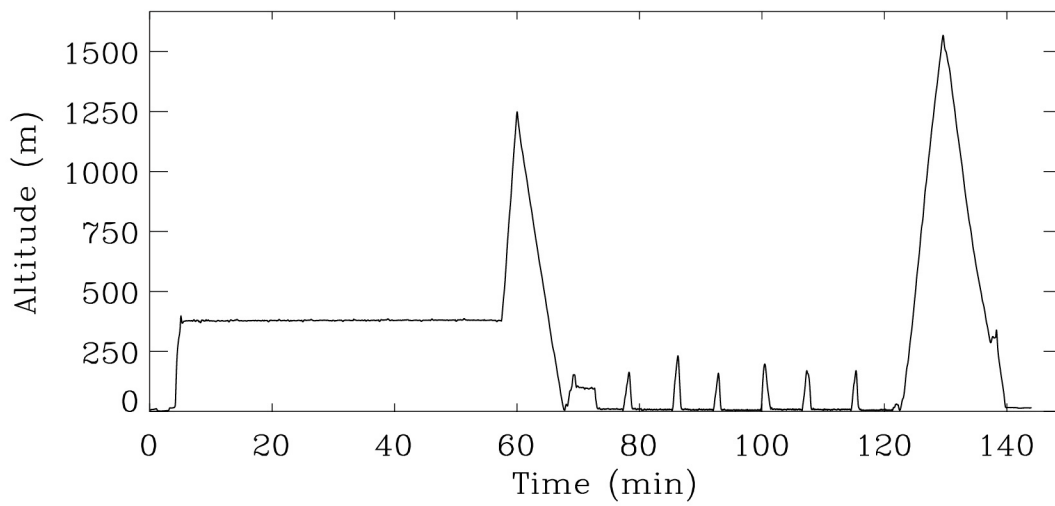
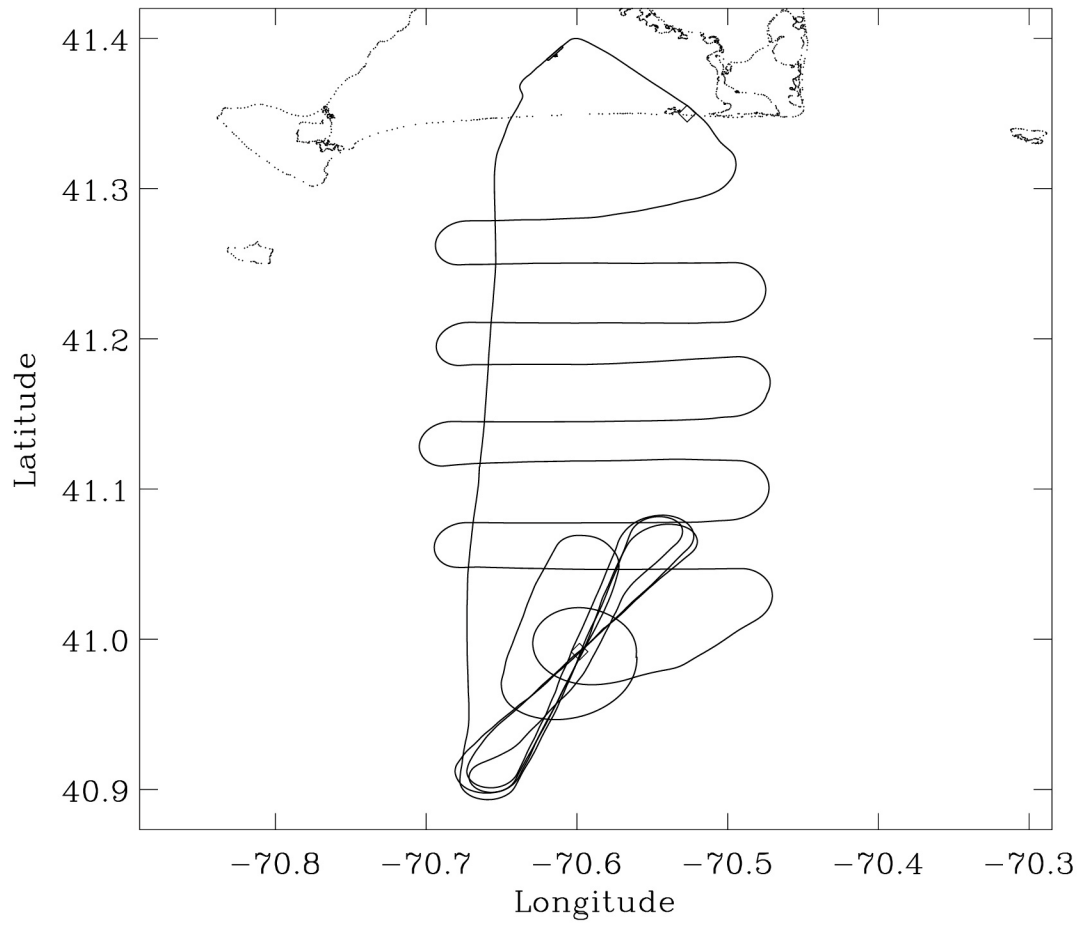


Fig. 29. N3R track for Flight 11 (31 JUL 01).

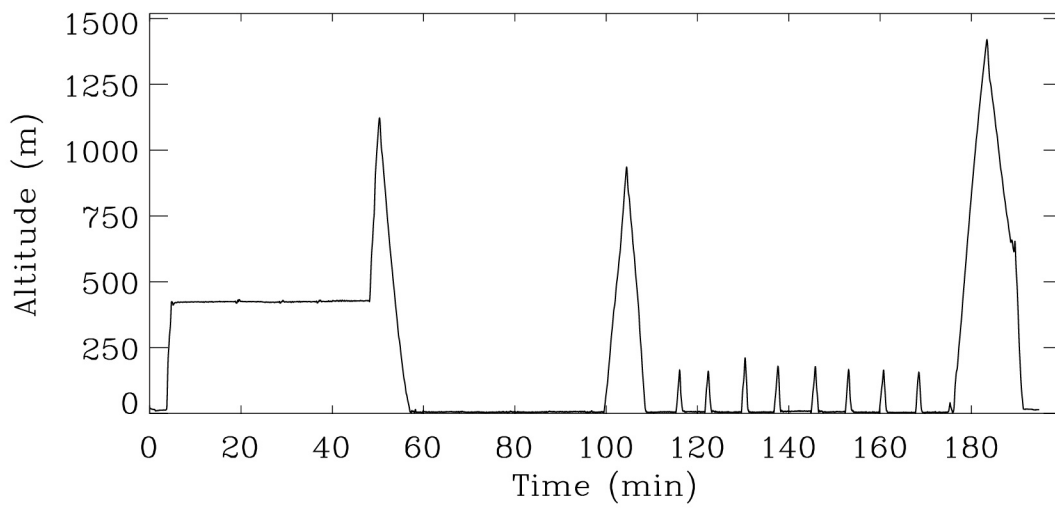
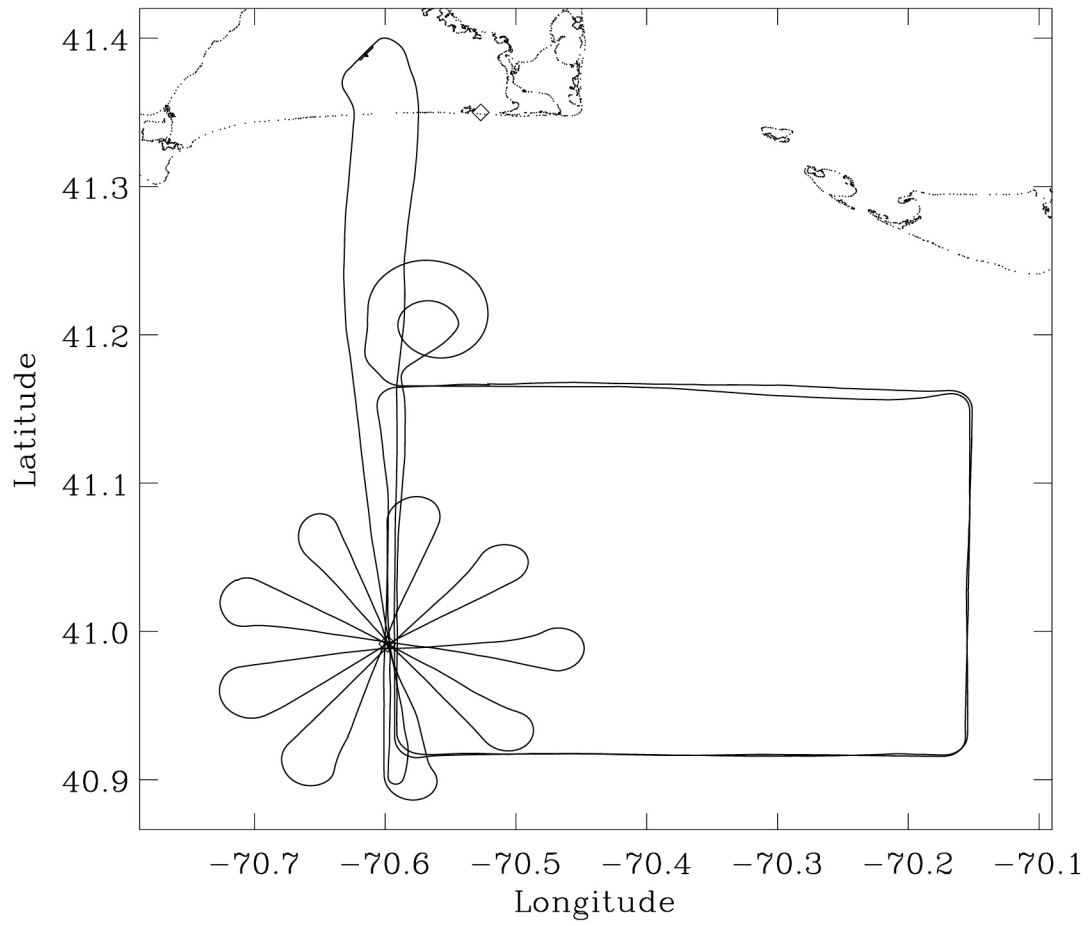


Fig. 30. N3R track for Flight 12 (01 AUG 01).

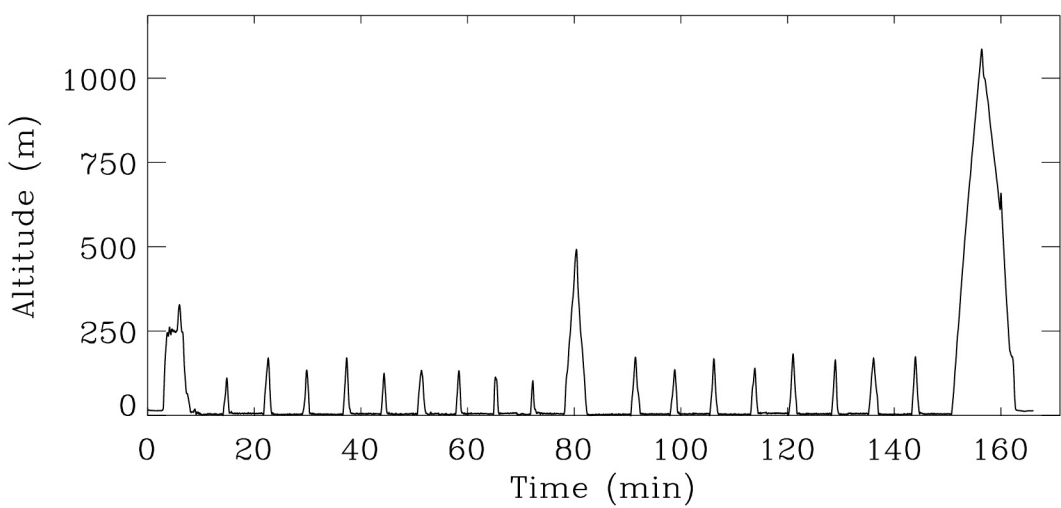
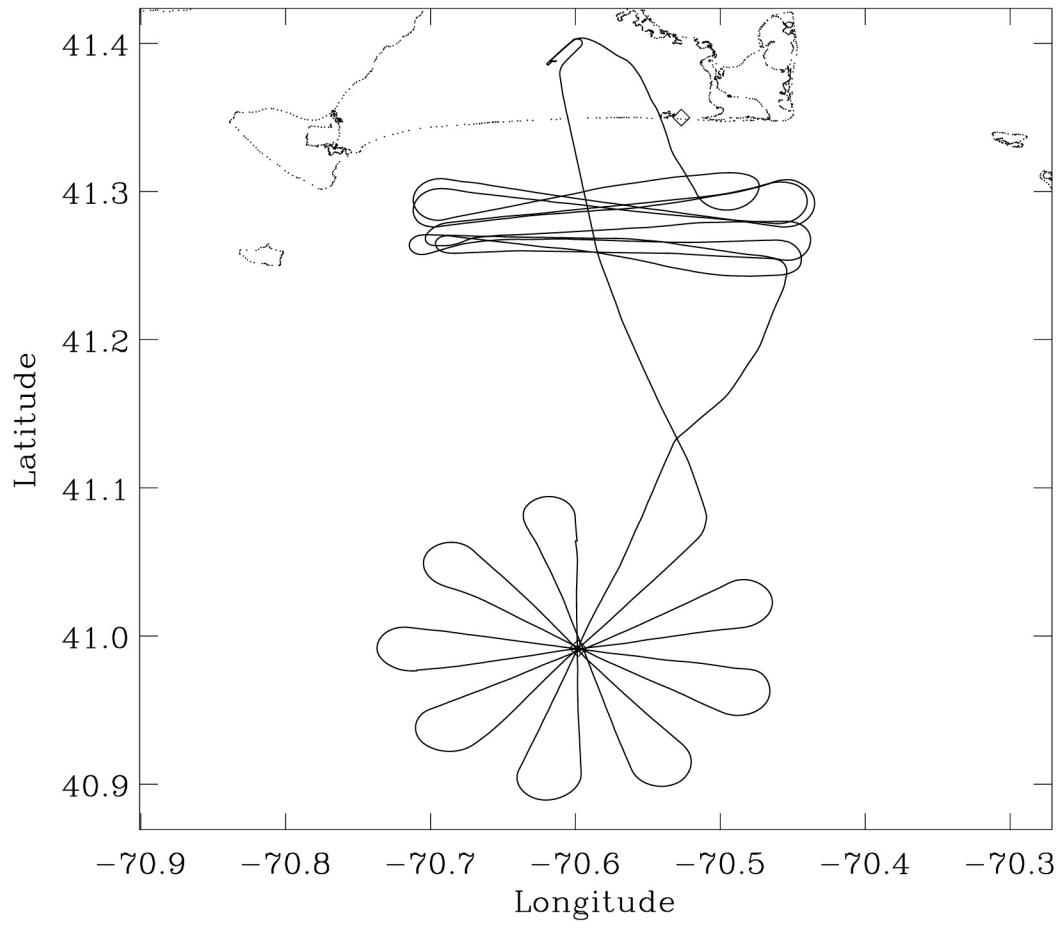


Fig. 31. N3R track for Flight 13 (01 AUG 01).

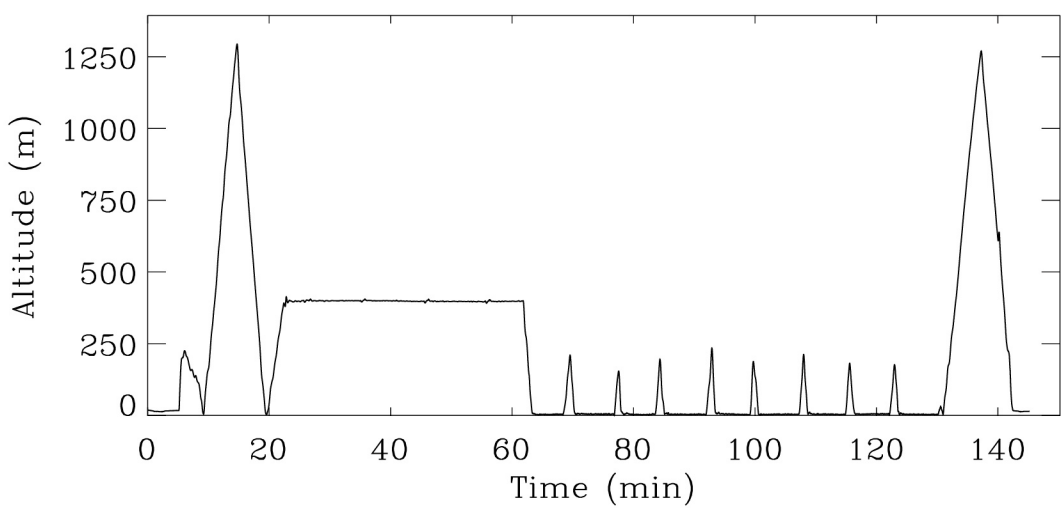
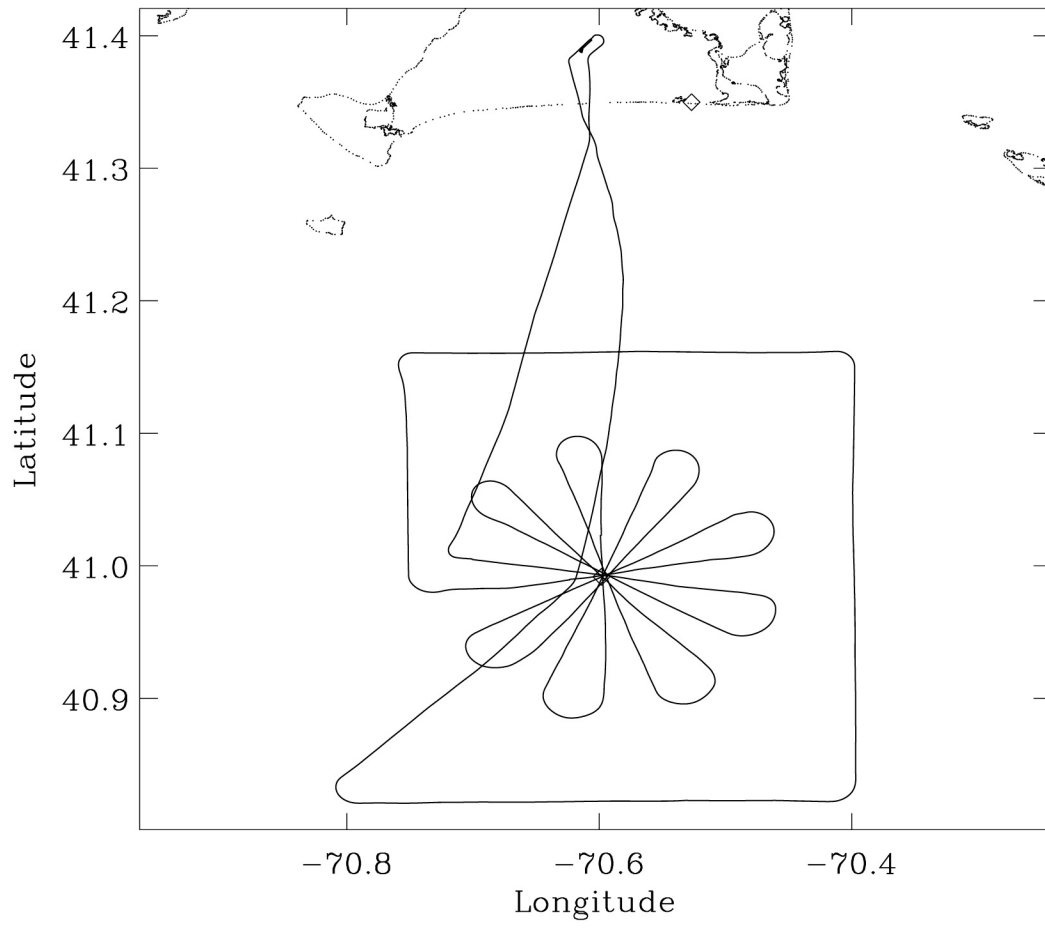


Fig. 32. N3R track for Flight 14 (02 AUG 01).

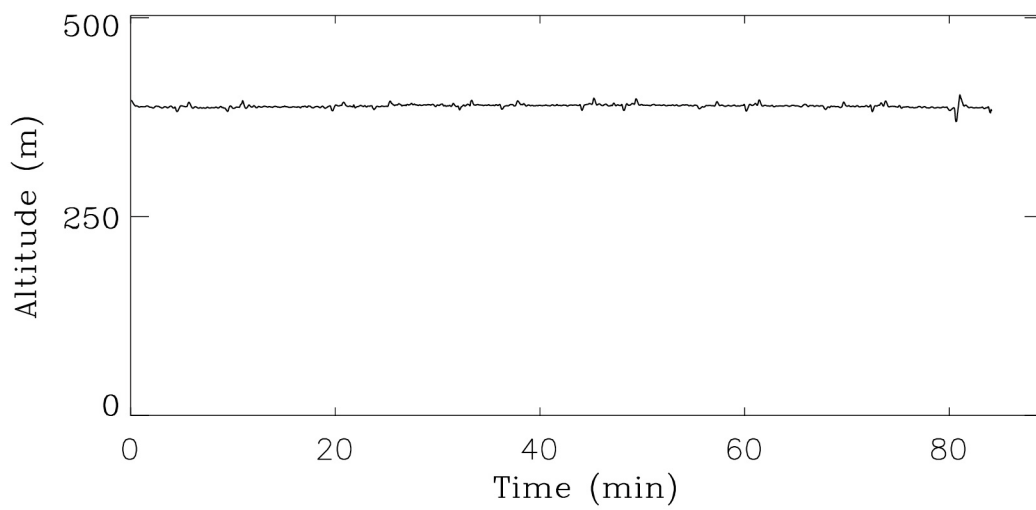
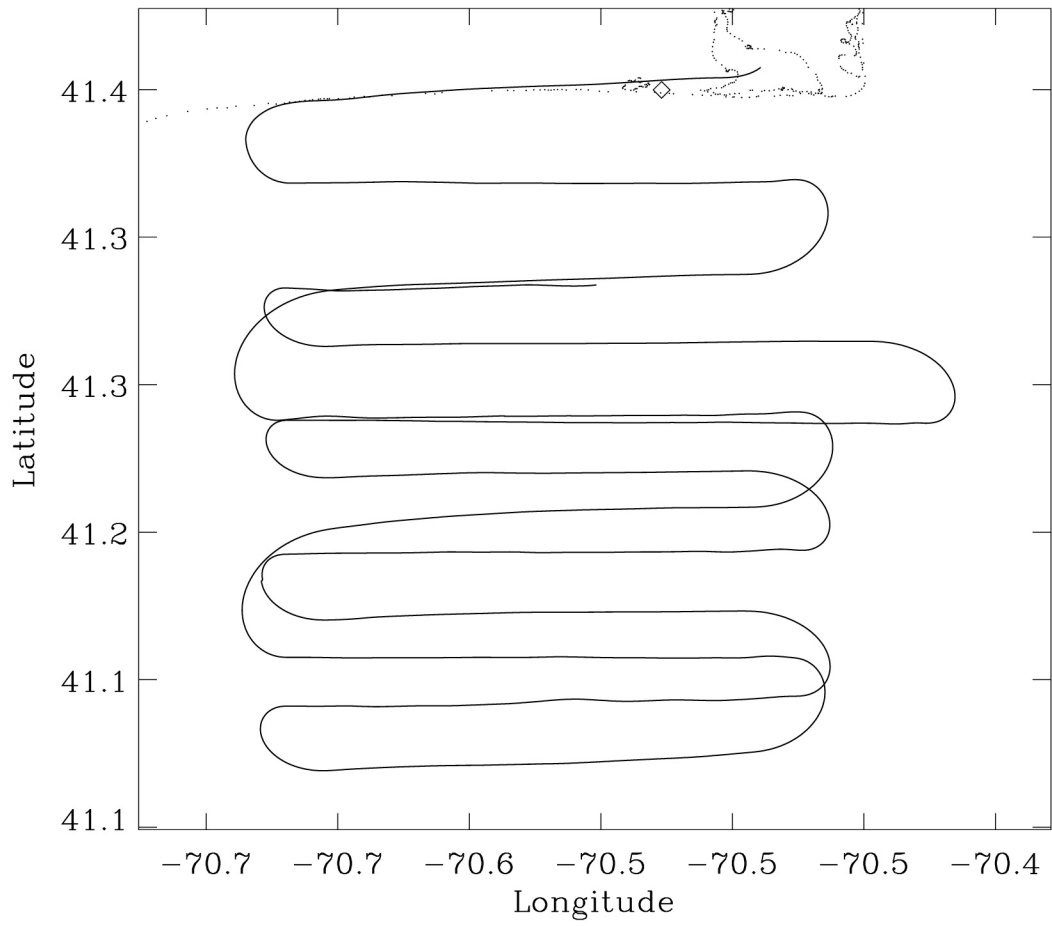


Fig. 33. N3R track for Flight 15 (03 AUG 01).

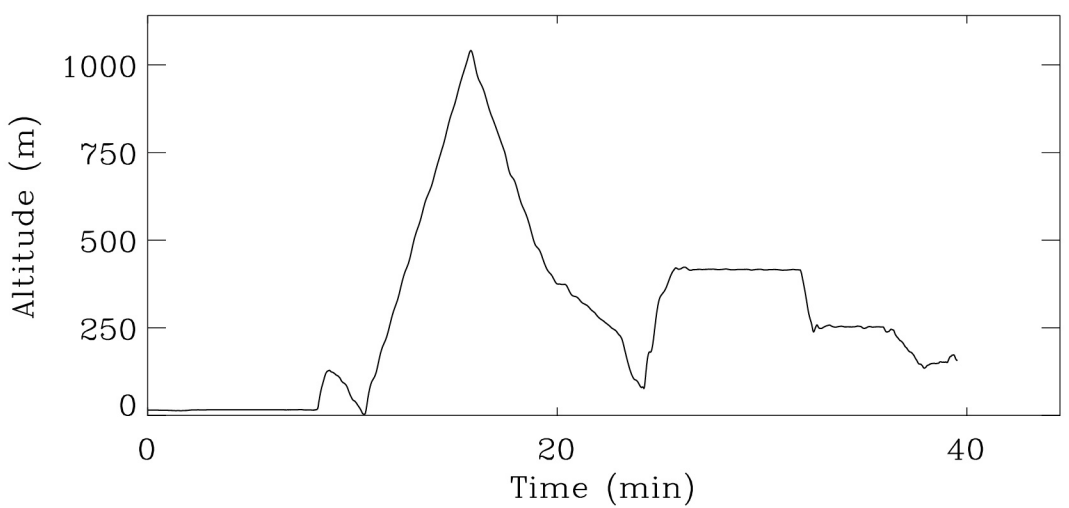
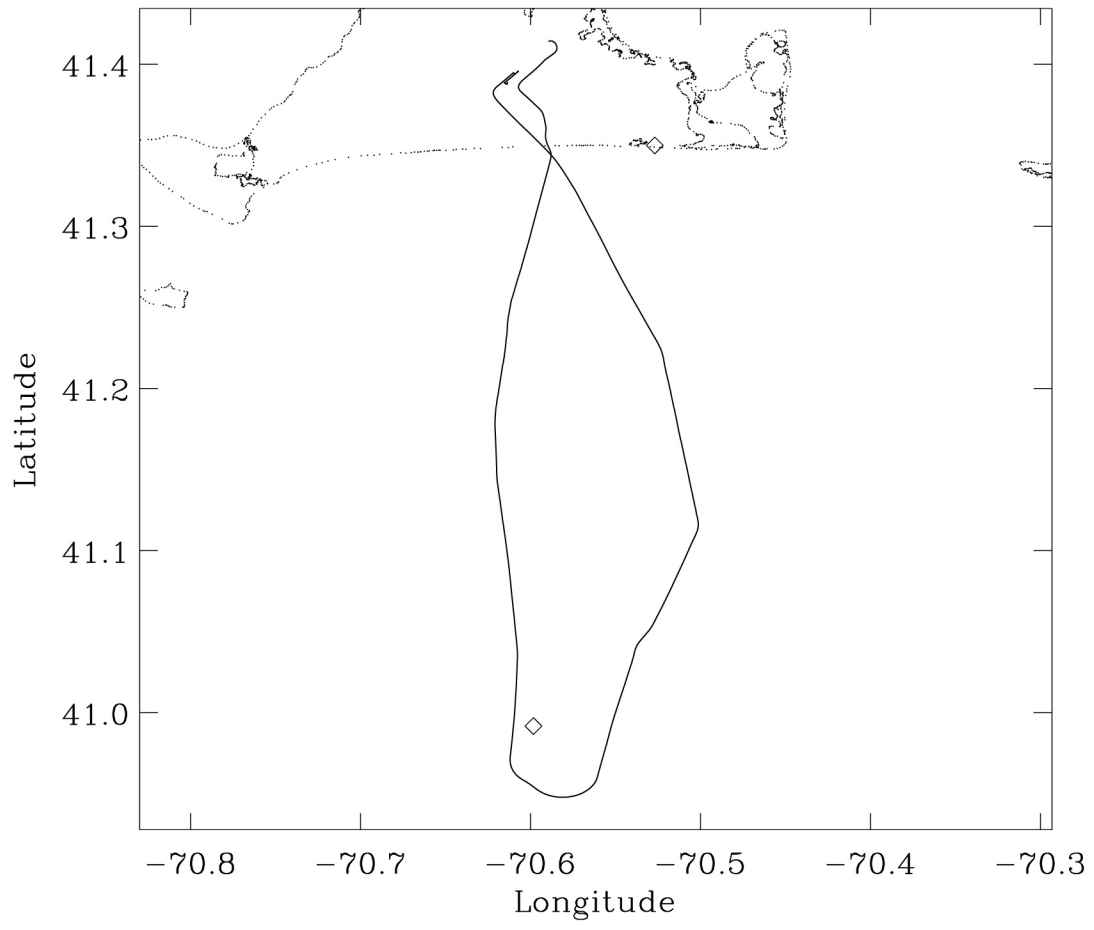


Fig. 34. N3R track for Flight 16 (05 AUG 01).

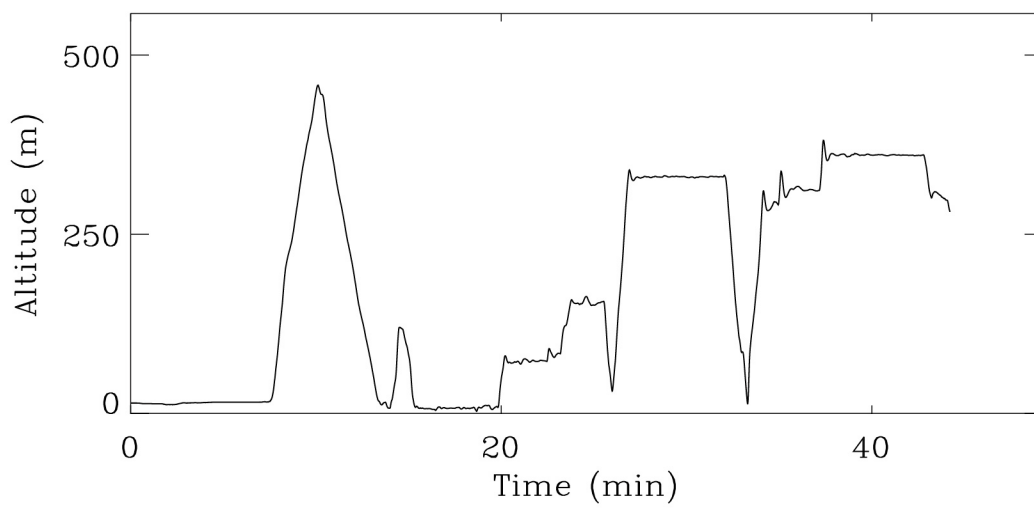
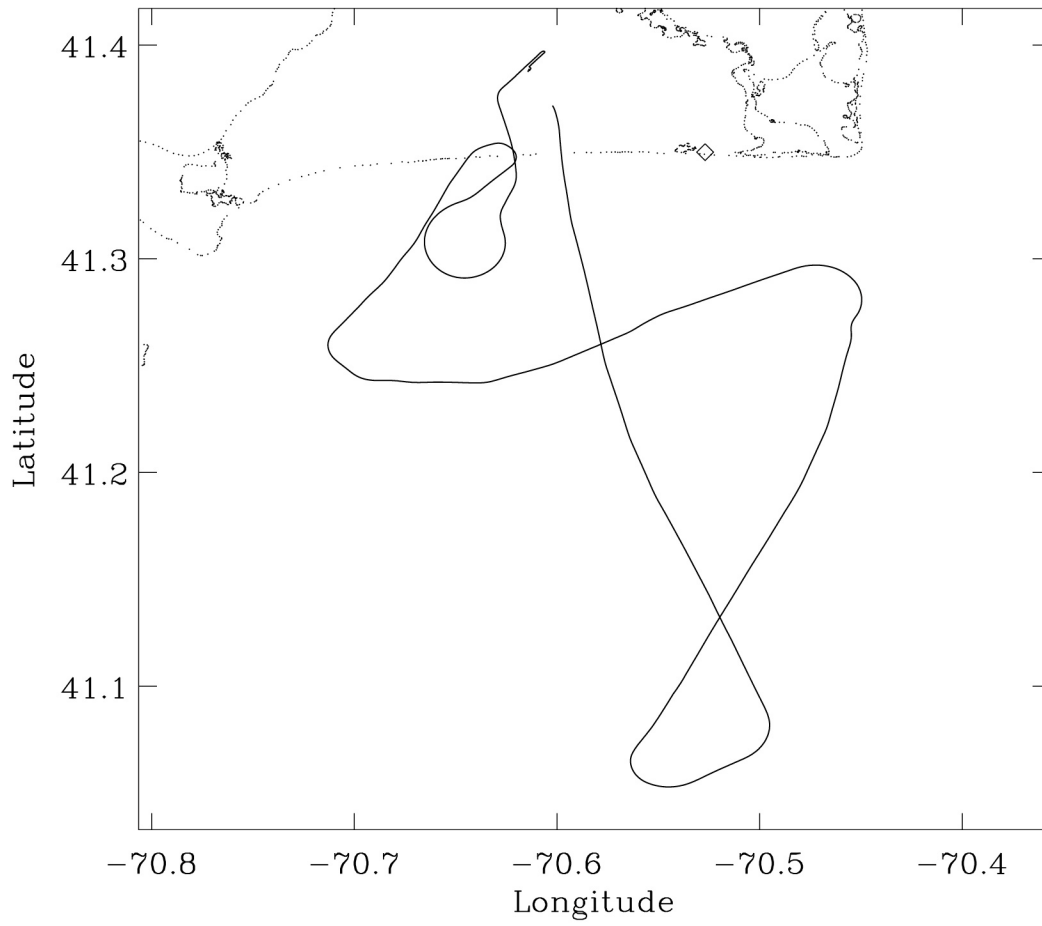


Fig. 35. N3R track for Flight 17 (05 AUG 01).

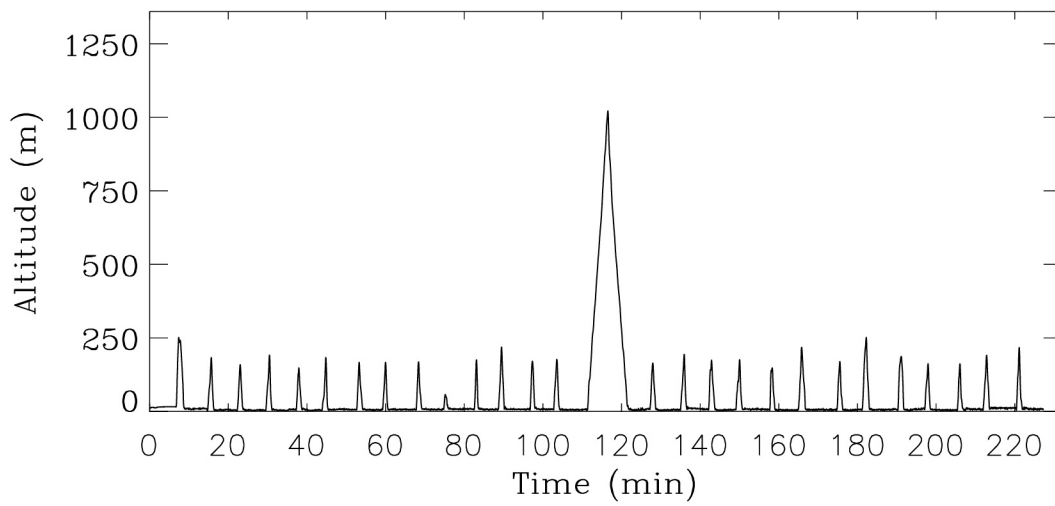
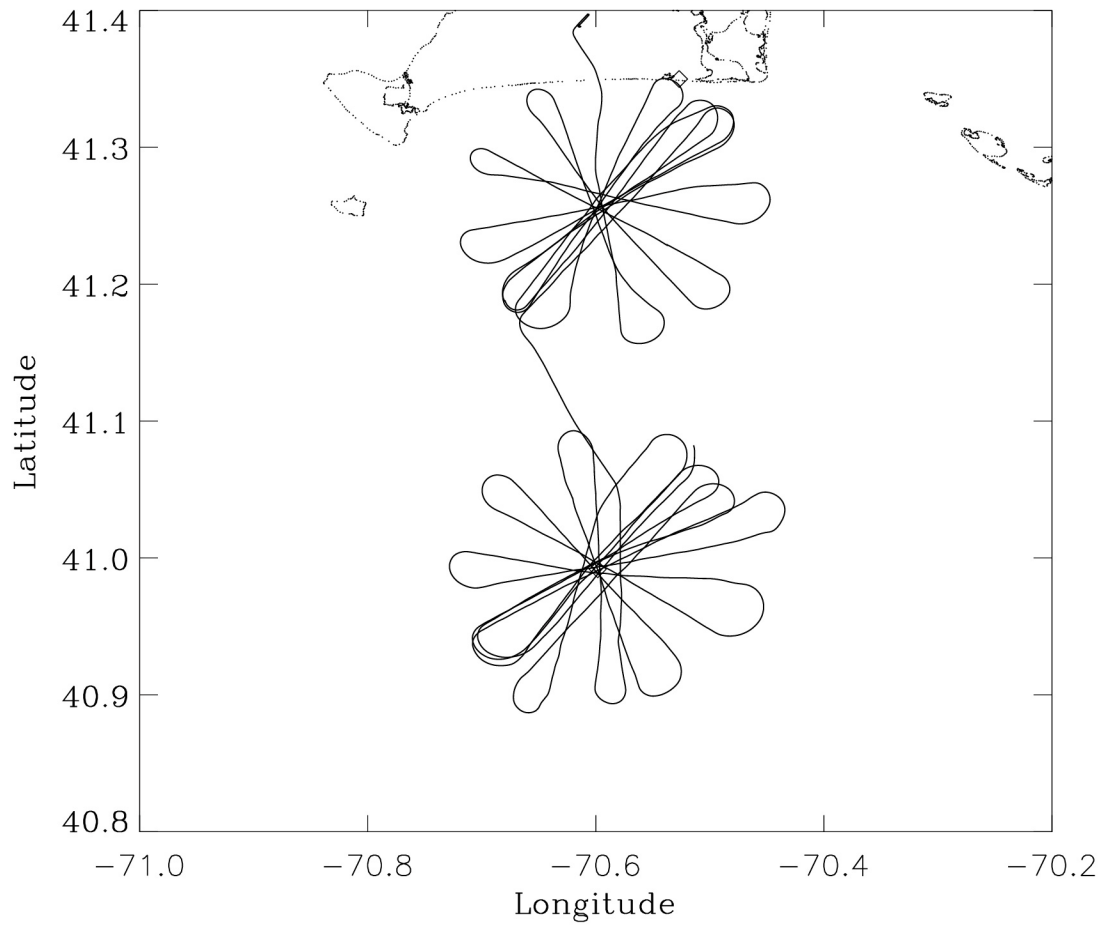


Fig. 36. N3R track for Flight 18 (07 AUG 01).

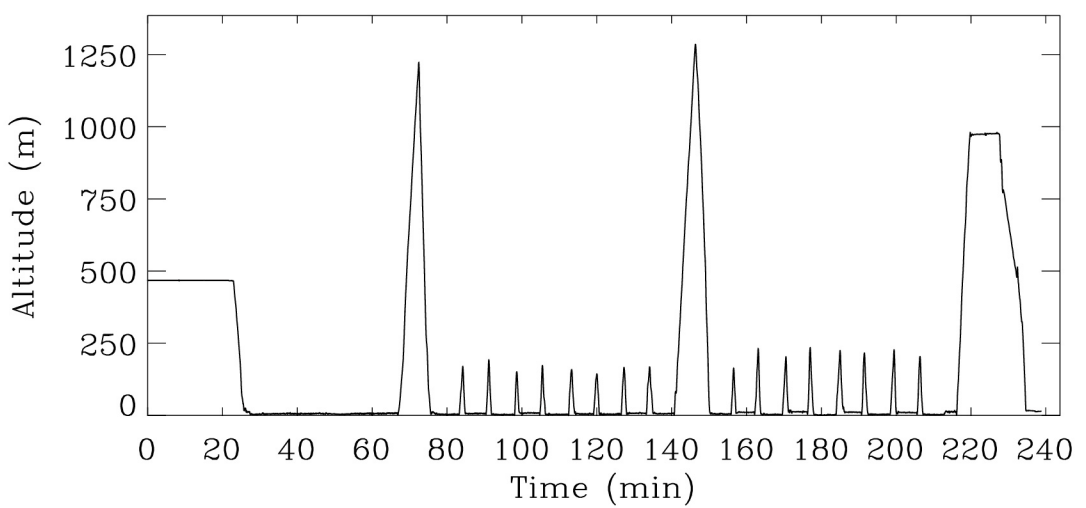
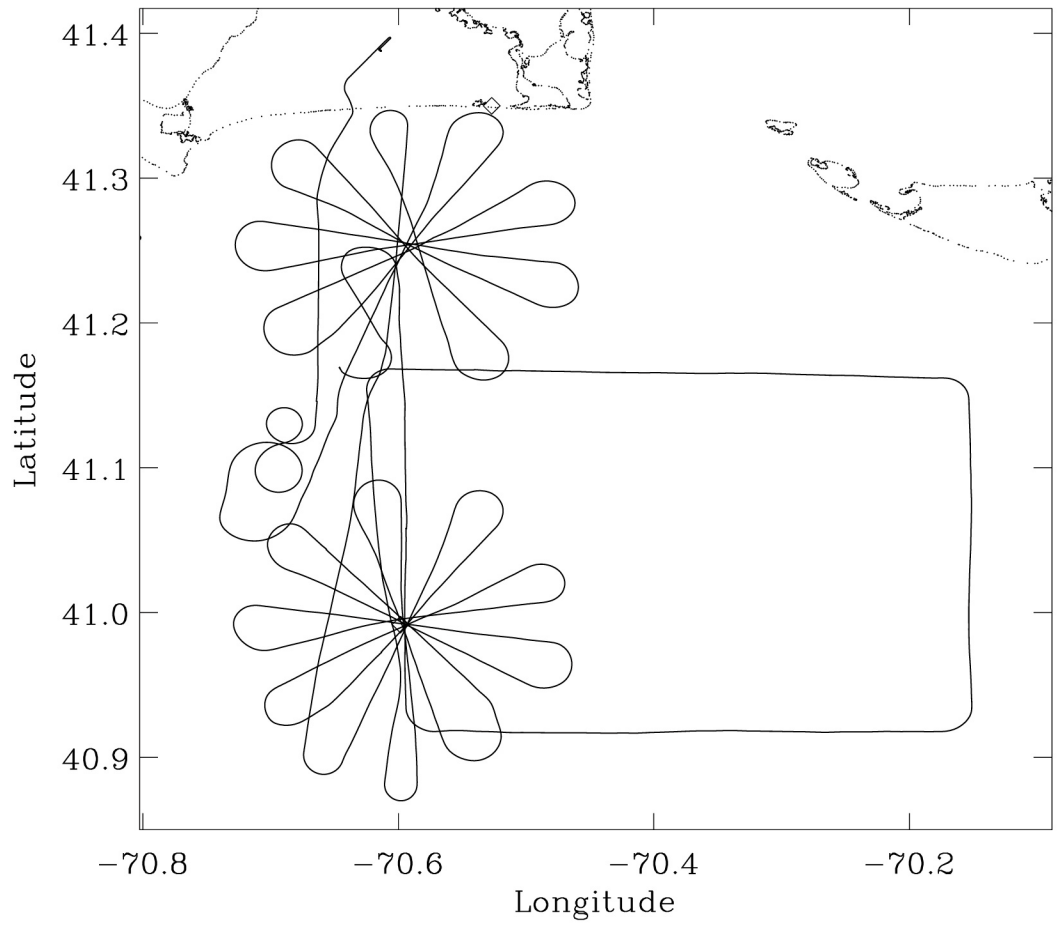


Fig. 37. N3R track for Flight 19 (08 AUG 01).

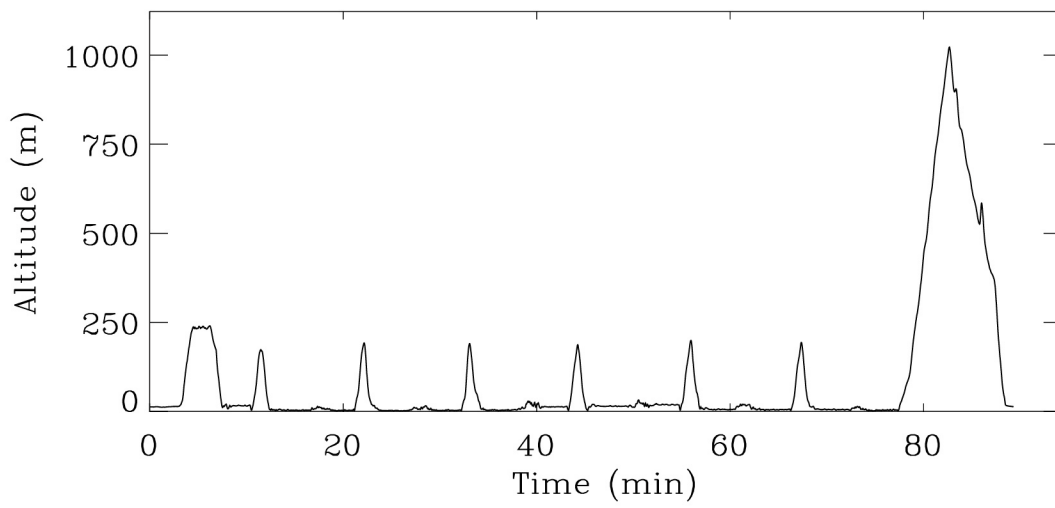
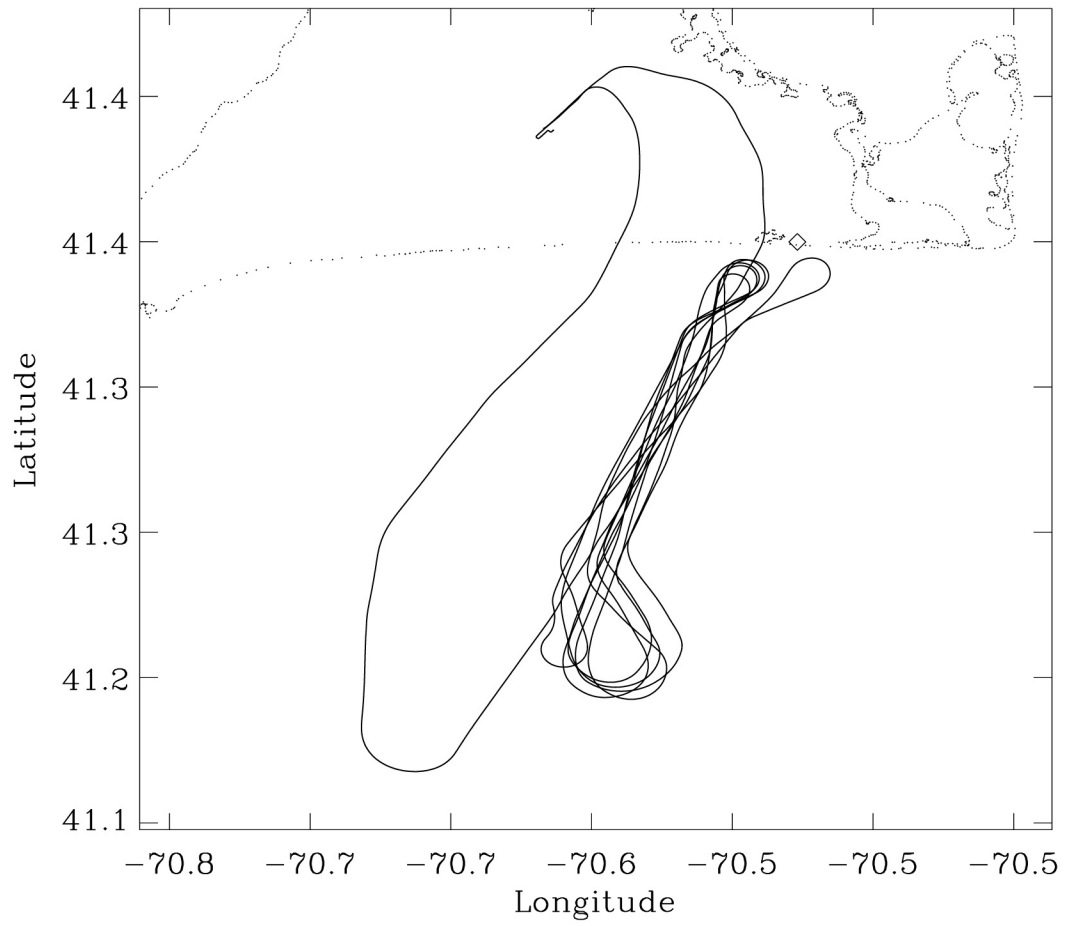


Fig. 38. N3R track for Flight 20 (08 AUG 01).